STUDIES OF SOLAR MAGNETIC AND

JAGADISH CHANDRA BHATTACHARYYA

Thesis submitted for the
D.Phil. (Science) Degree
of the
University of Calcutta

1969

ACKNOWLEDGEMENTS

The experimental work involved in the present thesis was carried out at the Kodaikanal Observatory, as a part of investigational work of the institution. I am thankful to the Director-General of Observatories for his kind permission to utilise the data obtained for the purpose of this thesis.

My heartfelt thanks are due to Prof. J.N.Bhar, who had taken so much pains to provide constant advice and guidance in course of my design and construction of this delicate equipment, and in the presentation of my results.

It is difficult to convey my indebtedness to Dr. M.K. Vainu Bappu, Director, Astrophysical Observatory, Kodaikanal, without whose valuable help and advice it would have been impossible for this work to progress. He had been my constant adviser in matters of design of the optical equipment, and the programmes for observations and analysis. No words can express my thanks for the ever helpful inspiration and guidance he provided during the whole course of this work.

I have great pleasure in expressing my thanks to Shri B.N. Bhargava, Director and Shri A. Yacob of the Colaba Magnetic Observatory for their help in the preparations of my data for computer analysis.

I am also to acknowledge the valuable advice rendered by Dr. V.E.Stepanov, Director, Sayan Observatory, U.S.S.R. and Dr. W.A. Baum, Director, Lowell Observatory, U.S.A. during the construction of the equipment at the time of their visits to Kodaikanal.

I have received help from various officers and staff of the Kodaikanal Observatory during my whole work. Special mention may be made of Shri A.P.Jayarajan, Shri K.C.A.Raheem and Shri K.S. Muthu for the design and construction of the optical parts, and of Shri M. Iqbal Ali, Shri L. Peter, Shri M. Paranjothi, Shri V. Germanappan and Shri Alfred Charles for the mechanical constructions. In Electronic design and construction, I have great pleasure in acknowledging the help of Shri S. Gopal, Shri Satya Prakash and Shri Mohd. Abbas.

During the observation and scaling of data, help of Shri Gopal, Shri Satyaprakash, and many others is gratefully acknowledged.

I am grateful to Shri K.R. Sivaraman, and Dr. Ch.V. Sastry of Kodaikanal Observatory, Dr. A. Chakravarty of Saha Institute of Nuclear Physics, Calcutta, and A. Kubicela of the Belgrade Observatory, Yugoslavia, for extremely helpful discussions about the method of analysis employed in my thesis.

The preparation of the art and manuscript of this thesis is greatly aided by the efforts of Sarvashri, A.M. Batcha, V. Ramasami, P. Shahul Hameed, A.M. Ghouse, M. Jan and C.G. Veeraraghavan and others, and I thank them for the help. I am also thankful to Sarvashri J.V. Narayana, U.V. Gopala Rao, T.K. Balakrishnan, A.Thulasidoss, B.K. Venkataraman and several others for their keen interest and useful help in the various fields.

Last, but not the least, I thank Shri T. Mark and Shri J. Anthonyraj for their help in maintaining the solar tower equipment during my observations.

Finally, I would like to record my sincere thanks to the remaining members of the staff of this observatory, who provided whatever help was needed.

Dt. 8-11-1969
Kodaikanal-3.

(J.C. BHATTACHARYYA)

TABLE OF CONTENTS

TABLE OF CONTENTS

TABLE OF CONTENTS

SUMMARY

The discovery of mass motions and existence of strong magnetic fields in active regions of the sun in the first decade of this century opened up new lines of investigation in the physical processes occurring in the hot plasma of the solar atmosphere. But owing to the inherently difficult nature of the measurements, the weak magnetic and velocity fields of the sun eluded detection for nearly half a century. The measurements posed a challenge to the experimental astrophysicists, who had attacked the problem time and again without success. At last aided by modern developments in the fields of electronics, electro-optics and spectroscopy, the first break-through was achieved in 1953 by Babcock and Babcock, when they showed the presence of weak magnetic fields on the sun. Within a decade Leighton and his co-workers were able to demonstrate the existence of the oscillatory nature of localized velocity fields that owe their origin to the deep seated hydrogen convection zone. In spite of these two striking developments further progress in this direction was hindered due to extreme requirements of precision and stability of the equipment. The very fact that only a few solar magnetographs exist at the different observatories of the

world to-day, point out to the difficulties encountered in making these measurements.

The basic requirements for making measurements of weak magnetic fields and granulation stimulated velocity fields, is a good solar telescope, a high dispersion high resolution spectrograph and a stable, precise electronic system for extraction and amplification of the weak electrical signals generated by means of sensitive electro-optic devices. The first two were already available at the Kodaikanal Observatory, and rigging up the remaining equipment conforming to the required precision and stability with the available resources has been my contribution towards the building of this new solar magnetograph. I have adopted the basic design principles of the Babcocks, but all individual electronic and optical units were completely designed to suit our existing spectrograph arrangements, and availability of various components required for the task. Needless to add that various alternative arrangements and circuits had to be tried in order to arrive at the present complete form of the instrument. Also, future modifications will continue to be made with a view to improve the performance of the instrument further, and to enlarge its scope of measurement.

The instrument in its present form is capable of detailed measurements in the solar spectrum. I have confined its use to some detailed studies of the oscillatory mass motions at various depths in the solar atmosphere and searched for the existence of similar possible variations of the longitudinal magnetic field. These two aspects are covered in my present dissertation.

I have given a brief review of the earlier work in sensitive measurements on solar absorption lines in Chapter I. The theoretical and observational aspects of solar velocity and magnetic fields are also discussed in this chapter.

I have discussed in Chapter II, the theories of measurement of longitudinal magnetic fields and of mass motions from the Zeeman splittings and Doppler shifts respectively of spectral lines, and described the construction of the instrument. I have included detailed design descriptions of the various units, in the hope that this will be useful to other observatories in the construction of such units in near future.

Various checks and calibrations performed on the instrument to test its capability for the measurements intended to be done with its help have also been described

in this Chapter. The sensitivity and limitations are also discussed in detail.

Chapter III consists of the presentation of my measurements on eight different spectral lines for studies of the oscillatory fields. The lines have been chosen in such a way as to represent various levels in the solar atmosphere. Characteristics of the predominant periods and amplitudes of the oscillation and their variations for different lines have been discussed. Detailed statistical analysis of the measurements have been given and the results discussed from various points of view.

In Chapter IV, I have presented results on more measurements of two chromospheric lines. The variation of the oscillation characteristics at different positions on the line wing have been presented. Results of harmonic analyses of the mean waveforms of one of the lines and spectral density curve variations at different distances from the centre of the solar disc are presented and discussed.

Chapter V, starts with the description of an attachment to the magnetograph for simultaneous recording

of velocity and magnetic fields and presents some results of such measurements. Possibility of correlation between the parameters of a magnetic field as well as the velocity field are discussed on the basis of a detailed statistical analysis of the simultaneous records.

--

CHAPTER I

A SURVEY OF CURRENT KNOWLEDGE OF SOLAR MAGNETIC AND VELOCITY FIELDS

1.1. Introduction

Ever since Kirchhoff's explanation about the origin of Fraunhofer's line of the solar spectrum, as due to selective absorption by gases in the solar atmosphere, these lines have proved to be the most powerful tools of solar research. Subsequent demonstrations by Young during the total solar eclipse of 1870 of the reversal of these absorption lines into emission lines in the flash spectra is one of the most thrilling experiments ever done in the realm of physics. The absorption spectrum seemed to contain an enormous amount of information about the chemical constitution and physical conditions of the atmosphere of the sun and other distant bodies. As more refined techniques started coming in, even the ambitious dreams of the earlier physicists appeared unduly modest compared to the possibility of the extent to which man's knowledge about the atmospheres of distant stars can be advanced by precise measurement of various aspects of absorption spectra.

The magnetic field of the earth was known to the scientists for a long time, the natural curiosity whether the sun also possesses a magnetic field had been troubling the minds of physicists for a long time. An indirect evidence of such an existence was first noticed during the total solar eclipse of 1878 when the remarkable structure of the solar corona bore resemblance to the lines of force surrounding a bar magnet. But first direct measurement of the existence of solar magnetic fields had to wait till Zeeman's discovery of the splitting of spectral lines in a magnetic field. Soon afterwards, in 1908, G.E. Hale at the Mount Wilson Observatory showed the typical Zeeman splitting of absorption lines in the light originating from sunspot regions. The measurements indicated that strong magnetic fields of a few thousand gauss exist over the sunspots and adjoining regions. By further refinement of the measuring techniques, Hale and Nicholson studied the magnetic field and its variations over the plage regions surrounding sunspot areas, and discovered the interesting laws about bipolar sunspot groups, the polarity reversals in adjacent sunspot cycles and many other features of the magnetic variations over the solar active regions.

1.2. Magnetic field measurements with electronic techniques.

All the measurements by Hale had been by high dispersion photography of the solar spectrum, and the method had, therefore, its limitations. The minimum field detectable was of the order of a hundred gauss, and he was unable to detect any field outside plage regions. In 1933, by using photoelectric cells and amplifiers employing thermionic valves, which had just come into use, Hale in collaboration with Dunham, Strong, Stebbins and Whitford made an attempt for measurement of the general magnetic field of the sun. The arrangement has been briefly described by Babcock and is as follows.

A powerful spectrograph, equipped with an analyser for circular polarization received light from a selected part of the sun's image. At the focus of the spectrograph, an exit slit was placed on a wing of a Fraunhofer line chosen for sensitivity to the Zeeman effect. Radiation transmitted by the second slit was received on a photo tube, the electrical output of which was connected to an amplifier having a meter at its output. If the line was affected by longitudinal Zeeman effect owing to the presence of magnetic fields in the solar atmosphere, a change of the analyser from the right handed to left handed condition would produce a slight

shift in the position of the line. Because of the sloping profile of the wing, the existence of magnetic fields will show up as a corresponding change in the indication of the output meter. However, owing to weakness of the sun's field and to the difficulty of eliminating systematic errors, Hale and his collaborators did not achieve positive results with their photoelectric equipment.

Variations of this basic method were applied by several investigators, notably by G. Thiessen (1946) who used a Fabry-Perot interferometer for high resolution measurements of Zeeman affected lines. An accuracy of $\pm$ 50 gauss could be achieved by him. Kiepenheuer (1953) introduced the fixed frequency modulation and selective amplification technique for extracting weak signals from large noise background, but his instrument had an inconvenient arrangement of compensation of instrumental polarisation introduced mainly by the coelostat mirrors. Although Kiepenheuer could reach a sensitivity of 1 gauss, he had to reckon with the uncertainties connected with the proper compensation of the instrumental polarisation and false modulation by moving optical modulator parts.

In a very subtle modification of the original arrangement, Babcock and Babcock (1952) eliminated this great hurdle. Instead of one slit, as had hitherto been tried, they used two slits to receive light from both the wings of the Zeeman affected line, and two photomultiplier tubes connected to a difference amplifier. Any instrumental polarisation, thus appeared in both the wings simultaneously, and was differenced out by the difference amplifier that followed. They also replaced the rotating optical modulator by incorporating an electrically excited retardation plate, thus eliminating the possibility of false modulation of the signal by moving parts. The arrangement in conjunction with a high resolution spectrograph and an automatic scanning device, was put into regular use in the Mount Wilson Observatory for measurement of weak magnetic fields on the sun.

Immediately afterwards, it was realised that this instrument is capable of measuring an equally important parameter of the solar surface, with an accuracy hitherto unknown. When a circular polariser is kept ahead of the optical modulator, the instrument becomes extremely sensitive to minute displacement of the lines. However, due to insufficient advancement in our understanding of the subject, the technique was used for the

first time by Howard (1962) soon after Leighton's classical demonstration of the small scale velocity fields on the solar surface (Leighton 1960).

1.3. Velocity Fields on the solar surface.

Although the existence of doppler shift of the solar Fraunhofer lines ascribed to solar rotation was shown in the last decade of nineteenth century, it was Evershed (1909) who first proved characteristic mass motion around sunspot groups, by observing doppler shifts in the spectra of sunspot regions. The existence of small scale velocity fields was also first demonstrated by him when he reported his observation of "innumerable small displacements of the lines equivalent to velocities of the order of a few tenths of a kilometre per second (Evershed 1922) when the slit lies across a well defined image of the sun. Evershed's findings were nearly forgotten over the decades and independently Richardson and Schwarzschild (1950), undertook the systematic measurements of the Doppler shifts of a few excellent plates of solar spectra, and determined the value of the magnitude of these shifts. McMath and his co-workers (1956) made similar measurements on spectra taken with the new vacuum spectrograph of the McMath-Hulbert Observatory and found almost identical results. But it was left to Leighton by

using his new technique of photographic subtraction of solar images obtained in opposite wings of an absorption line to prove the existence of vertical oscillatory velocity fields on the solar surface. The existence of this velocity fields, the oscillatory nature of the motions and the comparatively large size of the contributing elements were confirmed by Evans and Michard (1962), Howard (1962) and Leighton, Noyes and Simon (1962) almost simultaneously afterwards. As more information poured in, the process appeared to be more complex than what had appeared at first sight, as it so frequently happens in many an important physical discovery.

The rapid ionization of hydrogen that one encounters as one goes below the solar surface gives rise to the hydrogen convection zone. The presence of granulation in well defined solar images lends support to such an assumption. Biermann (1947) considered the possibility of theoretical grounds and contended that the granulation cells are due to convection occuring deep in the photosphere. Whitney (1958) worked out the possibilities of these convection cells setting up characteristic oscillatory motions in the upper photosphere and found that oscillations of periods of the order of a few minutes are possible. Discovery of oscillatory velocity fields soon afterwards windicated his stand. Whitney's computations

opened up a new possibility of determination of physical parameters of the outer solar atmosphere by study of the oscillation characteristics. The problem reduces to the question of understanding the wave propagations in the solar atmosphere. Propagation in idealised model isothermal atmospheres is comparatively simple, and was taken as a basis of Whitney's calculations. It is well known that an isothermal atmosphere is a dispersive medium, and that for a given direction of propagation, there is an interval of frequencies for which no propagation is possible. For the higher frequencies the waves are of compressive type, whereas for the lower frequencies, the waves are of gravitational type. Moore and Spiegel (1964), have thoroughly studied these properties and their work throws some light on the possible mechanism, by which the disturbances which have been produced in the deeper layers of the atmosphere, in the convective zone, can reach the upper layers. Schmidt and Zirker (1963) have considered the transmission by an atmosphere of the wave produced by a piston which suddenly begins to move upward at time t = o. Their results reflect essentially the dispersive properties of the atmosphere. The spectrum of the transmitted oscillations reflects both the properties of the impressed force and the filtering properties of the atmosphere. Schatzman (1964) reported that by

considering two atmospheric models, with a special choice of the parameters, such that the models are mathematically tractable, he finds that the transmitted wave bears some similarity with the oscillations observed by Evans and Michard, for an impressed force which was a step function. His calculations basically point out that the physical parameters connected with the wave propagation problem in solar atmosphere are intimately connected with the spectrum of the vertical oscillations noticed.

The importance of this wave propagation in the solar atmosphere is further augmented, since it is considered the most probable mode of energy supply to the chromosphere and the corona. Bierman (1948) and Schwarzschild (1948) independently suggested that pressure waves from the photospheric granules above a certain critical frequency travels up as sound waves, the amplitude increasing with height, so that the energy carried by them stays constant or decreases slowly. The dissipation of this energy occurs by radiative exchange in the lower chromosphere, heat conductivity and viscosity being found to be negligible. Schatzman (1949) considered the possibility of these sound waves being degenerated into shockwaves, the energy dissipation being controlled by the mechanism described by the theory of Brinkley and Kirkwood.

Alfven (1947, 1950) has suggested another possible mode of such an energy transfer. The motion of granules in a magnetic field should give rise to magnetohydrodynamic waves which would travel up in the solar atmosphere. The main dissipation of the energy is by Joule heating of the medium. This Alfven type of waves need not be considered as having a separate existence from sound waves and shock waves. Compression waves produced in the convection zone and reaching the lower chromosphere, propagate in regions of non-uniform density and non-uniform magnetic field. Through these gradients compression waves can generate Alfven waves which can propagate along the magnetic lines of force.

The actual mechanism of chromospheric and coronal heating still holds an important secret in our understanding of physical processes occurring in these regions. It is not illogical to assume that some insight will be provided through systematic study of the motions of the media traversed by these waves.

1.4. Magnetic Fields in active regions.

Active regions of the sun have all along been associated with strong magnetic fields. Energy of the solar flares are also believed to be drawn from energy

stored in the magnetic field. But the exact process by which these fields develop and contribute to the solar activity energy and decay is still a matter for speculation.

A possible explanation of the whole solar magnetic phenomena has been attempted by H.W.Babcock (1961). The postulate underlying Babcock's hypothesis is that the poloidal field of the sun and the torroidal field which is manifest in the active regions of the sun are both simply manifestations of the same general magnetic field. The non-uniform rotation of the sun is responsible for the production of the toroidal field.

The mechanism visualised by Babcock can be briefly described as follows. The sun is having a small general magnetic field, initially. The submerged lines of force of the dipolar poloidal field lie in the meridian planes in shallow upper layers. Because of non-uniform rotation of the sun, the equatorial layers move faster, pulling with them the submerged magnetic lines of force. In course of time the submerged lines of force are drawn considerably out in longitude and wrapped around the sun, several times over with a consequent amplification of field strength. The magnetic energy of these layers increases at the expense of rotational kinetic energy.

This winding up to form tight spirals proceeds until the magnetic field intensity of these submerged toroidal fields reaches at some point or points a value sufficient for instability to occur. Such regions tend to be buoyed up to the surface to form bipolar magnetic regions (BMR).

The variation of differential rotation explains the first emergence of BMRs at middle latitudes. The model also gives semi-quantitative interpretation of many of the characteristic features of sunspot and the solar cycle, but a detailed working out of its implications will require some fundamental progress in basic magnetohydrodynamics.

Babcock's theory visualises more or less regular poloidal field's outside BMR's but actual observations by refined techniques have proved the existence of much finer structure of these magnetic elements. Howard (1966) suspects the elements to be of a scale of 1 second of arc. From simultaneous measurements on two lines of slightly different heights of formation Severny (1966) concludes that the extents of these elements are equally limited in the vertical direction. The elements are apparently unaffected by vertical mass motions (Severny, loc. cit) and remains on such accounts an enigma.

Finally, the question of periodic oscillations in the value of magnetic field was investigated by Severny (1967). From simultaneous record at two spectral lines he appeared to notice a periodicity of a few minutes, but the experimental conditions do not allow enough confidence to be placed on that observation. A new feature has, however, been noticed by him, when he observed that the magnetic field observed in integrated light from the sun has a definite periodicity of 15 days, like some other variable magnetic stars. It is perhaps by collection of such different facets of information, that our knowledge of the magnetic behaviour of the sun and the stars can be properly synthesised in near future.

—

CHAPTER II

THE SOLAR MAGNETOMETER

2.1. Theory of Measurement.

The instrument designed for this work follows the basic pattern of the solar magnetograph of Babcock and Babcock. A solar telescope images the solar disc on to a screen; a small aperture selects a small area of the solar disc and the light from this area is dispersed by a high dispersion, high resolution spectrograph. A suitable spectral line is re-imaged on to a "Detector head", in such way that the light from the two wings and the core of the line are separated and received on three separate photomultipliers. An appropriate electro-optic modulator introduced in the beam modulates the electrical outputs of the photomultiplier tubes. A narrow band selective amplifier amplifies the modulated signal and a phase sensitive synchronous detector demodulates it. The output, a varying D.C. signal, is recorded on a strip chart recorder.

The parameters intended to be studied in our set-up are (i) the longitudinal magnetic field and (ii) the velocity field. The electro-optic light modulator for (i) is a mounted crystal of ammonium-dihydrogen-phosphate

(ADP) backed by a polaroid. The ADP is operated by a sinusoidally varying voltage of appropriate magnitude. The arrangement alternately cuts off the oppositely circular-polarised light from the wings of a Zeeman affected line. The difference of outputs of the two photomultipliers that receive the light from the two wings are amplified by a difference amplifier; the output of the third photomultiplier monitors any variation of the experimental conditions.

For (ii) the modulator consists of an additional fixed circular polariser ahead of the ADP-polaroid assembly. The arrangement modulates the complete light beams in the operating frequency, and hence the output currents of all the three photomultipliers. The difference amplifier gives a non-zero output whenever there is a difference between the outputs of the two photomultipliers receiving light from the two wings of a line; when the line is properly centred the output is zero. This makes the equipment extremely sensitive to line shifts.

The theory of measurement of the longitudinal magnetic field and the velocity from the Fraunhofer lines has been described in detail by many authors

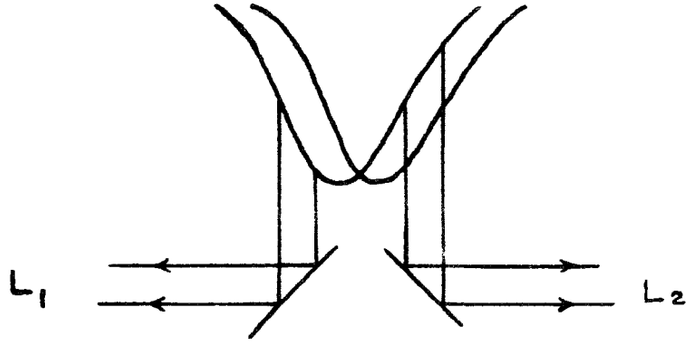

Fig. II-1.

(Babcock (1953), Nikulin et al (1958), Deubner et al (1961). So, I shall give only the salient points about it. In the direction of the magnetic field, most of the spectral lines split up into two components, both circularly polarised, but in opposite sence. The shift in wavelength of each component is related to the magnetic field strength by the following relation:

$$\Delta\lambda = 4.67 \times 10^{-5} g \lambda^2 H \qquad (2.1)$$

where $\Delta\lambda$, λ are in cms, and H is in gauss, g is the Landé splitting factor for the particular line. If by introducing a quarter wave plate and a polariser, one of the components is removed, only the other component will be seen and the line will appear shifted. In an arrangement as in Figure II-1 which separates the light from the two wings into components L_1 and L_2, the difference $\Delta L = L_1 \sim L_2$ will be zero if the line is properly centred, but introduction of a quarter wave analyser will result in a fractional change,

$$\frac{\Delta L}{L} = 4.67 \times 10^{-5} \frac{1-R}{1+R} \frac{2}{B} g \lambda^2 H \qquad (2.2)$$

in a Zeeman affected line, R being the residual intensity at the centre of the line and B the half width of

the line assuming a straight triangular profile. If the light is received on two photomultiplier tubes of identical and linear response, then a small change in photomultiplier current should result with the introduction of a circular polarisation analyser, given by,

$$\frac{\Delta i}{i} = 4.67\ 10^{-5}\ \frac{1-R}{1+R}\ \frac{2}{B}\ g\lambda^2 H \qquad (2.3)$$

where 'i' is the mean current delivered by the photomultipliers receiving light from the wings of the spectral line.

In the velocity mode, the shift of any spectral line results in a differential output of the two photomultipliers that receive light from the wings. The proportionate change in the differential photomultiplier output is given by:

$$\frac{\Delta i}{i} = \frac{v\lambda}{c}\ \frac{1-R}{1+R}\ \frac{2}{B} \qquad (2.4)$$

where v is the line of-sight component of velocity of source and c is the velocity of light both expressed in the same units.

The signal in both cases is very small and completely submerged in the noisy photomultiplier output

currents. To amplify the signal out of the noise background, the selective amplification technique is employed. To achieve this, the ADP is operated at one fixed frequency. In the magnetic mode, this results in chopping off the right and left circular polarised radiation in alternate half cycles. The differential output of the two wing photomultipliers thus contains a single frequency signal whose amplitude is proportional to the longitudinal magnetic field. This, when channelled through the narrow band selective amplifier, rises above the noise level and makes it possible for it to be recorded after suitable further amplification, filtering and synchronous detection.

In the velocity mode, action of the alternating voltage operated ADP together with the pair of polarisers and a fixed quarter wave plate is to modulate the total light falling on the photomultipliers. Since the modulations are all in phase, the differential output when present is also modulated. The frequency selective amplifier amplifies this signal in preference to the noise background and the final synchronous detector output is proportional to the Doppler velocity of the source.

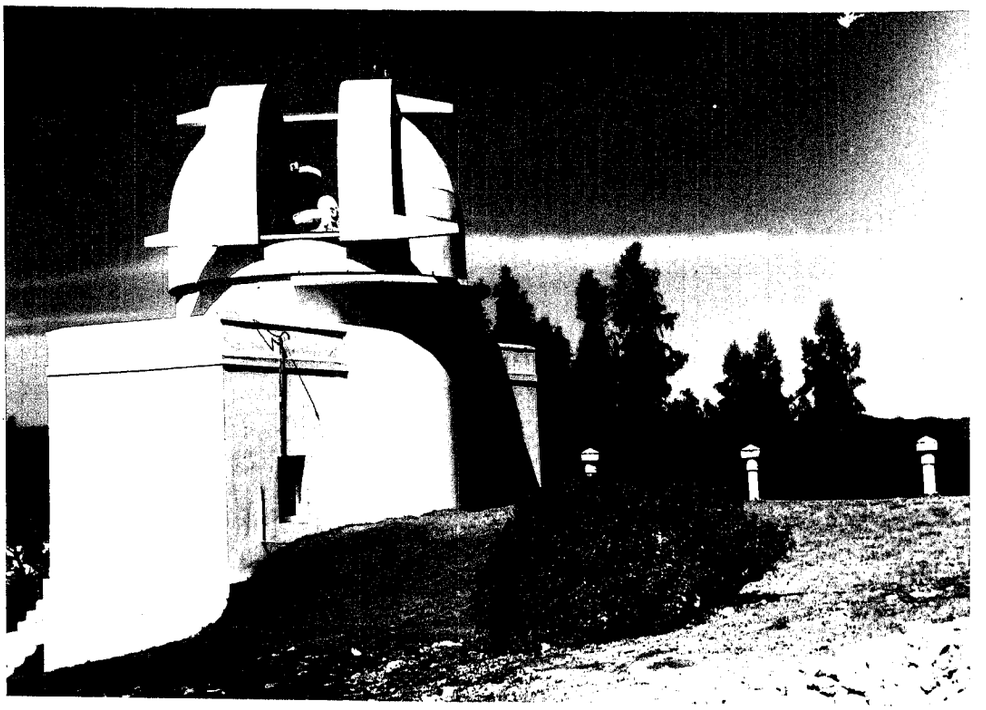

Fig. II-2

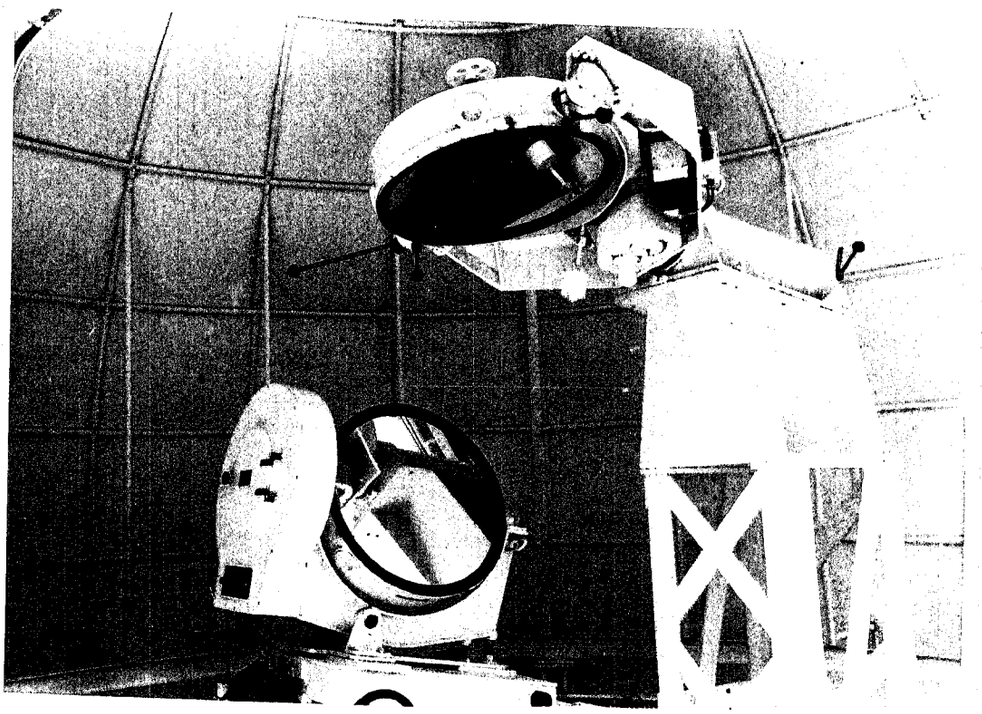

Fig. II-3

2.2. The Optical Arrangement.

The equipment is housed in the solar tower at the Kodaikanal Observatory. It consists of a three mirror coelostat arrangement with the first two mirrors mounted on a tower 11 meters above ground level. These two mirrors are fused quartz optical flats of 61cm diameter with aluminium coated reflecting surfaces and housed in two cells with equatorial mounting. Figures II-2 and II-3 show two photographs of the solar tower and the first two coelostat mirrors respectively. The first mirror is driven by a synchronous motor which is run by a precision frequency generator and is geared in such a way as to follow the sun accurately. The precision frequency generator consists of a Wien Bridge Oscillator with the bridge elements in a thermostatically controlled oven, and generates a frequency of 47.333 cycles per sec., nominally. A separate control allows the frequency to be varied over a small range to accommodate variations in the sun's apparent motion. The oscillator output is phase-split and amplified by three power amplifiers to produce a 3 phase 440V supply with a very stable frequency.

The second mirror which is also equatorially mounted has independent remote controlled slow and fast

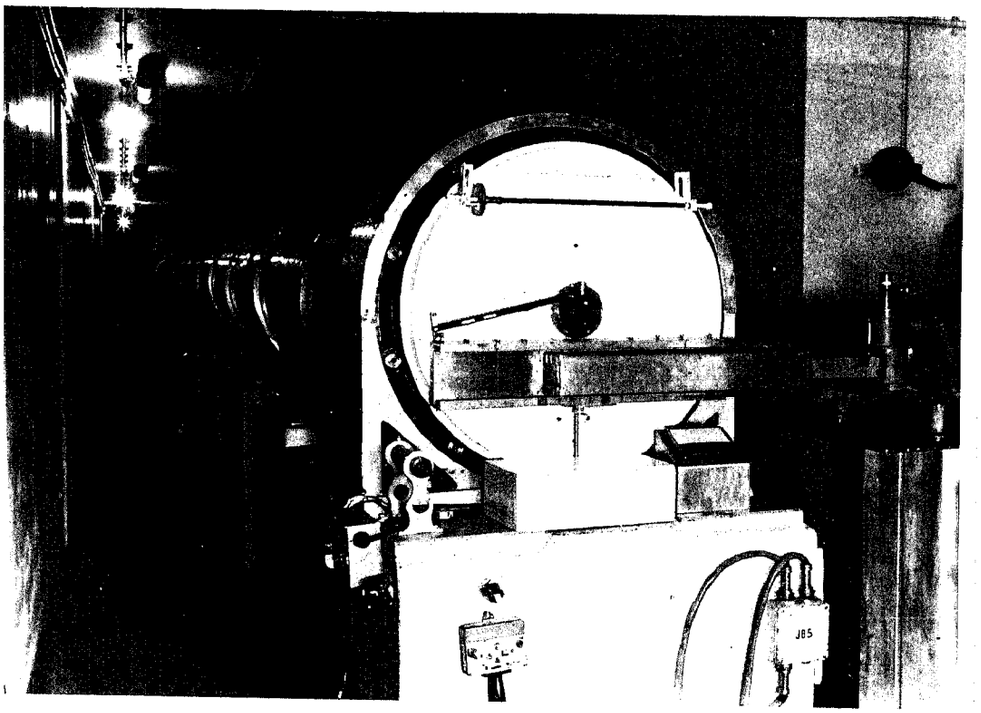

Fig. II-4

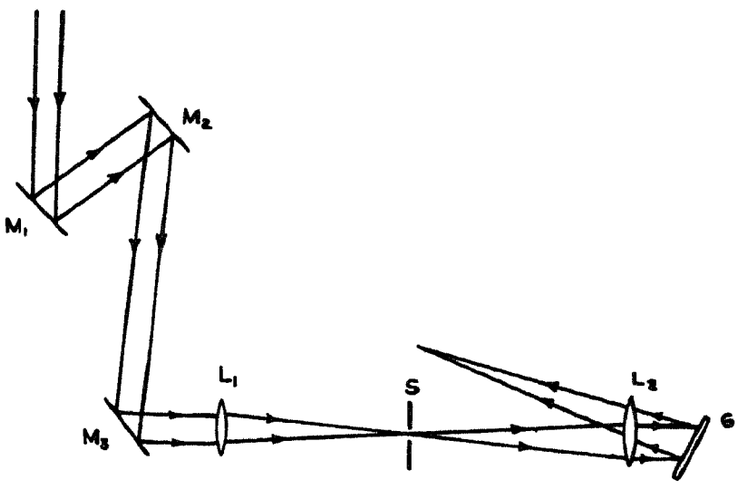

Fig. II-5.

movements around two perpendicular axes, enabling the observer to centre any part of the solar image on to the spectrograph slit.

The third mirror situated at the bottom of the tower is also a 61cm aluminised fused quartz blank but is fixed at 45° to the vertical so as to render the beam from the tower coelostat mirrors horizontal along the axis of the 60 meter long under-ground tunnel.

The horizontal solar beam falls on a 38cm dia, f/90, two element achromat objective lens, which forms a 34cm solar image 36 meters away. The lens is coated with thin film of magnesium fluoride to reduce loss of light due to reflection at the surfaces. The colour curve is flat over a major part of the visible spectrum. The lens is mounted on a remote controlled traction carriage to carryout small changes in focussing when working at extreme edges of the spectrum.

To facilitate visual inspection, the solar image is focussed on a white metal screen, which forms the end plate of the 18 meter diffraction spectrograph. Figure II-4 shows a photograph of the spectrograph. The diffracting element is a 600 lines/mm plane reflection Babcock grating blazed in the fifth order green. It has a ruled area of 153mm x 203mm and is used in a Littrow arrangement

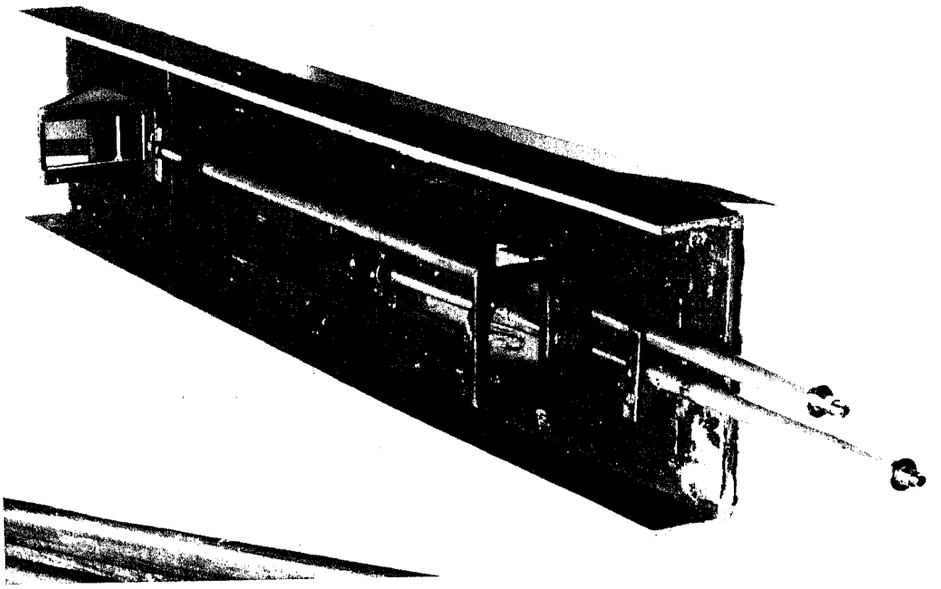

(a)

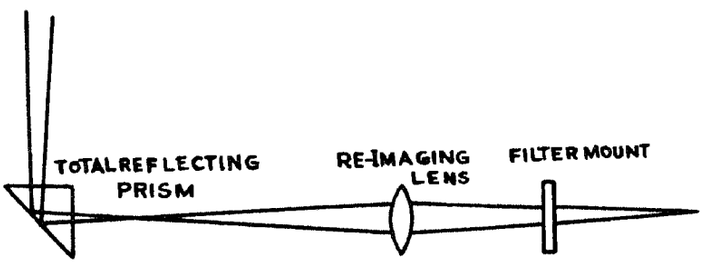

(b)

Fig. II-6

with one 20cm, f/90 two element achromat lens, for collimation and imaging of the spectra. In the fifth order green, where it is blazed, a dispersion of 9mm/A is obtained with a resolving power of 600,000. A schematic arrangement of the solar tower equipment consisting the three mirror coelostat, horizontal telescope and the spectrograph is shown in figure II-5.

The instrument as described above is used on several different research projects on the sun. As such it would be difficult if the complex and heavy magnetograph head is designed to fit permanently in the standard focal plane of the spectrograph. I have overcome this difficulty by locating the magnetograph head adjacent to the spectrograph and reimaging the spectrum on the analysing slit of the magnetograph. Thus within a few seconds, the spectrograph can be changed from a magnetographic mode of operation to the conventional photographic one. This re-imaging attachment is shown in figures II-6(a) and II-6(b). A total reflecting prism placed just ahead of the focal plane of the spectrograph bends the beam at right angles and is reimaged by a small good quality lens of 20cm focal length, without magnification. The lens position is adjustable for accurate focus, which can be monitored at the detector

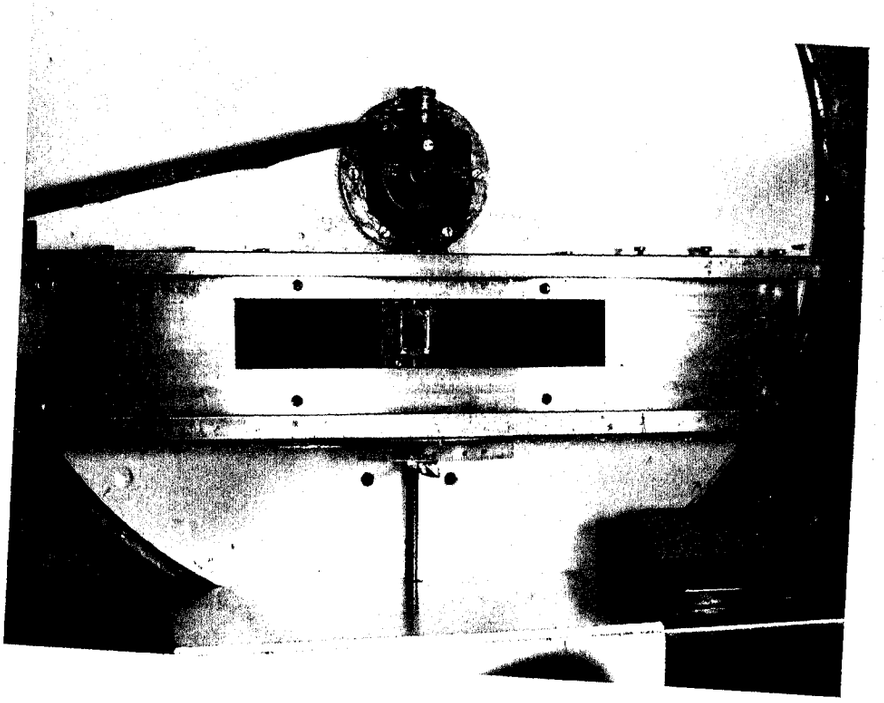

Fig.II-7

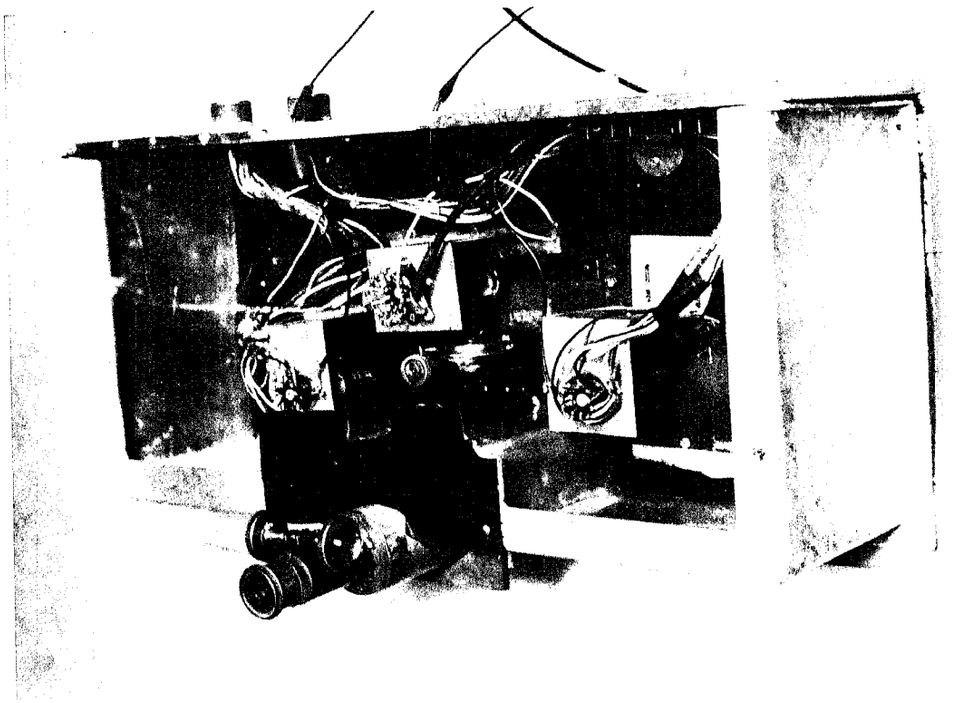

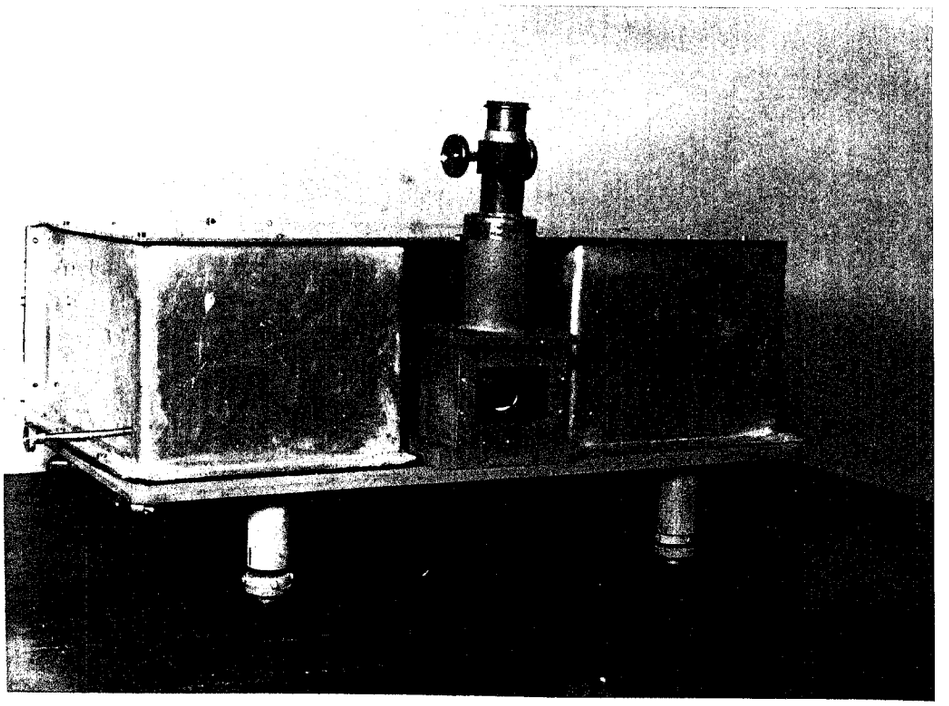

Fig. II - 8 (a)

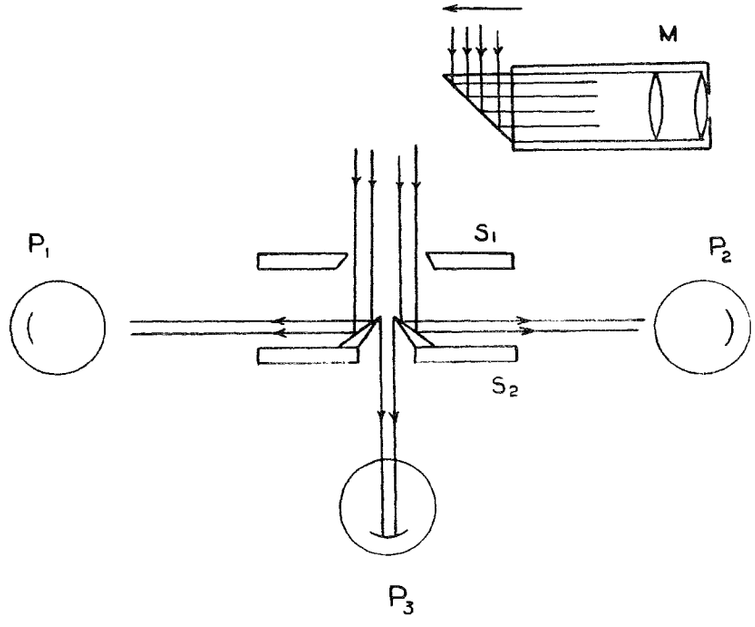

Fig. II-8 (b)

head on which the spectra are re-imaged. A light-tight mount for 5cm x 5cm filters is provided in this unit, to enable working in the higher order spectra by interposing suitable filter combinations to cut out the unwanted overlapping orders.

A plane parallel quartz line shifter is mounted in front of the re-imaging attachment to enable minute shifting of spectral lines and for automatic Doppler corrections. The plate is optically worked to an accuracy of $\lambda/2$ and has a thickness of 3.085mm. It is mounted on a rotatable axis which extends below and is connected to a two phase servo-motor. The axis also has a pointer moving over cylindrical scale which is directly calibrated in degrees. A photograph of the line shifter arrangement is shown in figure II-7.

The photomultiplier detector head is shown in figures II-8(a) and II-8(b). The re-imaged spectrum is allowed to fall on a combination S_1S_2 of two adjustable slits, so that if a spectral line of proper width is focussed, the two wings will be reflected to two photomultipliers P_1P_2 while the core will pass through to the third photomultiplier P_3. The slit S_1 is a standard Hilger bilateral slit of length 18mm and adjustable upto

a maximum width of 1800 . The slit S_2 is a bilateral arrangement of two optically worked reflecting jaws of speculum coated with Aluminium in a vacuum deposition chamber at a precisely controlled rate. This is also adjustable upto a maximum opening of 1500μ . A very fine precision screw attached to S_2 enables precise alignment of the two slits.

The three photomultipliers tubes $P_1P_2P_3$ are RCA 1P21 photo tubes with S_4 cathode surfaces. The multipliers P_1, P_2 form a matched pair selected from about 2 dozen tubes, and show almost identical characteristics. To improve their performance they are operated with double the normal stage voltages across the cathode and the first dynode and slightly reduced voltage between the ninth dynode and anode. The photomultiplier P_3 is provided with equal voltages at all stages, the potential divider chain being located at the base of the tube. But the supplies to tubes P_1 and P_2 are independently given to individual electrodes by means of multicore cables, voltage division being controlled by elaborate networks in the main instrument panel. The outputs of the two 'wing' photomultipliers P_1P_2 are taken out by a pair of shielded cables for feeding into the difference amplifier. A small monitor viewer M

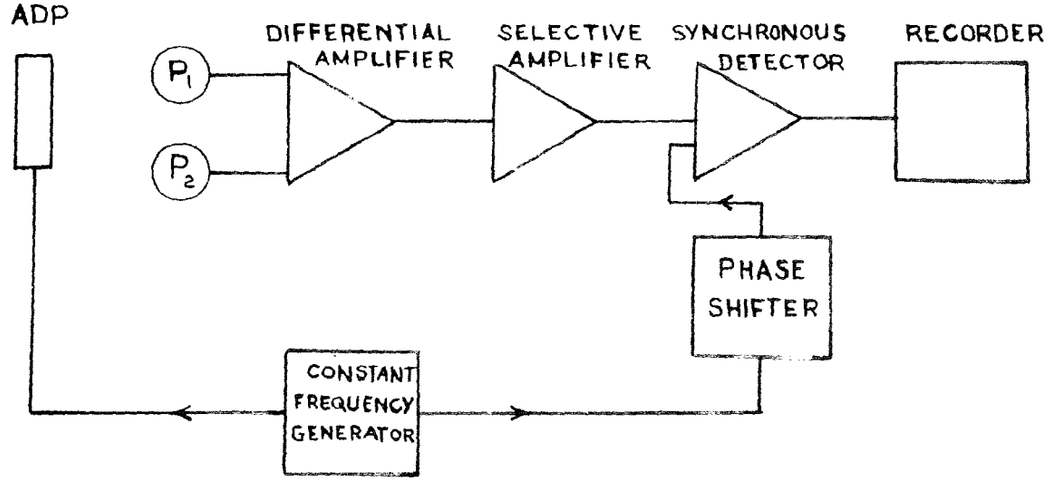
ADP
DIFFERENTIAL AMPLIFIER
SELECTIVE AMPLIFIER
SYNCHRONOUS DETECTOR
RECORDER
P1
P2
PHASE SHIFTER
CONSTANT FREQUENCY GENERATOR

Fig. II-9.

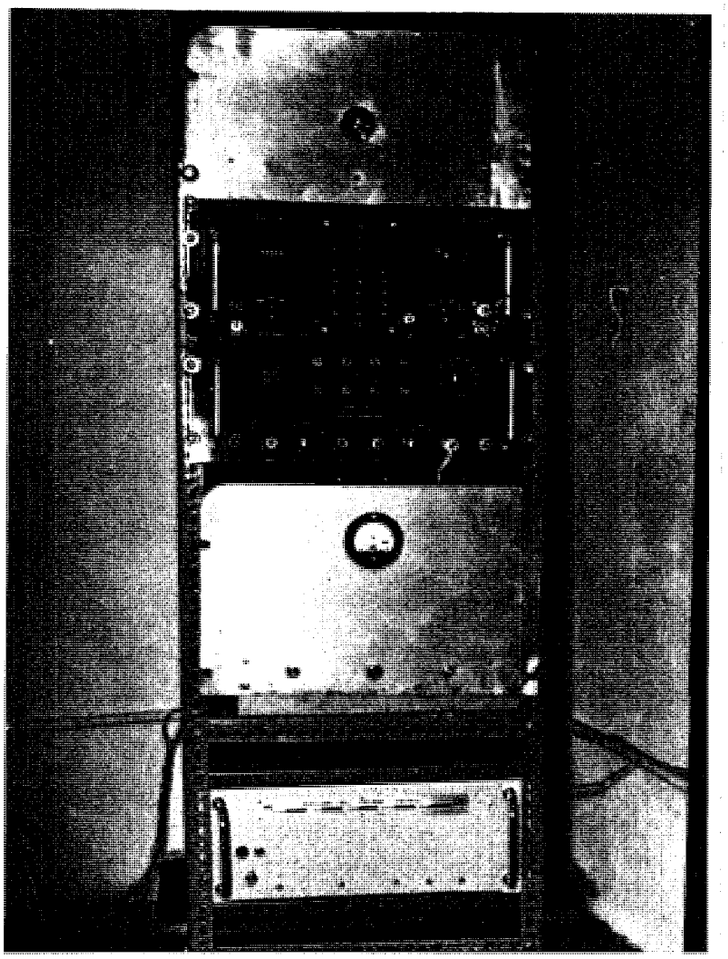

Fig. II - 10

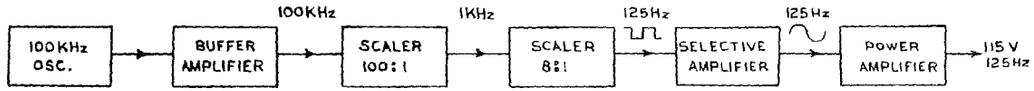
100KHz
OSC.
BUFFER
AMPLIFIER
100KHz
SCALER
100:1
1KHz
SCALER
8:1
125Hz
SELECTIVE
AMPLIFIER
125Hz
POWER
AMPLIFIER
115 V
125Hz

Fig II-11

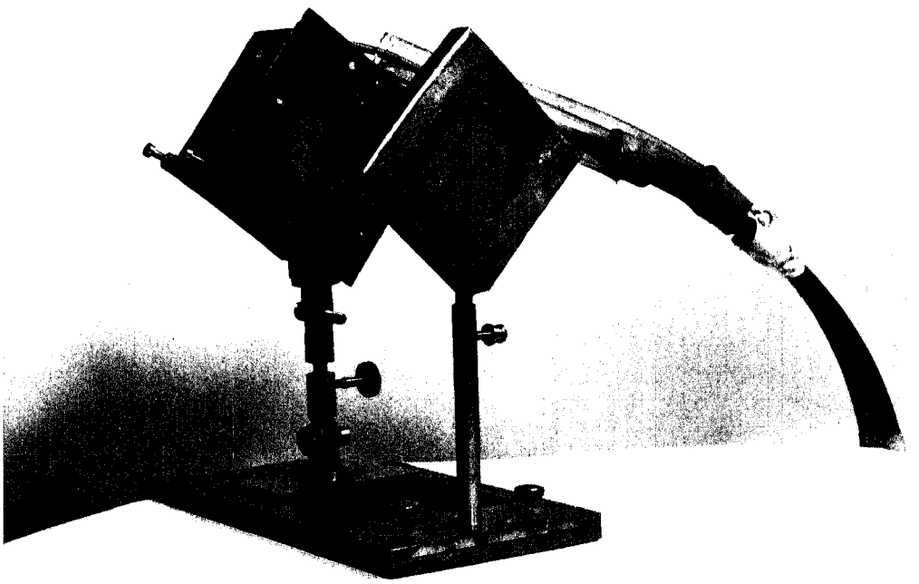

Fig. II-12

consisting of a total reflecting prism and an eye piece is mounted on a draw tube which can be brought in or out of the beam by manual operation. The monitor helps identifications of spectral region and approximate centering of the line on the slit combination.

2.3 The Electronic Design.

The electrical arrangement for modulation, selective amplification and detection is shown schematically in figure II-9. The modulating frequency employed in our case is 125 Hz obtained from a crystal controlled oscillator and a scaler chain. Figure II-10 shows the constant frequency generator unit consisting of a 100 KHz crystal controlled oscillator, a buffer amplifier, two scaler units providing a scale of 800, and giving a square wave of frequency 125 Hz, an active filter comprising of a selective amplifier at 125 Hz with a twin T network at its feed back loop, and finally a push-pull Class AB power amplifier delivering 40 Watts at 125 Hz, 115 volts. The whole set up is shown schematically in figure II-11. Separate transformers have been used in our equipment to supply the light modulator at 2500 volts and the phase shifter unit at 230 volts for operating the 6.3 volt chopper vibrator.

The heart of the light modulator is a Baird Atomic mounted ADP crystal type AM-2, with optically transparent Nesa electrodes. The mounted crystal is fixed on an adjustable stand and introduced in the solar beam just before the spectrograph entrance slit. A polaroid is also fixed on a rotatable frame following the ADP. The stand has facilities for accommodating a fixed circular polariser for converting the equipment for velocity recordings. Two separate heavily insulated conductors supply the 2500V A.C. needed for the crystal to switch $\pm \lambda/4$ retardation between the two polarised components of the light beam. A photograph of the stand with the different elements is shown in Figure II-12.

The difference amplifier used is a commercial DA-102 low level differential amplifier manufactured by EPSCO Incorporated, U.S.A. This accepts two inputs and amplifies the difference by means of a cascode input stage. Common mode rejection is high, rejection ratio at 125 Hz being 50,000 to 1. Differential gain is adjustable from 100 to 2000 in five steps. The amplifier has a very wide band-width from D.C. to 200 KHz inversely proportional to gain, the gain-bandwidth product being equal to 20 MHz. The equivalent input noise between 0-50 Hz being less than 3 microvolts rms, the amplifier

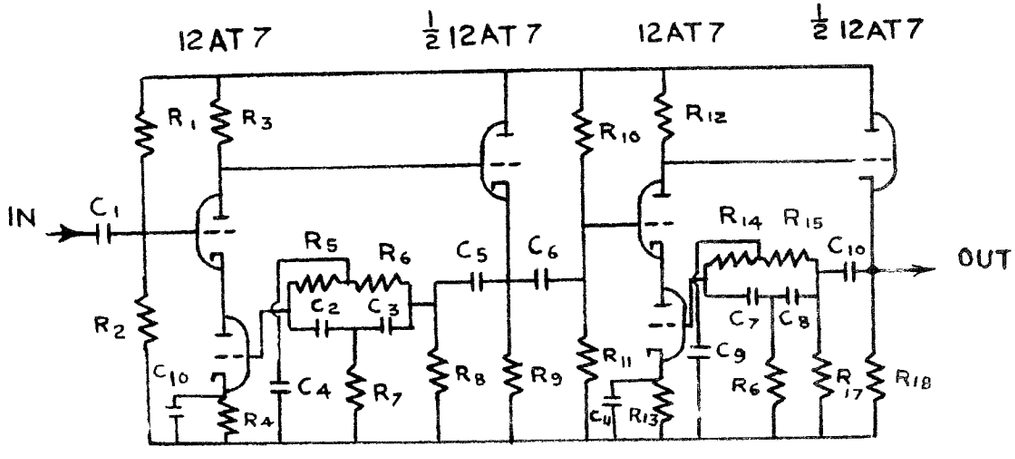

R_1, R_{10}	=	2M	C_1, C_5, C_6, C_{10}	=	0·11 µF
R_2, R_{11}	=	820K	C_2, C_3, C_7, C_8	=	0·11 µF
R_3, R_{12}	=	150K	C_4, C_9	=	0·22 µF
R_4, R_{13}	=	1 K	C_{10}, C_{11}	=	100 µF. 12V.
$R_5, R_6, R_{13}, R_{14}, R_{15}$	=	10K+2K variable			
R_7, R_{16}	=	5·1K+1K variable			

Fig. II-13.

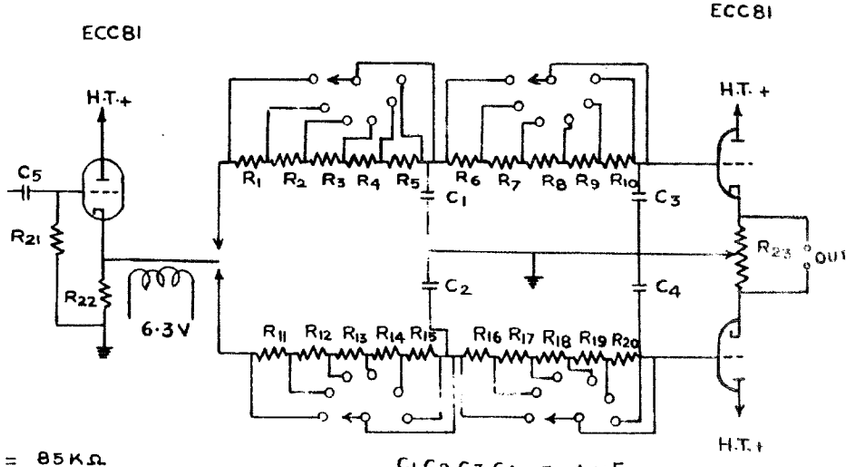

$R_1\ R_6\ R_{11}\ R_{16}$ = 85 KΩ
$R_2\ R_7\ R_{12}\ R_{17}$ = 240 KΩ
$R_3\ R_8\ R_{13}\ R_{18}$ = 470 KΩ
$R_4\ R_9\ R_{14}\ R_{19}$ = 1 MΩ
$R_5\ R_{10}\ R_{15}\ R_{20}$ = 1 MΩ
R_{21} = 1 MΩ
R_{22} = 5 KΩ
R_{23} = 10K turn helipot

$C_1\ C_2\ C_3\ C_4$ = 4 μF
C_5 = 0·1 μF

Fig. II-14.

is ideally suitable for amplification of low photomultiplier signals. Simultaneous amplification of D.C with the 125 Hz signal frequency permits D.C to be separated at the output and used for operating a servo system keeping the line continuously centered on the double slit of the photomultiplier detector head, when the equipment is used as a magnetograph.

The selective amplifier consists of two stages. The individual units are of a cascode input stage with a twin-T rejection network in its feedback loop. Figure II-13 shows the circuit diagram of one of the two identical stages. Use of a cathode follower stage in the feedback path improves the frequency response characteristics, the half power points being $\pm$ 5 cps. away from the centre frequency of 125 cps. The amplifier is intrinsically found to be very stable. High precision stable resistors have been used in the construction of the twin-T networks.

The phase sensitive synchronous detector employs an electro-mechanical single pole 2 way chopper driven at the synchronous frequency of 125 cps. The circuits arrangements are shown diagrammatically in figure II-14. The four pole 6 way switch can select 6 different R-C

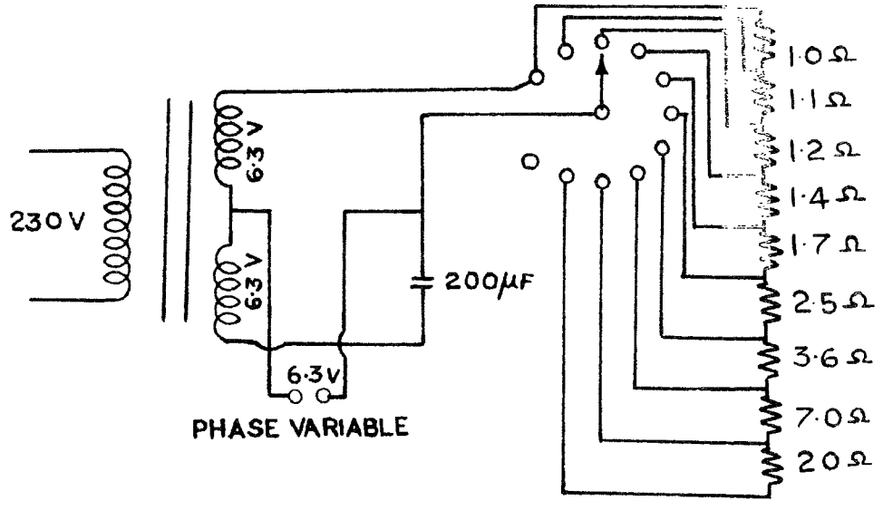
230 V
6·3 V
6·3 V
6·3 V
200μF
PHASE VARIABLE
1·0 Ω
1·1 Ω
1·2 Ω
1·4 Ω
1·7 Ω
2·5 Ω
3·6 Ω
7·0 Ω
20 Ω

Fig. II-15.

combinations to vary the time constant of the synchronous detector. The values of the time constant which can be chosen this way are 0.3, 1.1, 2.8, 6.8 and 11 secs. Feeding into the detector is done through a cathode follower stage with D.C. coupling, and the output is obtained from a pair of balanced cathode followers in differential arrangement. The balance point is adjustible by a precision ten turn helical potentiometer connected between the two cathodes and the ground.

For proper adjustment of the phase sensitive detector a phase shifting arrangement for the driving voltage has been provided. The network is shown in Figure II-15. The resistances are chosen in such a way that each step in the eleven point switch shifts the phase by about 18°. The output impedance of the network is kept low, so that the connection of the chopper drawing about 100mA at 6.3 volts does not affect the operation of the network.

The recorder used is a Honeywell Brown potentiometric recorder with a standard resistance box at its input. The recorder has a full-scale sensitivity of 10mV with a response time for full scale reflection of 1 sec. The chart used is of standard 10 inch width, being drawn at the rate of either 1/2-inch/min. or

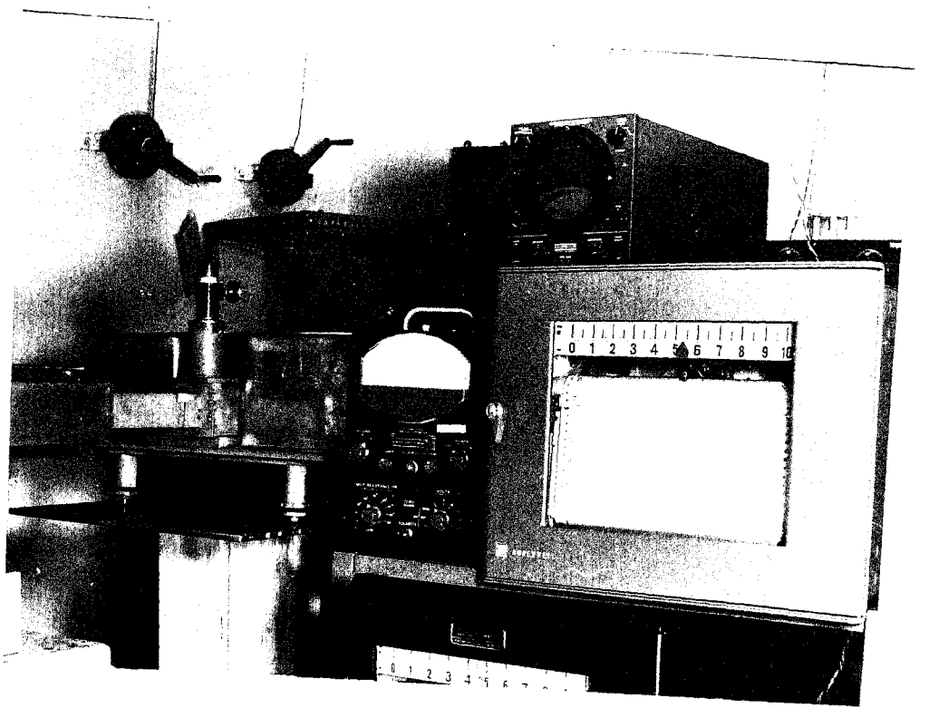

Fig. II-16

2-inches/min. depending on the requirement. The output stage of the synchronous detector is kept slightly off balance so that the zero can be adjusted at the centre of the chart.

The output of the central photo tube is amplified directly by a D.C. electrometer amplifier* and recorded on a strip chart recorder. To smooth out the noise fluctuations of the photoelectric output current, an R-C time constant of 1 Sec. is introduced at the input of the amplifier. A photograph showing the amplifier recorder assembly is shown in Figure II-16.

The H.T supplies of the three photomultipliers are derived from a transistorised E.H.T unit with high stability**. The H.T is taken to a distribution panel where two stable resistance networks divide the voltage for application to different dynodes of the photomultiplier pair P_1P_2. A variable resistance introduced in one chain allows small differential adjustment to be

---

* Electrometer D.C amplifier and voltmeter type 1230A manufactured by Messrs. General Radio Company, U.S.A

**Transistorised E.H.T unit type HV205 manufactured by Electronic Corporation of India.

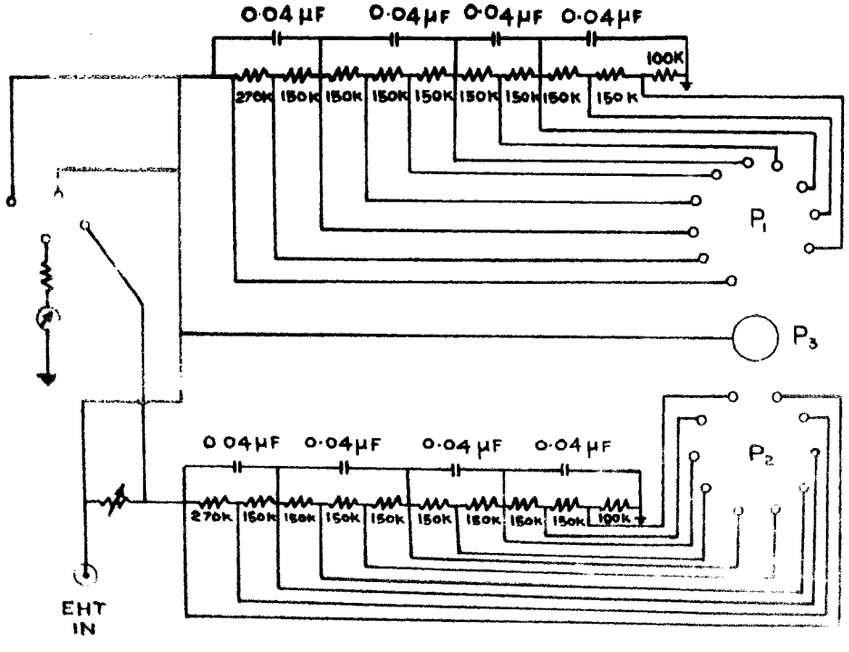
0·04 μF
0·04 μF
0·04 μF
0·04 μF
100K
270K
150K
150K
150K
150K
150K
150K
150K
150 K
P1
P3
0·04 μF
0·04 μF
0·04 μF
0·04 μF
P2
270K
150K
150K
150K
150K
150K
150K
150K
150K
100K
EHT
IN

Fig. II-17.

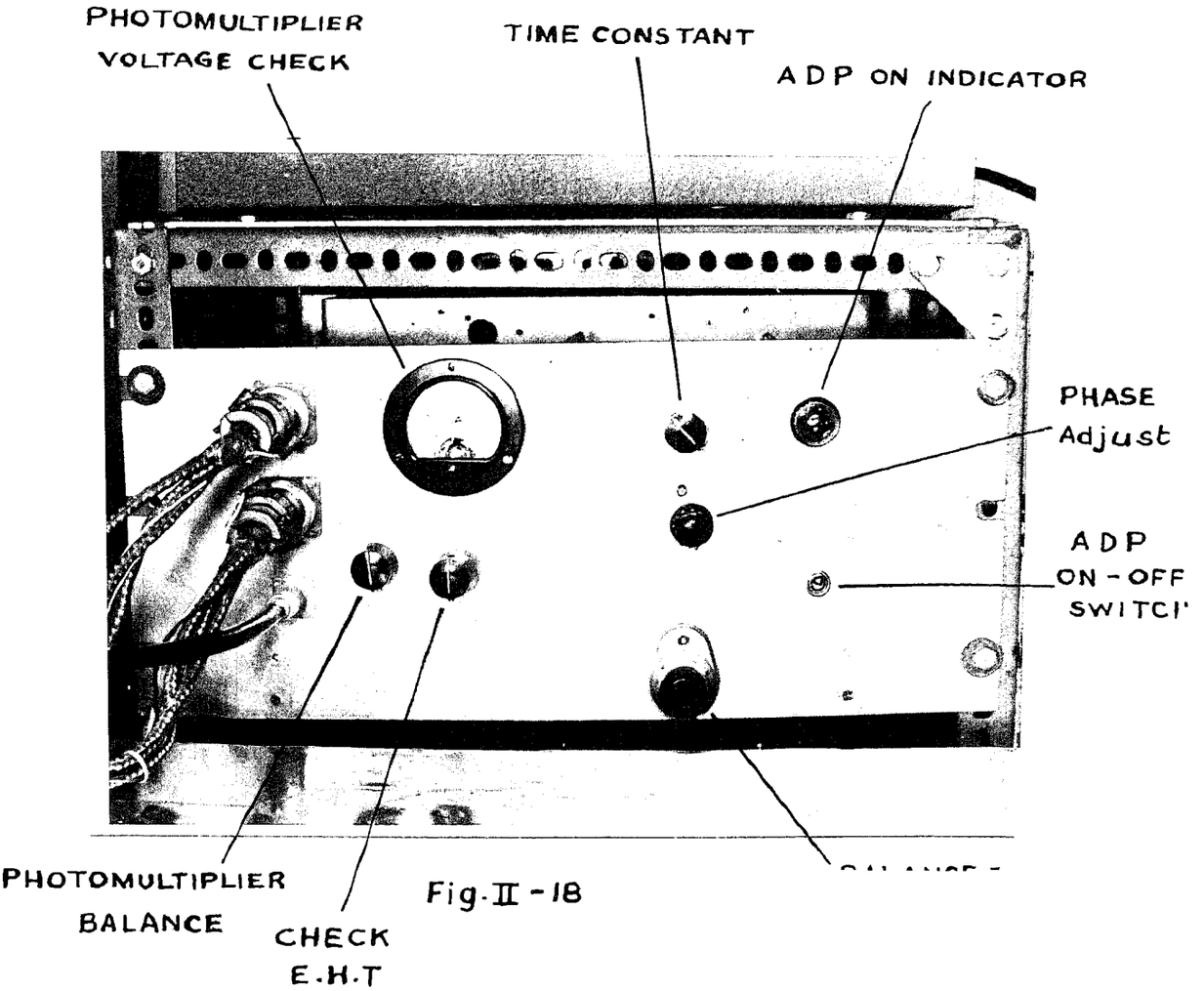
PHOTOMULTIPLIER
VOLTAGE CHECK
TIME CONSTANT
ADP ON INDICATOR
PHASE
Adjust
ADP
ON - OFF
SWITCH
PHOTOMULTIPLIER
BALANCE
CHECK
E.H.T

Fig. II - 18

made between the pairs, which may become necessary in course of aging of the two photomultipliers. A three way switch with a voltmeter enables the operator to check the voltages on the three photomultipliers independently. A circuit diagram of the E.H.T. distribution panel is shown in Figure II-17.

All the essential controls for operation of the equipment have been brought out to a front control panel. The individual controls include (1) the E.H.T. distribution check, (2) Photomultiplier balance potentiometer, (3) Synchronous detector zero adjustment potentiometer, (4) the R.C. time constant selector, (5) phase control of the synchronous detector and (6) the light modulator on-off switch and indicator. A photograph of the control panel is shown in Figure II-18.

A cathode ray oscilloscope with associated amplifiers capable of D.C amplification* has been included in the equipment to check several adjustments in the equipment. Besides the regular use as indicator in synchronous detector phasing and photomultiplier balancing, the oscilloscope is also used for initial signal tracing and in the calibration of the amplifier stages of the equipment.

---

* Dumong 304-A, D.C. Oscilloscope.

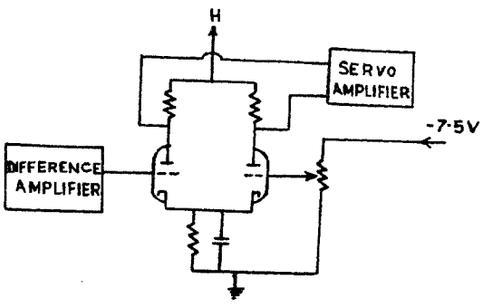
H
SERVO AMPLIFIER
-7·5V
DIFFERENCE AMPLIFIER

(a)

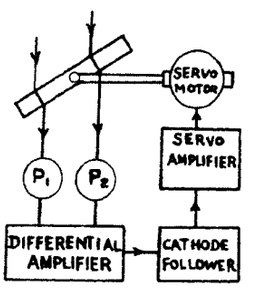
SERVO MOTOR
SERVO AMPLIFIER
P1
P2
DIFFERENTIAL AMPLIFIER
CATHODE FOLLOWER

(b)

Fig. II-19

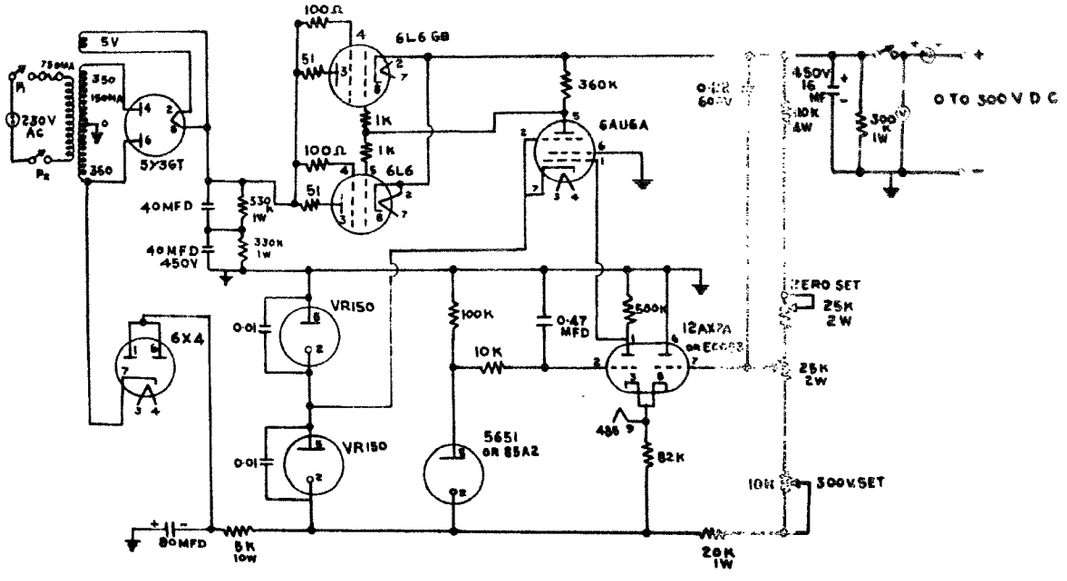
100Ω
6L6 GB
51
1K
360K
6AU6A
100Ω
1K
6L6
51
40MFD
330K 1W
40MFD 450V
330K 1W
5Y3GT
350
150MA
360
250V AC
P1
P2
5V
VR150
0.01
6X4
100K
10K
0.47 MFD
500K
12AX7A OR ECC83
5651 OR 85A2
VR150
0.01
486
82K
80MFD
5K 10W
20K 1W
450V 16 MFD
10K 2W
300V 1W
0 TO 300 V D C
ZERO SET
25K 2W
25K 2W
10K
300V SET

Fig. II-20.

During observations the oscilloscope is used in conjunction with a photoelectric guiding arrangement, as a two dimentional indicator to help extremely accurate guiding.

The automatic doppler compensator unit used in the equipment, consists mainly of a servo motor driving the parallel plate line shifter. The amplifier used is a commercial servo amplifier employed in Honewell continuous balance units in their strip chart recorders. The input is derived from the EPSCO differential amplifier described earlier, which delivers the amplified D.C difference voltage between the two photomultiplier P_1P_2 outputs. This is fed into the servo amplifier through a D.C. buffer amplifier stage. The output controls the two phase servo motor which in turn rotates the line shifter seeking null position. The arrangement is diagrammatically shown in Figures II-19(a) and II-19(b).

The power supply unit for operating the selective amplifier and cathode follower stages is a stabilised H.T. unit of conventional design. Figure II-20 shows the circuit diagram of this unit. To achieve further stability necessary for this equipment, a transistorised voltage stabiliser* employing saturable core action employed between the mains supply and the equipment.

---

*Ether transistorised voltage stabiliser Model LT-T-1000

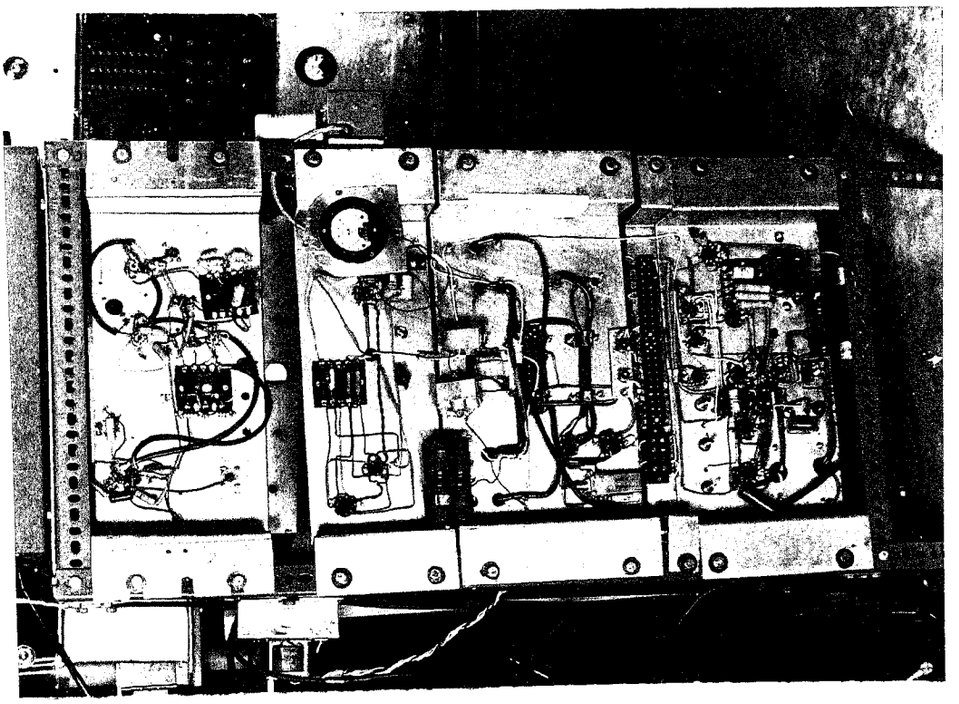

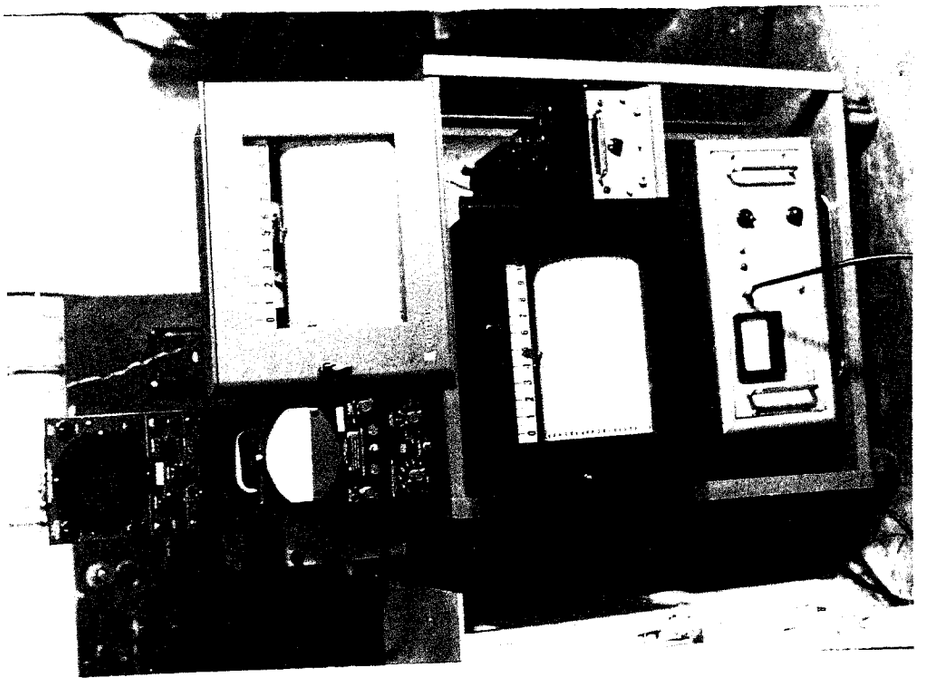

Fig. II-21

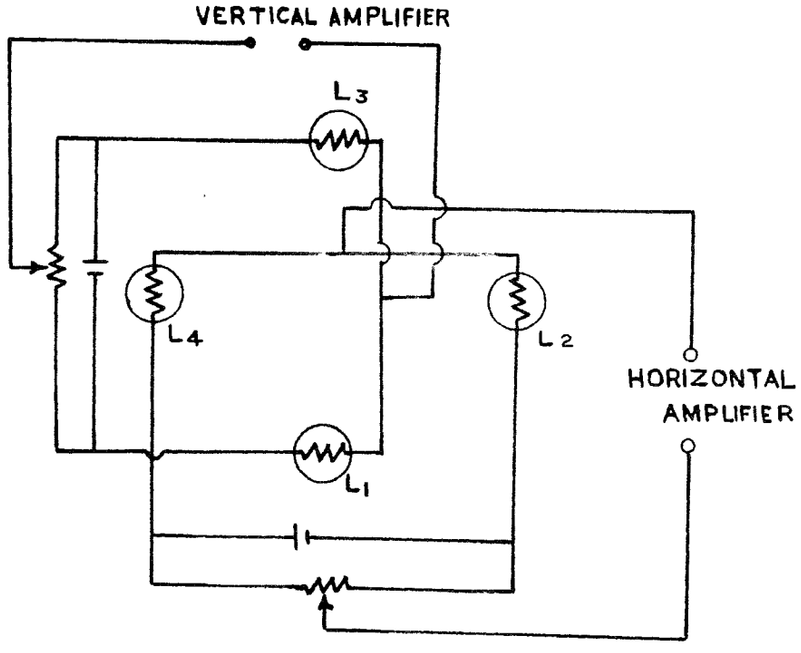

Fig. II-22.

For convenience of operation the electrical units have been mounted on two vertical frames with rack type assembly. To accommodate further in the limited space of the spectrograph room one of the rack assemblies has been mounted on movable trolley with casters. Figure II-21 shows a photograph of the electrical units.

For accurate guiding of the solar image, a photo-electric guiding unit has been employed during our observations. The property of the limb darkening gradient has been utilised for this purpose. As most of the observations were at the disc centre, the limb of the solar image was free for such usage. Four light dependent resistors Philips type LDR are mounted behind a screen in such positions as to receive light from two perpendicular pair of diametrically opposite points near the sun's limb. Each pair of LDRs is connected in a Wheatstone bridge arrangement as shown in Figure II-22. The unbalance voltages are fed into the vertical and horizontal amplifiers of the Dumont D.C oscilloscope which deflected the cathode ray spot on the screen according to the unbalance voltages in corresponding directions. Because of strong gradients of solar limb darkening, any small shift of the solar image resulted in appreciable unbalance voltage, which could be

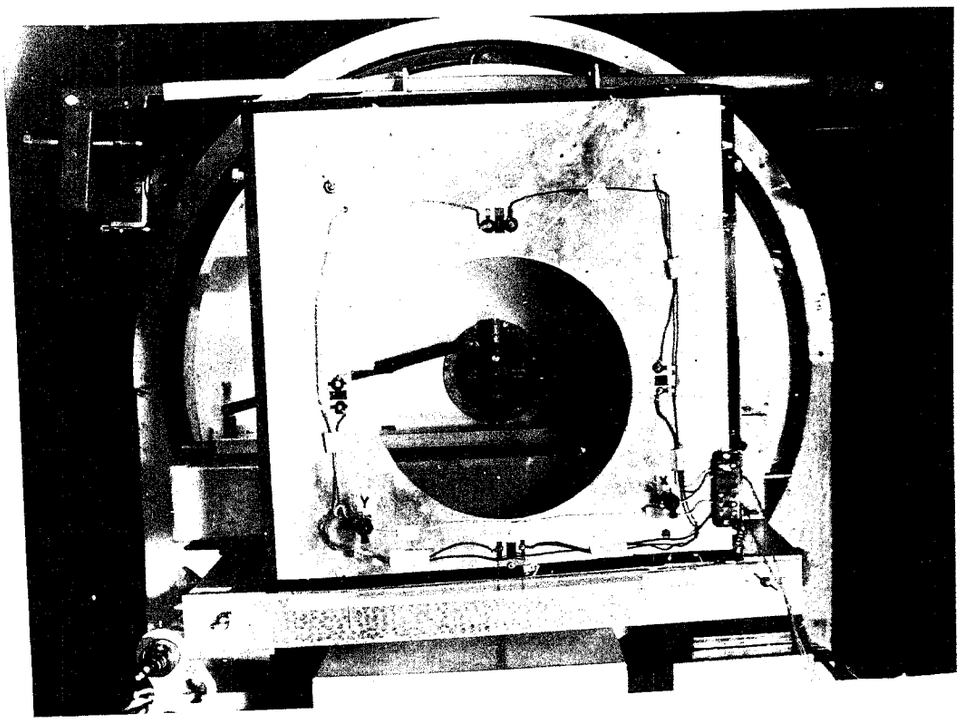

Fig. II-23

corrected by recentering the image by operating the guide buttons of the coelostat arrangement. A photograph of the photoelectric guiding frame is shown in Figure II-25. The frame is capable of movement in two perpendicular directions controlled by two fine precision screws. Two calibrated sensitive dial gauges were used to determine the movements of the frame during my observations.

2.4. Instrument Characteristics.

For proper evaluation of the readings obtained by the instrument described above, a thorough controlled calibration and checking of various key units as well as the instrument as a whole is essential. The method and results of such operations are now described in the successive paragraphs.

The gain frequency characteristics of the selective amplifier is a factor which determines the minimum signal detectable by the instrument. For the sake of proper maintenance of the instrument, it is preferable to have this checked periodically. Facilities are provided in the equipment for doing this. Output of a Laboratory standard oscillator is fed through a calibrated attenuator to the input of the selective

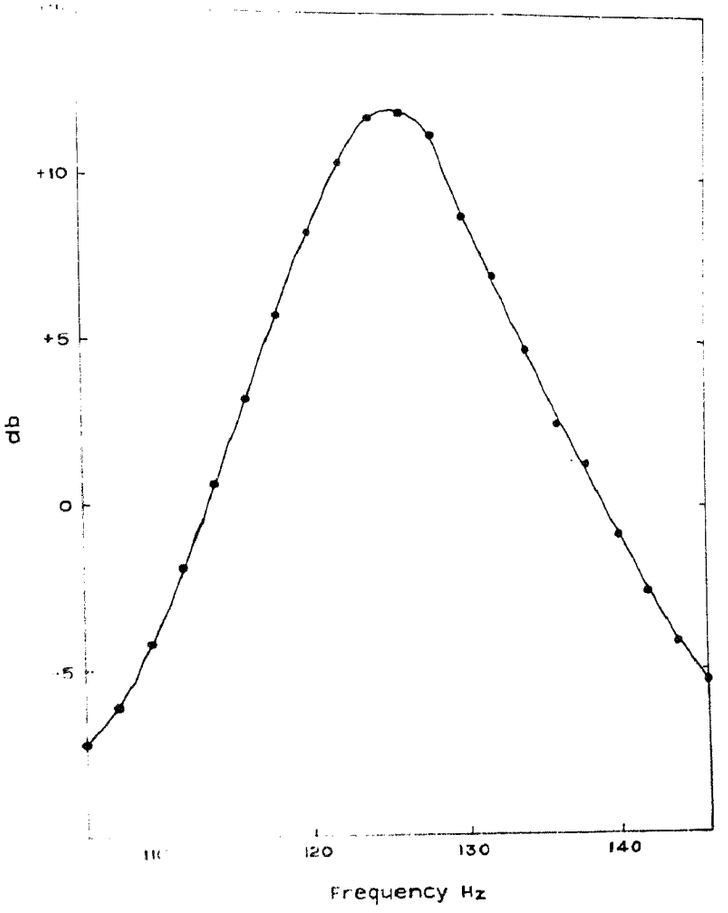

Fig. II - 24

Differential Amplifier
Gain setting: 1000

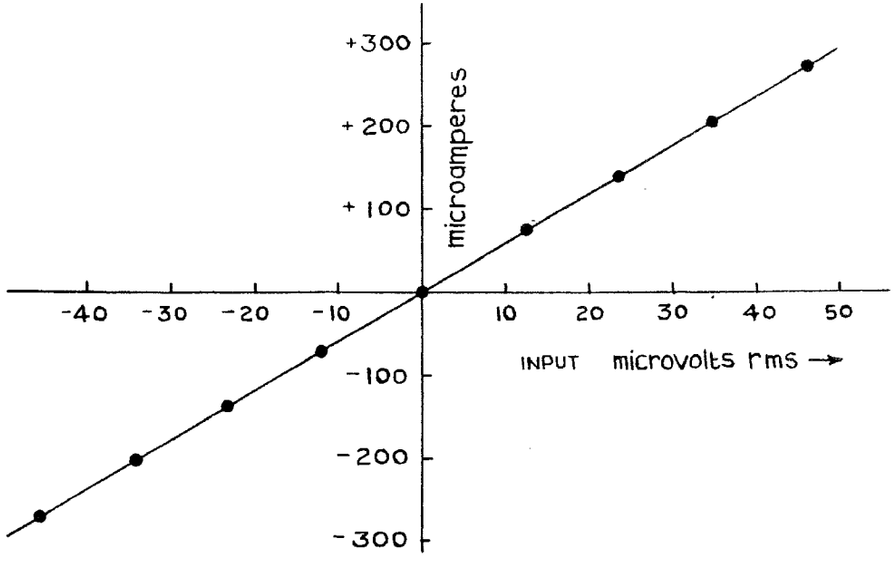

Fig. II-25

amplifier, the input from the differential amplifier being removed, and the output measured directly on the cathode ray oscilloscope screen. An alternate path bypassing the amplifier is made for measuring the input on the same scope. The output/input ratios are measured at frequencies around the operating frequency. Figure II-24 shows the gain-frequency characteristics of the selective amplifier used in our equipment.

The linearity characteristic of the entire amplifier-detector chain is extremely important, as variation in this may introduce large errors in our measurements. This is checked by the following arrangement. The input to the differential amplifier is removed and a small fraction of the generator voltage fed instead, through the calibrated attenuator. The output is directly measured on the recorder, taking care to keep the phase of the synchronous detector reference voltage properly adjusted. Measurements are done at various input levels, and the input vs output characteristics determined and compared with the original. Figure II-25 shows one such characteristic obtained from our equipment. Reversing the input connections enables us to obtain points on the negative side.

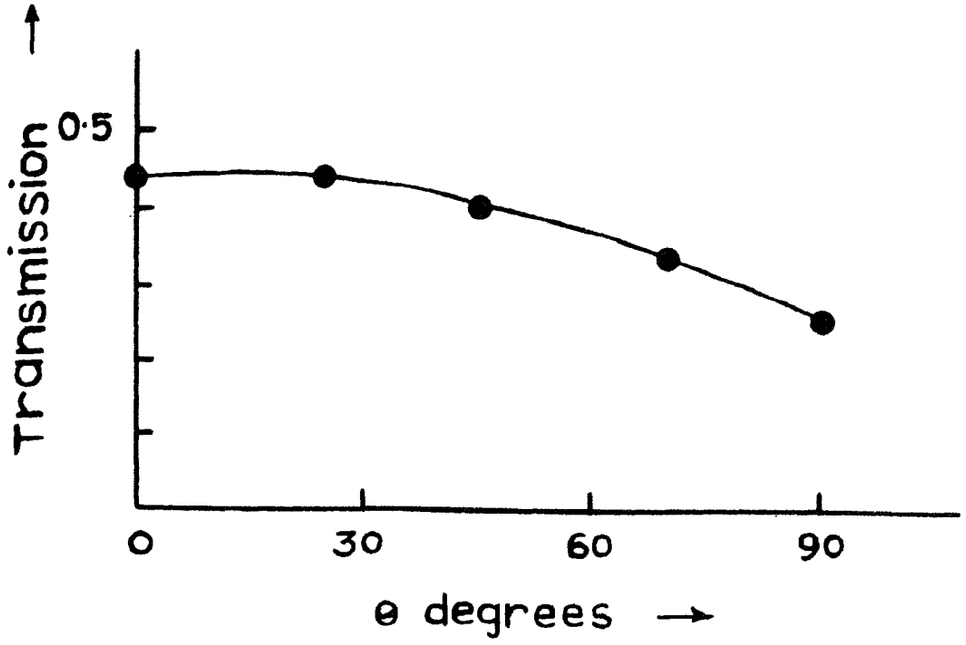

Fig. II -26

The light passing through the ADP-polaroid assembly is completely polarised and has large variation for different orientations of the grating ruling and photo cathodes. Since the orientation of the photomultiplier cathode is fixed with respect to the grating ruling, it is necessary to know the variations of the photoelectric output for different orientation of the ADP-polaroid assembly. This is easily done by noting the third photomultiplier response for different orientations of the assembly. Figure II-26 shows the transmission characteristic for the ADP-polaroid assembly in the green region. The maximum value of response, it may be seen, is only 0.44. Similar transmission characteristics for the fixed circular polarisers is also determined. When used as a circular polariser, the response do not vary with its orientation. Its transmission is found to be only 0.40 in unpolarised light.

For accurate measurements, it is essential that the linear drift of the output should be a minimum. From systematic studies, it has been seen that the equipment almost completely stabilises after half-an-hour's warm up time. During observations care is taken not to record data before such stabilisation is achieved.

Stabilisation of the photomultipliers, however, is much more difficult to obtain. There is a tendency of large differential drifts after EHT is switched on, which may require hours to come down to a reasonable value. To avoid such drifts the photomultiplier voltages are continuously kept on during the observing period lasting over days. The photomultiplier pair is balanced at the beginning of each observation by focussing a portion of continuum on the slit-pair, and the balance checked at the end of observation.

Adjustment of the reference voltage phase can be done without ambiguity by looking at the C.R.O. wave forms at the electromechanical chopper outputs. The phase once adjusted do not require frequent changes.

2.5. Calibration.

The checks described above are mainly necessary for optimum adjustment of the equipment, but an overall calibration is essential for every set of observations recorded with the equipment. In our equipment we have used the sun as the calibrating source. It is known that the axial rotation of the sun on its equator results in a linear velocity of 2 Km/sec. On the east limb this results in a blue-shift of the lines of equivalent amount

and on the west limb also of equal magnitude, but in opposite direction. If we correctly centre a line on our slit-pair, with the instrument working in the velocity mode, then the instrument output will be zero. Supposing that we have managed to do this, with the centre of the solar disc shining on the spectrograph slit, then on moving the sun so that a point on the east limb shines on the slit, some non-zero detector output will result. By moving similarly in the other direction, we shall get an output of equal magnitude but of opposite sense. On the recording chart the pen will deflect from one side to another for such movements and the difference between the two deflections will be equivalent to a Doppler shift of 2+2 = 4 Kms/sec., and this can be used as a standard, provided certain other factors are taken care of.

The first difficulty one encounters is the random shifts of the spectral lines, resulting in an unsteady output. The effect is most pronounced at the centre of the solar disc, but very much less at the limbs, at least for some lines. For such lines one can get a reasonably steady deflections for the two limb positions. For others it is necessary to take a large number of readings at the two positions to work out the mean values.

The fall in light intensity near the limbs also require correction. The electrical signal, as per equation (2.4) is proportional to the product of the Doppler shift and the mean intensity. To compensate for this variation, it is also necessary to know the proportionate reduction of intensity in the nearby continuum region at the calibration points on the East and West limb positions. For the sake of convenience of measurement, it is the line core intensity which had been measured at the two limbs, as well as at the observation point. The centre to limb variation of the core-intensities of these lines have been neglected for this purpose.

With the above two corrections, it is possible to determine the scale co-efficient of the instrument for any particular line. The deflection obtained d in our instrument can be given by:

$$d = K v I \qquad (2.5)$$

where v is the line of sight velocity in metres/sec. and I the intensity of the adjacent continuum as measured from the photomultiplier output and K the instrument constant working under certain conditions. Suppose further that D is the difference of the two

deflections at the calibration points (which are taken close to the limb on the solar equator) whose theoretical Doppler velocities differ by M metres/sec. (which is very close to 4000 metres/sec), and I_L is the mean intensity of the adjacent continuum at those points, then

$$D = K M I_L \qquad (2.6)$$

by the same reasoning.

Eliminating K between equations (2.5) and (2,6)

$$v = M \frac{I_L}{I} \frac{d}{D} \text{ metre/sec} \qquad (2.7)$$

In the magnetic mode an additional factor need be taken into account while using the sun as the calibration source. Here, also the well known Doppler shifts of the line in question is measured. The line used in our magnetic scans is the FeI line of λ = 5250.218A with a Lande factor of 3. Substituting these values in equation (2.1), the separation of the two longitudinal Zeeman components become

$$\Delta\lambda_H = 2\left[4.67 \cdot 10^{-5} g \lambda^2 H\right] \qquad (2.8)$$

$$= 7.72 \cdot 10^{-5} H$$

$[\Delta\lambda_H$ in Å, H in gauss$]$

The Doppler shift of the same line is related to the line of sight velocity by the relation:

$$\Delta\lambda_v = \frac{\lambda}{c} \cdot v = 1.75 \cdot 10^{-5} v \quad [\Delta\lambda_v \text{ in } \text{Å}] \tag{2.9}$$

where v is expressed in metres/sec. So, other things remaining equal, the equivalence between the Doppler and longitudinal magnetic shifts is given by

$$1.75 \cdot 10^{-5} v = 7.72 \cdot 10^{-5} H$$

$$\text{or,} \quad H = 0.225 v \tag{2.10}$$

But as we have to introduce a fixed circular polariser in front of the electro-optic modulator, the light transmitted in the Doppler mode is usually a fraction of that in the magnetic mode. The transmission loss of our fixed circular polariser is determined separately as described in Section 2.4. If we designate this fraction by p, the final relation between the two quantities will be given by

$$H = 0.225 \text{ p.v.} \tag{2.11}$$

H being given in gauss when v is in metres/sec.

It may be mentioned that the value of this fraction p as measured in our arrangement is highly dependent on the relative orientation of the two polaroid axes. To avoid any error due to this, the value of the transmission is determined separately for every magnetic record by noting the third photomultiplier readings with and without the circular polariser in actual orientations of the two elements in the optical modulator.

2.6. Accuracy and Limitations.

The noise introduced by our amplifier-detector chain is extremely small, by proper choice of tubes and voltage feeding network, the two photomultipliers also introduce very little dark noise, the individual dark currents at the operating voltage of 900V being about 2×10^{-9}A. But it is the random nature of the photo-electron cascades which limits the ultimate accuracy of our whole measurements. The scale of the solar image in our optical set up is 5".6 per mm. and a standard spectrograph slit of width of 250μ and length 1mm has been used throughout our measurements, except in a few special programmes where the variation is specifically stated. The angular dimensions of the solar disc covered by the slit is thus 1".4 x 5".6. At the detector head slit pair, the spectrum is re-imaged without magnification

and to quote a typical dimension, the wing photomultipliers view a portion of spectrum 1 mm x 350 μ each. In the fifth order where it is mostly used, the dispersion is extremely high and the level of illumination at the photomultiplier cathodes is low indeed. In the Doppler mode with the fixed circular polariser introduced in the beam a typical order of photo-current generated in each photomultiplier is of the order of 10^{-8}A. At this level of illumination the random nature of the photoelectron pulses dictates the limits of gain and resolution that can be achieved in our set up.

To improve the signal to dark noise ratio for low light levels a scheme of acceleration field gradients inside the photomultipliers has been used. Following suggestions by Dr. Baum of Lowell Observatory, the voltage between the cathode and the first dynode has been made double the normal stage voltage, and that between the ninth dynode to the anode, kept at 60% of the stage voltage. The arrangement is common among astronomers doing faint star photometry, and it is believed that this has also improved the performance of our equipment, enabling us to reduce the slit size to low values.

A good spatial resolution, which is a major objective of our experiments is thus limited by the

availability of light flux. In the f/90 system used by us, the standard slit size of 1".4 x 5".6 has been chosen after several months' observations, as the optimum dimensions that can be used in our set up. Longer slits have been used at the cost of spatial resolution, only when the weakness of the signals compelled us to adopt such a procedure.

Another limiting factor encountered by us is the seeing at the observation site. Owing to its location on a high peak surrounded by uneven terrain, the period of good seeing at Kodaikanal is limited to only an hour or so after sunrise. For long continuous records, observation had to be carried through periods when the seeing was no better than 2-3 seconds of arc. Lowering the slit dimensions under such conditions was obviously useless.

For experiments requiring scanning over an extended area, the rate of scan was chosen to be in conformity with the time constant of the detector. Higher time constants had to be used with higher gains which were necessary for weaker signals, thus requiring longer times for such scans. The spatial nature of certain time varying features of weak intensity could thus be studied with only limited accuracies.

CHAPTER III

SOME CHARACTERISTICS OF THE BURSTS OF THE QUASI-PERIODIC OSCILLATIONS

3.1. Quasi-Periodic Oscillations.

The quasi-periodic oscillations of solar photospheric layers were observed and their characteristics studied from photographic records of spectra and spectroheliograms by Leighton et al (1962), Evans et al (1962) and others. Photoelectric methods were first employed by Howard (1962), when he observed oscillatory motions of the photospheric cells by the Mount Wilson solar magnetograph in the Doppler mode. Orrall (1964), Frazier (1968) as well as the groups already mentioned made further studies in the oscillatory nature of solar velocity fields. The existence of such oscillations were expected from the theoretical standpoint by several authors before Leighton's discovery, who had invoked the theories of vertical acoustic waves and horizontal gravity waves from thermodynamical properties of the solar atmosphere Biermann (1947), Schwarzschild (1948), Whitney (1958). The data obtained thus far, however, do not completely reveal the actual nature of these oscillations. Because

of the small sizes and complex nature of these oscillating elements, the actual observations have to be limited to periods of best seeing conditions when fluctuations introduced by the observing conditions are least. Also considering the possibility that the nature of these oscillations may vary significantly over the depth of the solar atmosphere and with varying magnetic conditions, the bulk of observational data collected on various spectral lines at different positions on the solar disc is quite inadequate for a complete understanding of the oscillation mechanism. Current investigations on this subject are being conducted at various observatories and are aimed at obtaining more detailed data. These coupled with improved methods of statistical analysis will certainly bring out most of the information contained therein.

The main features of the oscillation phenomena known to date are briefly summarised below:

i) The oscillatory motions are confined to small cells of dimensions of the order of six to seven seconds of arc, and are possibly directly connected to the granular structure seen in white light photographs under the best seeing conditions.

ii) The mean period observed is about 300 seconds and is believed to be dependent on the mean photospheric height at which the observations are recorded.

iii) The oscillations occur in discrete bursts, interspersed with periods of relative quietness. Even during the burst, the oscillations are not of homogenous nature, random changes of phase being frequently noticed. It is believed that the mean duration of an unambiguous oscillation is not more than one or two cycles.

iv) The maximum amplitudes of the line-of-sight velocities are of the order of a fraction of a km/sec. and are predominantly radial.

v) The amplitude of oscillation gets reduced in the presence of strong magnetic fields.

The techniques employed so far can be broadly classified into three types:

i) Rapid-time-sequence photography of selected spectral lines over a fixed area on the solar disc.

ii) Time-sequence of Doppler spectroheliograms by Leighton's technique, and

iii) Continuous velocity records over a guided small region on the solar disc by photoelectric techniques.

The relative advantages and disadvantages of the three techniques are discussed below:

In the rapid-time-sequence photography of selected spectral lines employed by Evans and his co-workers, minute Doppler shifts of small areas along a narrow rectangular aperture on the solar disc are obtained every few seconds. The method gives the spatial variation of the velocity field in one dimension together with the information about the relative phases of the oscillation in different cells. The spatial resolution is limited by the photographic graininess and the atmospheric seeing, when used with narrow slits in high resolution high dispersion spectrographs. Time resolution is dependent on the exposure time required and the rapidity with which the successive frames can be exposed. Reduction process is laborious, which has to be overcome by special measuring equipment. Data obtained are not continuous in time but discrete, spaced by the time delays between exposures and integrated over the exposure time.

Basic spatial accuracy in Leighton's Doppler spectroheliographic technique is comparable to that above; the added advantage being the unfolding of the two dimensional aspect of cellular structure of the oscillation

field. Time resolution is poorer because of longer interval necessarily introduced between successive exposures of the same region of the solar disc. The technique is very good for study of large cellular structures, but definitely poor for detailed time study of oscillations at a single location on the solar surface.

In the photoelectric technique the main method is to use a Babcock-type magnetograph in the Doppler mode. In this way continuous records of oscillatory nature of individual cells can be obtained. The spatial resolution is limited by the size of the aperture used, and is poorer compared to those obtained by the other two methods. But this disadvantage is more than off-set by the technique's capability of bringing out fine features of the oscillation. The time resolution is in fact limited by the noise introduced in the photomultiplier tubes which are subsequently much reduced by narrow band selective amplifiers, and by the noise introduced due to atmospheric seeing. The sensitivity of this method is the highest of the three, and much longer records can be obtained by this technique, because of less stringent demands on the seeing quality.

The major observations reported so far are tabulated below:

Table 3.1

Year	Investigator	Spectral lines used	Technique.
1961	Leighton et al	FeI 6102 CaI 6103 NaI 5896	Doppler spectro-heliograph.
1961	Evans et al	TiI 5173 MgI 5172, 5183 FeI 5171, 5187, 5170 FeI 8514 CaII 8498 CaII 8542	Rapid-sequence Spectra
1962	Howard	FeI 5250	Doppler Magnetograph
1962	Evans and Michard	FeI 5171 MgI 5172 TiI 5173 FeI 5324	
1963	Evans, Michard and Servajean	TiI 5173 MgI 5172 FeI 5171 FeI 8514 CaII 8498 CaII 8542	
1964	Orrall	FeI 3931	Rapid-Sequence Spectra
1967	Howard	FeI 5250 CrI 5247	Doppler Magnetograph
1968	Frazier	FeI 6355 FeI 6364 SiII 6371	Rapid-Sequence Spectra

3.2. Details of Observation.

My study of the temporal variation of the Doppler velocities follows the photoelectric technique. The Kodaikanal magnetometer has been operated in the Doppler mode by placing a fixed circular polariser in front of the ADP as described in Chapter II. A small area measuring 5".6 x 1".4 at the centre of the solar disc has been observed continuously by this arrangement. One of the aims of this observation was to have as long as continuous record of velocity at a certain location as possible and the records were terminated only when the seeing became poor. Spectral lines have been chosen so as to represent various depths in the solar atmosphere. The table below lists the details of the various observations obtained.

Table 3.2

Height Km.	Line	Equivalent width mÅ	Excitation potential of lower level.	Length of record
-140	C_2 5094.026	8.5	-	$3^h\ 28^m$
-	NiI 5094.418	25	3.83	$2^h\ 47^m$
-	FeI 5072.677	60	4.22	$4^h\ 05^m$
-	TiI 5210.392	86	0.05	$3^h\ 30^m$
610	MgI 5172.698	1259	2.71	$2^h\ 47^m$
580	BaII 4554.036	159	0.00	$3^h\ 03^m$
620	NaI 5889.973	752	0.00	$1^h\ 57^m$
2220	H 4861.342	3680	10.20	$3^h\ 30^m$

In choosing these lines my aim was to have oscillation records at various heights of the solar atmosphere. The height of the chromospheric lines were roughly assessed from the detailed observations of flash spectra taken during the 1962 solar eclipse by Dunn et al (1968) of the Sacramento Peak Observatory group. The height at which the observed intensity falls to $1/\epsilon$ of the value just outside limb has been taken as the mean height of formation of the line. The line C_2 5094 was selected because detailed depth calculations of this molecular line by Subrahmaniam (1965) ar e available and it is possible to tie up the relative levels of other lines with respect to this one originating in the shallow low temperature level at the photosphere-chromosphere interface. However, owing to the extreme shallow depth of this line, the signal was very low during observations, and the highest gain in the amplifiers had to be used, which resulted in rather noisy outputs. The heights of the three photospheric lines cannot be properly determined by this technique, for which detailed contribution function calculations are necessary. For the purpose of my studies, they have been grouped together below the molecular carbon line, and the mean properties of the oscillations noticed in these lines have been used for comparative studies.

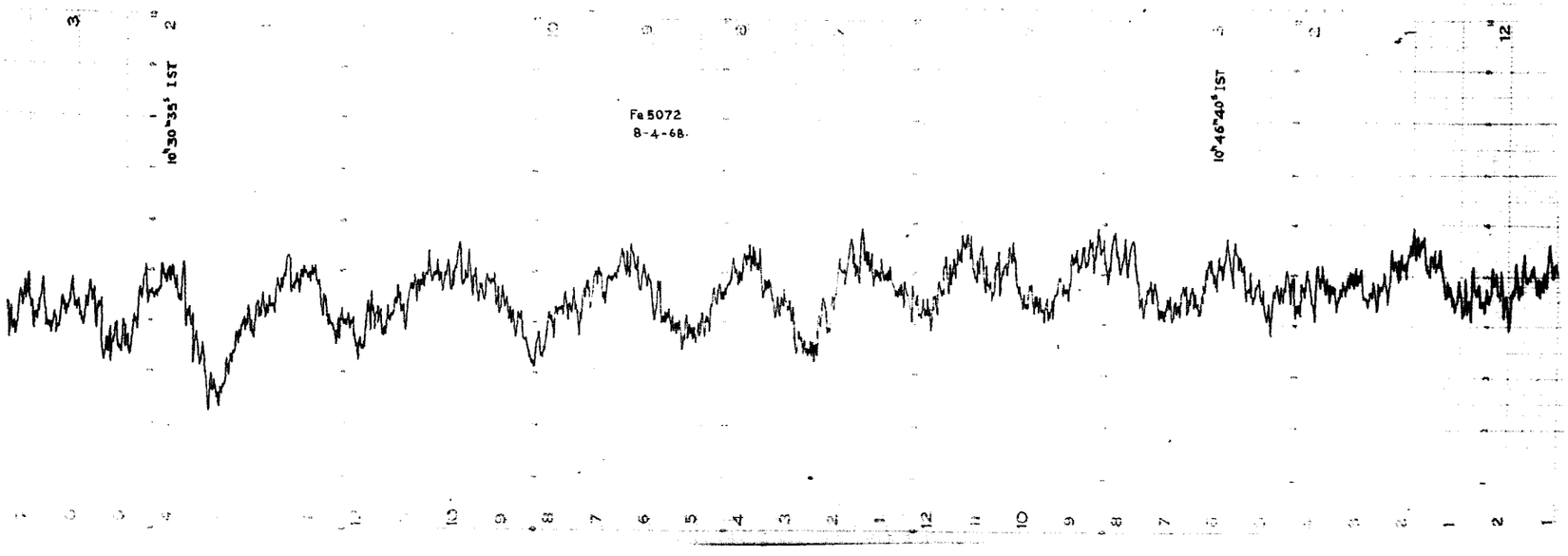

Fig. III-1

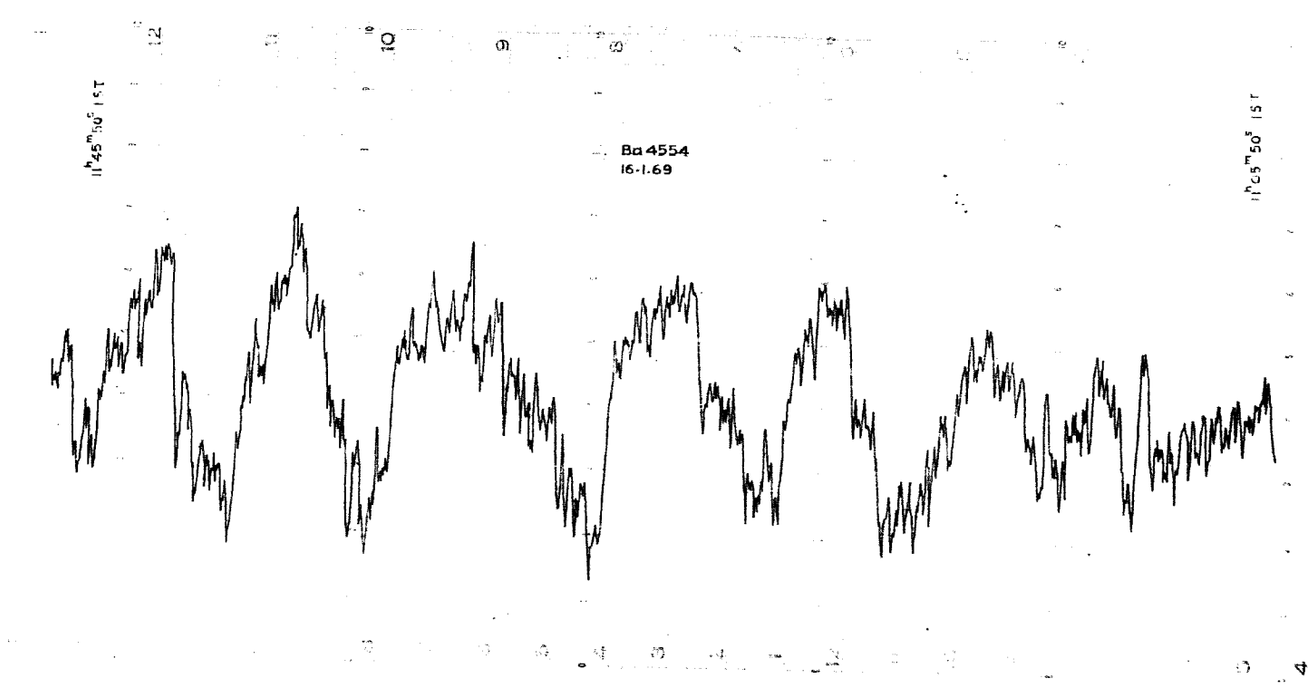

Fig. III-2

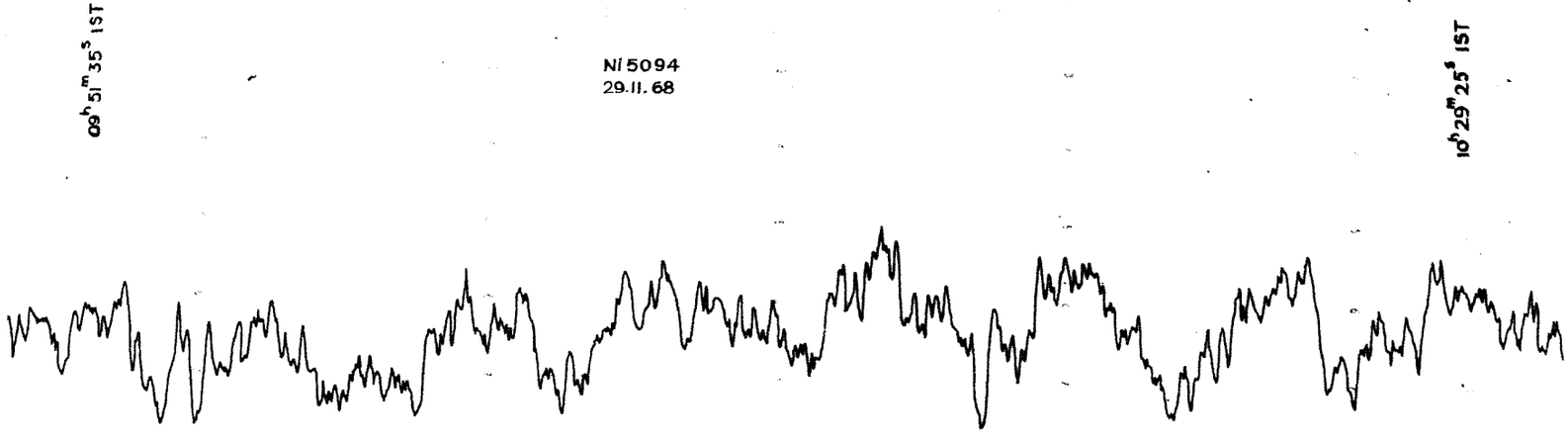

Fig. III - 3

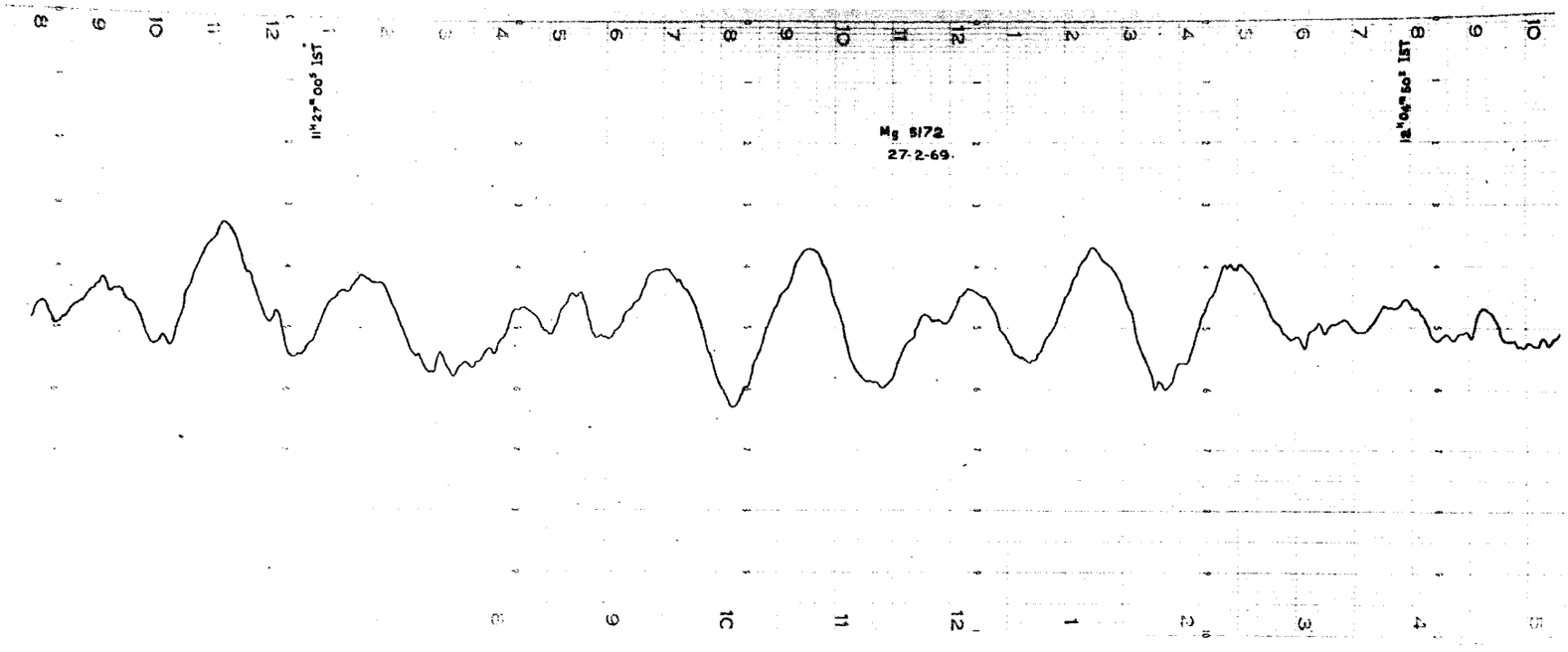

Fig. III-4

The slits were located at the steepest part of the line profile to ensure maximum sensitivity. The length of record indicated in column 5 is the maximum stretch of continuous observations at a single location, guided photoelectrically. To allow for solar rotation over this interval, the guiding frame was adjusted by precalculated discrete minute steps throughout the observation. Parts of a few typical velocity records are shown in Figures III-1 through III-4.

The analog quantity recorded in the strip chart recorder is the electrical output of the solar magnetograph in the Doppler mode and a few mathematical operations are necessary to convert these into velocity values. Every record is preceded and concluded by two sets of calibration records, from which the mean calibration co-efficients are first calculated as described in Chapter II. The chart readings have then been measured at regular small intervals together with the intensity readings at corresponding points. The mean of the readings of the first half hour are worked out and this is taken as the initial zero line for further calculations. Since the records extended over long periods it was also necessary to adjust the zero line for Doppler shifts due to the

earth's diurnal rotation. This has been done by calculating the relative line of sight velocities of the sun from any point of the terrestrial globe by the equation:

$$v = -0.465 \sin t \cos \delta \cos \lambda$$

where t is the hour angle of the sun, δ its declination and λ the latitude of the observing station, which in our case is $+10^{\circ}\ 14'$. The values were calculated for every fifteen minutes for the period of these observations. These velocity values have then been converted into equivalent chart deflections by using appropriate calibration factors and the initial zero line readjusted after accounting for these changes every fifteen minutes. The corrected zero line thus has a continuous drift over the observation period very nearly following a cosine function. This is drawn on the chart and the chart deflections at close intervals determined from the zero line. These are then converted into velocity values by using appropriate calibration factors. Since the drift of the final D.C cathode follower of our instrument has been found to be negligible, the velocity series is virtually free from any artificial long period drifts. The corrected velocity-time curves also generally confirm this. In some of the records, mean value changes over extended periods have been noticed, which must be taken as real.

PERCENTAGE DISTRIBUTION OF PERIODS

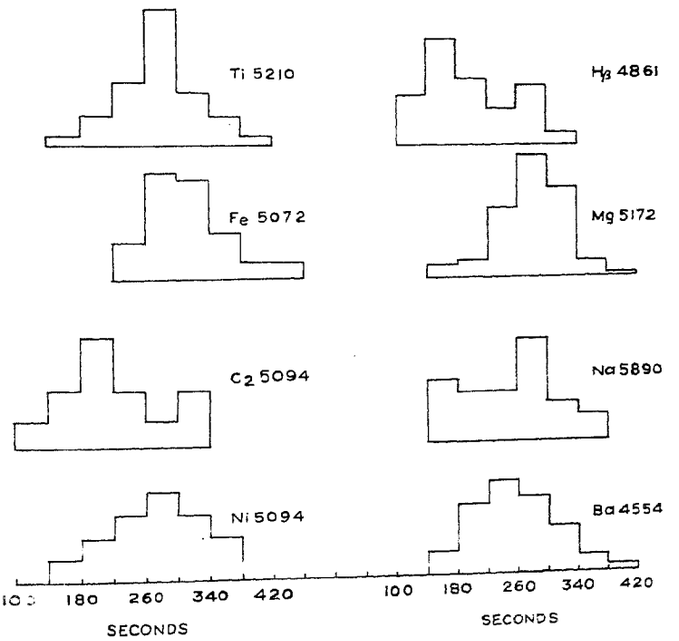

Fig. III-5

Fig. III-6

3.3. Nature of Oscillations.

In the records the oscillations stand out quite clearly against the noise background and this prompted me to have a preliminary survey of the regularity or otherwise of the oscillations. The lengths of individual cycles have been picked up from the velocity records and the data arranged in the forms of histograms. The results indicate quite a lot of scatter around mean values. Figures III-5 and 6 shows the histograms arranged separately for photospheric lines (Ti 5210, Ni 5094, C_2 5094, Fe 5072) and chromospheric lines Ba 4554, Mg 5172, Na 5890 and H_β . Ba 4554 is bound to have a very appreciable chromospheric contribution and hence is being treated herein along with other chromospheric lines. If we neglect the observations on C_2 5094, since the record is excessively noisy, it is seen that the predominant period in the photosphere is one in the 260-300 seconds range. In the chromosphere the period is not so consistent, and about the height of H_β a second peak of lower period appears to be more frequent. These histograms, however, do not indicate relative strengths of these oscillations for which detailed statistical analysis for estimation of power spectra is necessary. These have been done and the results are discussed later in this chapter.

From Figures III-5 and 6, one important information about these oscillations is apparent. The scatter of the periods around the mean values are apparently of gaussian type, indicating the random nature of the agencies affecting the oscillating medium. This point appears to be in variance with the observation of Frazier (1968) who feels that a steady state reasonance was shown in the records obtained by him. Generally it is believed that these oscillations are essentially a transient response to individual granular disturbances. In such a case the phases of these oscillations will shift in a random nature. This will also result in random changes of periods as reckoned from the individual peaks as in the present case. This is exactly what is being exhibited by the histograms. The histograms, however, do not disprove or contradict Frazier's "steady state resonance" in the vertical oscillations, but as found from the detailed power spectra analysis from our records, the corresponding amplitudes must be negligible. This has been discussed later.

3.4. Bursts of Oscillations.

The oscillations are seen to occur in definite bursts lasting for 5 minutes to an hour in different lines. The mean duration of bursts are seen to be longer in the lines originating low in the solar atmosphere compared to

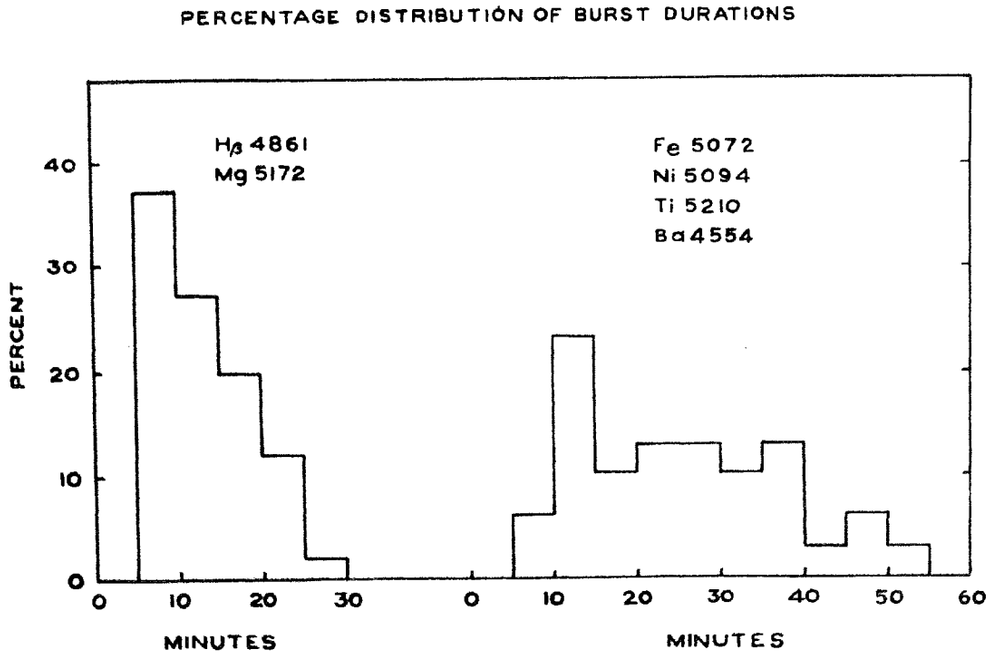
PERCENTAGE DISTRIBUTION OF BURST DURATIONS
Hβ 4861
Mg 5172
Fe 5072
Ni 5094
Ti 5210
Ba 4554
PERCENT
0
10
20
30
40
MINUTES
0
10
20
30
40
50
60
MINUTES

Fig. III - 7

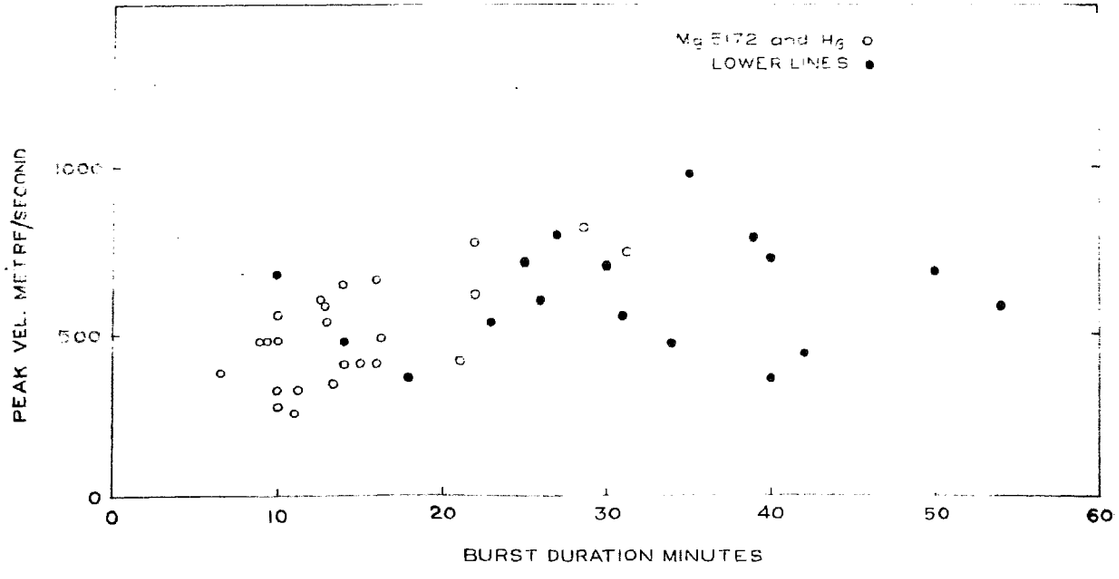
Mg 5172 and Hg o
LOWER LINES •
PEAK VEL. METRE/SECOND
1000
500
0
0
10
20
30
40
50
60
BURST DURATION MINUTES

Fig. III - 8

those observed in the higher lines. Figure III-7 shows the distribution of the durations of various bursts noticed during my observations. The mean duration of bursts noticed in Mg 5172 and H_β , is 14.2 minutes whereas these recorded in Ti 5210, Ni 5094, Fe 5072 and Ba 4554 lines is 31.4 minutes. The peak velocity amplitude attained during a burst appeared to be higher for longer bursts; this is seen to be the case for the lines of MgI 5172 and H_β 4861. The other lines do not appear to exhibit this correlation. It is possible that the very long bursts noticed in the photospheric lines may be composed of more than one burst occurring close to each other. This may occur if we consider that the damping in the lower layers is comparatively small, so that the oscillation stays for a longer period. Or, perhaps, the physical conditions in the lower layers are such as to respond to granular disturbances more easily. But whatever be the prevalent mechanism, much longer intervals exhibiting clear oscillations were noticed in these photospheric lines than in MgI 5172 and H_β . Figure III-8 shows a scatter diagram of the burst amplitude against burst duration, which illustrates this point.

During the burst periods the medium shows definite oscillatory mass motions, the nature of the oscillations,

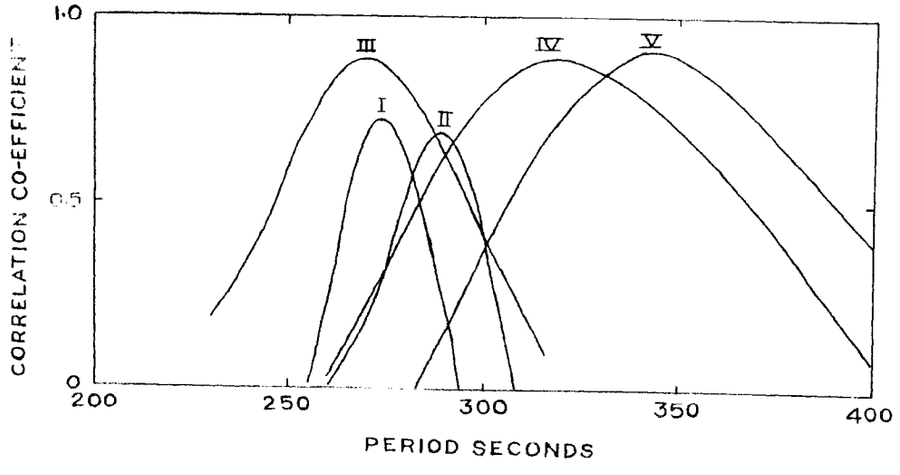
1.0
0.5
0
CORRELATION CO-EFFICIENT
200
250
300
350
400
PERIOD SECONDS
I
II
III
IV
V

Fig. III - 9

however, is quite complex. On close scrutiny, sudden changes in the phase of oscillations appear quite frequently, thereby changing the apparent period of the oscillations. The scatter noticed in the period histograms described earlier must be mainly caused by this effect. Because of the random nature of these phase changes, the characteristics of these bursts appeared to have little in common.

To establish this point on a more definite basis, I have tried a statistical test on the variations bursts recorded during my observations. The idea is briefly stated below: If the bursts are resonant oscillations built up in the medium by external impulses followed by a decay due to damping, then it should correlate well with a sinusoidal function of appropriate period and phase. The proper period and phase can be found out with a series of trials. For the same spectral line the periods at which maximum correlation occur should be consistently close together. On the other hand the existence of random phase changes will shift the correlation peak at random for different bursts and even in two parts of the same burst. A computer programme to work this out was written up and the burst characteristics checked on the CDC 3600 computer of the Tata Institute of Fundamental Research. Figure III-9

shows a few typical plots of correlation co-efficients against periods of the theoretical sinusoidal series for a few bursts noticed in the observations in the line of MgI 5172. The peaks indicate a statistical estimation of the periods of oscillation during a burst, assuming sinusoidal nature of variation of velocities. No consistent correlation peaks were noticed for any two bursts on the same spectral line which confirmed the assumption about the random phase changes during the burst.

Table 3.3 shows these correlation estimates of the periods of several bursts tested by this method. The consistency in the period is apparently lacking completely, pointing to the possibility of severe random disturbances during these bursts.

Table 3.3

Line	burst No.	Correlation Period (Seconds)
Mg 5172	1	274
	2	288
	3	270
	4	318
	5	343
Ba 4554	1	293
	2	354
	3	317
	4	354
Na 5890	1	307
	2	265
Ti 5210	1	285
	2	280
	3	318
	4	273
H 4861	1	283
	2	190
	3	185

3.5. Autocorrelation and Power Spectra analysis.

For more reliable determination of predominant periods and the amplitudes of these velocity oscillations, the autocorrelation and power spectra analysis of these velocity records have been done by me. The theory, scope and limitations of the method have been discussed in detail by several authors (Blackman and Tukey, 1958, Goodman 1957). I shall briefly outline the procedure followed by me.

If we have a continuous record of finite length T of velocity of an element on the solar disc represented by v(t), the autocovariance function for a lag τ is defined by:

$$C(\tau) = \lim_{T\to\infty} \frac{1}{T} \int_{-T/2}^{+T/2} v(t)\, v(t+\tau)\, dt \qquad (3.1)$$

and the power spectral density at frequency f,

$$P(f) = \int_{-\infty}^{+\infty} C(\tau)\, \epsilon^{-i 2\pi f \tau}\, d\tau \qquad (3.2)$$

The relation between these two formations may be expressed more simply as a one sided cosine transform, i.e.

$$P(f) = 2 \int_{0}^{\infty} C(\tau) \cos 2\pi f \tau\, d\tau \qquad (3.3)$$

Both the functions can thus be estimated from a long continuous record. The mean amplitude of the stationary oscillatory component of frequency f contributing to the spectral density P(f), can be estimated noting that P(f) in the positive frequency interval contains only half of the total power or variance (Blackman and Tukey, 1958). If A(f) denotes the amplitude of the oscillatory component at frequency f, then

$$2P(f) = \frac{A^2(f)}{2}$$

$$\text{or} \quad A(f) = 2\sqrt{P(f)} \qquad (3.4)$$

For convenience of computation, discrete values of the velocity at close intervals are used, instead of the continuous records. If v_1, v_2, ... v_n are the values picked up at uniform small intervals, the autocovariance function C_r can be given by

$$C_r = \frac{1}{n-r} \sum_{1}^{n-r} v_i \, v_{i+r} - \left[\frac{1}{n}\sum_{1}^{n} v_i\right]^2 \qquad (3.5)$$

The stability of the estimate is a function of r/n, getting progressively poorer as r approaches n. Therefore, in practice the maximum value of r has been kept at a small fraction of n. Denoting this maximum value by m, the series of autocovariances, C_1, C_2 .... C_m are

calculated. Using these values, the finite cosine series transforms are then calculated, the general term of which being:

$$V_r = C_0 + 2 \sum_{q=1}^{q=m-1} C_q \cos \frac{qr\pi}{m} + C_m \cos r\pi \qquad (3.6)$$

actually gives an unsmoothed spectral estimate for a frequency of r/2m cycle per observation. Smoothing is next done by the application of a correction for a suitable lag window. In my analyses, I have used "hanning window", which modifies the spectral estimates according to the following set of equations:

$$\begin{aligned} U_0 &= 0.5\, V_0 + 0.5\, V_1 \\ U_r &= 0.25\, V_{r-1} + 0.5\, V_r + 0.25\, V_{r+1} \qquad (3.7) \\ U_m &= 0.5\, V_{m-1} + 0.5\, V_m \end{aligned}$$

The limits of confidence for these estimates is best determined by treating them as if they follow the χ^2 distribution, with K-degrees of freedom. Detailed tables showing the behaviour of this variate with various degrees of freedom are available. The co-efficient of variation of χ_K^2, i.e., the ratio of r.m.s. deviation to average value, is $(2/K)^{\frac{1}{2}}$, so that as K increases χ_K^2

becomes less variable. It is only necessary to estimate the value of K, the equivalent number of degrees of freedom, to determine the confidence interval for any estimate.

Exact values of K are somewhat dependent on the nature of spectra and the type of lag window used. An approximate relation useful for this estimation is given, however, by

$$K = \frac{2n'}{m} \qquad .. \quad (3.8)$$

where n' the effective length of record is approximately,

$$n' = n - \frac{m}{3} \qquad .. \quad (3.9)$$

For broken records, the number of independent pieces, p, must be taken into account, so that the effective length of records is given by,

$$n' = n - \frac{pm}{3} \qquad .. \quad (3.10)$$

Since the value of K is by definition given by twice the ratio of average value of P(f) squared to the variance of P(f) itself, the r.m.s. deviation of the estimates is $\sqrt{\frac{2}{K}}$ times the average value. The value of the r.m.s. deviation for some of our estimates is calculated this way.

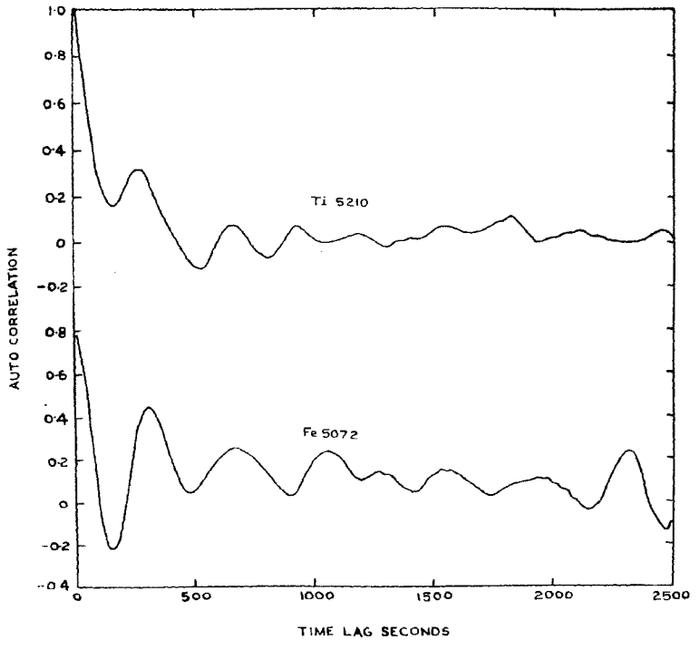
1·0
0·8
0·6
0·4
0·2
0
-0·2
0·8
0·6
0·4
0·2
0
-0·2
-0·4
AUTO CORRELATION
Ti 5210
Fe 5072
0
500
1000
1500
2000
2500
TIME LAG SECONDS

Fig III-10

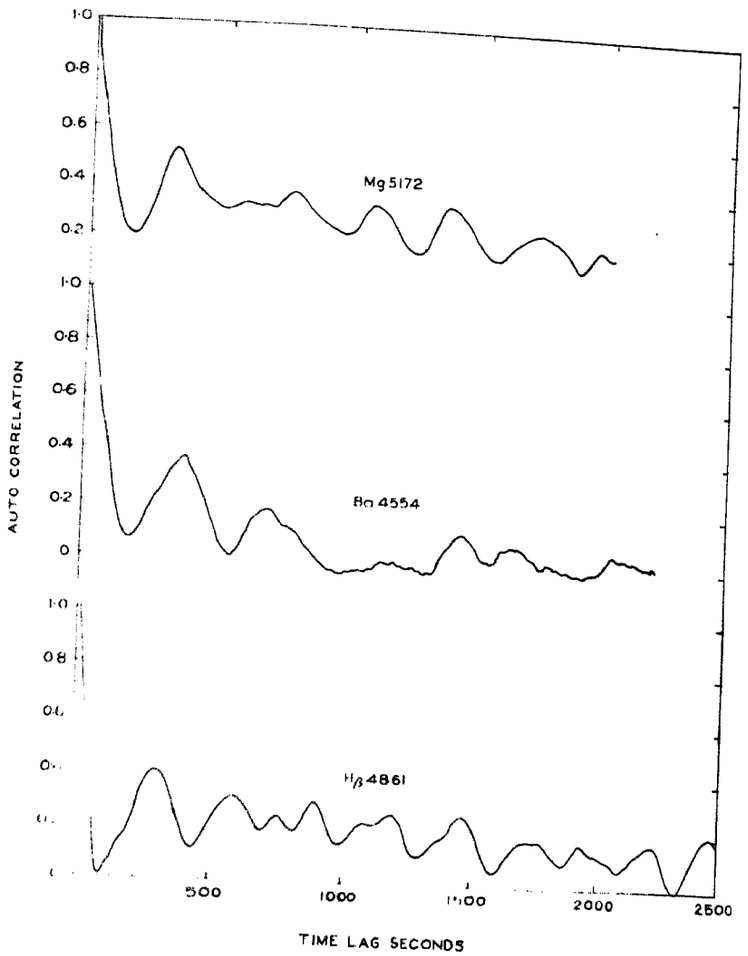
AUTO CORRELATION
1·0
0·8
0·6
0·4
0·2
Mg 5172
1·0
0·8
0·6
0·4
0·2
0
Ba 4554
1·0
0·8
Hβ 4861
500
1000
1500
2000
2500
TIME LAG SECONDS

Fig. III - 11

Data points in my case have been picked up at uniform intervals of 10 seconds, and the maximum values of lag m limited to within 0.2n. The calculations have been performed by the CDC 3600 computer.

3.6. Discussions on results of Power Spectra Analysis.

Values of autocorrelation co-efficients, i.e. normalised autocovariances are plotted against corresponding lags. Figures III-10 and III-11 shows some of the plots both for high and low level lines. All these curves confirms our preliminary findings about the persistant periodicity with a period of about 300 seconds. The plots have the appearance of damped sinusoidal functions. These are possibly due to constant change of phase of individual oscillations, and also due to presence of periods of bursts followed by relative quietness. Some of the curves exhibit increased fluctuations at greater lags, pointing to the existence of the second possibility. One question that troubles the minds of investigators of solar velocity oscillation is whether the oscillating solar layers have a tendency to repeat identical motions after a lapse of many minutes. If an affirmative answer could be found for this, it could have explained the increase of the amplitudes of the autocorrelation patterns at

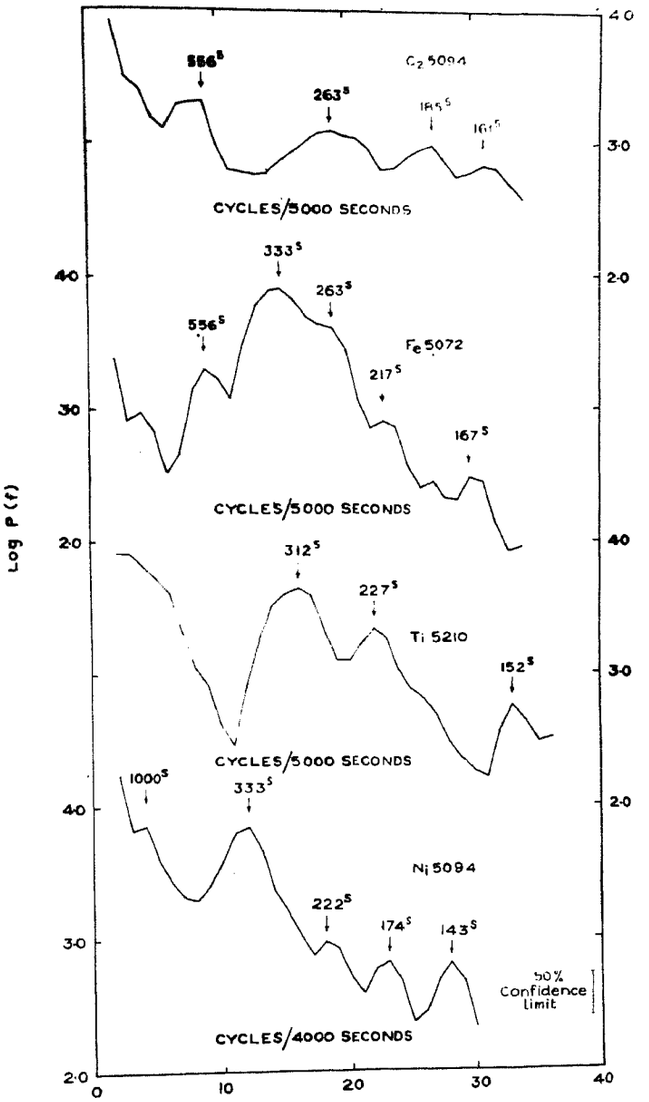
Log P (f)
556^S
263^S
C$_2$ 5094
CYCLES/5000 SECONDS
333^S
263^S
556^S
Fe 5072
217^S
167^S
CYCLES/5000 SECONDS
312^S
227^S
Ti 5210
152^S
CYCLES/5000 SECONDS
1000^S
333^S
Ni 5094
222^S
174^S
143^S
90% Confidence limit
CYCLES/4000 SECONDS
4·0
3·0
2·0
0
10
20
30
40

Fig. II-12

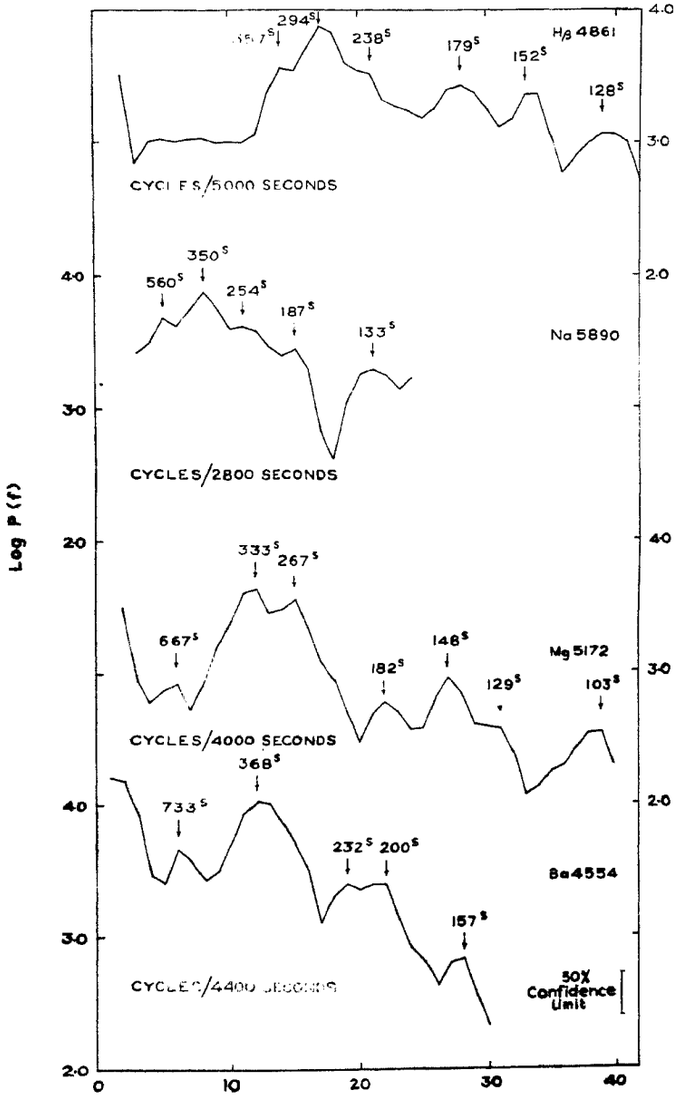
Log P (f)
4·0
3·0
2·0
294S
238S
179S
152S
128S
Hβ 4861
CYCLES/5000 SECONDS
350S
560S
254S
187S
133S
Na 5890
CYCLES/2800 SECONDS
333S
267S
667S
148S
182S
129S
103S
Mg 5172
CYCLES/4000 SECONDS
368S
733S
232S
200S
157S
Ba 4554
50% Confidence Limit
0
10
20
30
40

Fig. III - 13

greater time lags. But considering that on detailed tost, no two bursts in the same line observed by me, showed even consistent characteristics, this possibility can perhaps be ruled out. It is more likely that the effect is not physically real, but created artificially due to insufficient length of data required for such investigations. Although the observations lasted for several hours, relatively few bursts were actually noticed and the probability of getting a good correlation in the phases of distantly separated bursts is good. Howard (1967) in his detailed analysis of oscillations in the photospheric lines of FeI 5250 and CrI 5247 also arrived at the same conclusion.

The spectral density plots for these lines gives more detailed information about these oscillations. Figures III-12 and III-13 shows the values of log P(f) against f for all the lines observed. The curves reveal the complex nature of the oscillations, and indicate the presence of other minor oscillatory components besides the main period of around 300 seconds. Of noteworthy significance is the persistent presence of a relatively strong component around 220 seconds for the photospheric lines and several others between 100 and 200 seconds for the chromospheric lines. Records obtained on the

Distribution chart for predominant periods and corresponding root mean square velocities

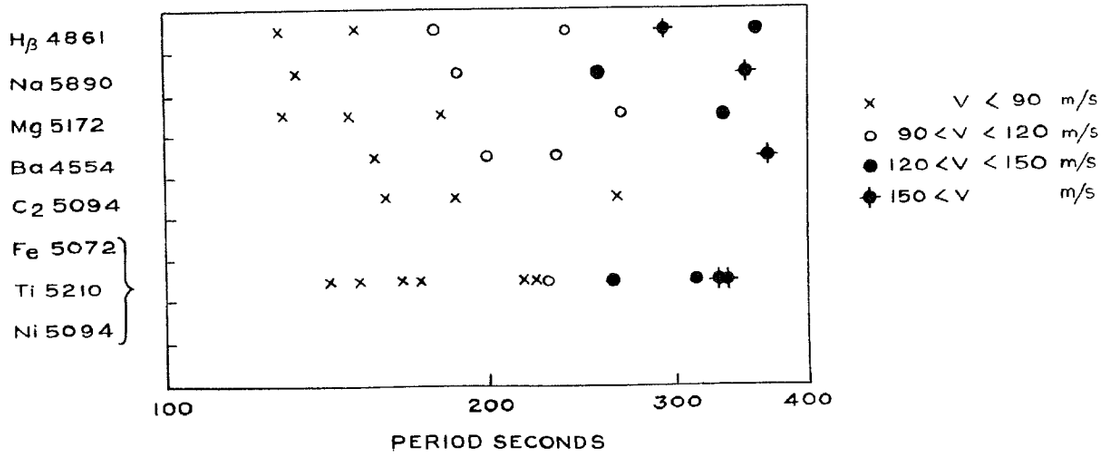

Fig. III - 14

chromospheric lines also indicate that the main period around 300 seconds is perhaps made up of two equally strong components on either side of 300 seconds. The peaks shown at periods larger than 500 seconds have to be treated cautiously as I feel that the resolution of the data is not good enough in these regions. Other investigators have attributed the low frequency tails noticed in deep forming lines as being due to the convective compohent, (Edmonds, Michard and Servajean, 1963, Frazier 1968). The additional spatial information obtained by their rapid-sequence spectral photography method enabled them to draw this conclusion. In absence of that, it is difficult, from the power spectra curves alone, to attribute such characteristics to the low frequency peaks noticed.

With a hope to detect any systematic variation of these peaks of the power spectral curve, I have arranged these on a chart indicating (Figure III-14) relative strengths of the oscillation peaks therein. The lines are arranged in order of their mean heights of formation in the solar atmosphere as assumed by my rough estimation from the Sacramento Peak flash spectral plates. As it is difficult to arrange the photospheric lines this way, they have been grouped together. The molecular carbon line with its mean height of formation in the temperature

minimum layer in the photosphere-chromosphere interface has been shown at its calculated height of formation.

Subject to the basic limitations of the data collected and the method of analysis, the following remarks may be made regarding the velocity oscillations:

i) There appears to be more than one mode of oscillation at all layers.

ii) The strongest mode is one with a period of over 300 seconds. This period remains virtually unchanged with height in the photosphere and low chromosphere but shifts to a lower period around $H\beta$ level.

iii) The weaker modes have a tendency to move to lower values of periods with increasing height.

Frazier (1968) in his observation of photospheric lines has noted the presence of two distinct periods of oscillation, the primary one being of a frequency of 3.8 milli-cycles/sec. i.e. of a period of 263 seconds. Although some of the lines observed by me originate in the same regions, I have found no evidence of this frequency being the primary one. The main photospheric periods are seen to be on the higher side of 300 seconds.

Also, although the period around 263 seconds showed a peak in one record only, three records showed a secondary peak around 220 seconds. The results of my present observations and those of Frazier are thus at variance. There is ofcourse, a fundamental difference in the two methods of observation; whereas Frazier has 55 minutes of observation over several point elements on the solar surface, my observations consist of the integrated behaviour of a larger area, but extending over a period, a few times longer. The period resolution and the confidence limits of the estimates of both the analyses are comparable, however. As such the non-conformity of these two results perhaps, point out that the precise oscillation frequencies noticed by Frazier is perhaps due to a chance coincidence, or some other hitherto unexplained reasons. It may be mentioned that Howard (1967) in his calculations of power spectra of oscillations observed in FeI 5250 and CrI 5247 noticed a prominent peak around 350 seconds period and not at 263 seconds.

The mean amplitudes of oscillation at the major peaks have been calculated from the power spectra curves, as per equation (3.4). These are tabulated in Table 3.4 below:

Table 3.4

Line	Period secs.	r.m.s. Amplitude m/s
Fe 5072	333	178
Ni 5094	333	163
Ti 5210	312	129
Ba 4554	368	205
Na 5890	350	174
Mg 5172	333	129
H 4861	294	170

The periods and the corresponding velocity amplitudes do not appear to have any systematic variation. This result is somewhat, unexpected, as the velocity amplitudes in general are known to have a tendency to increase with height (Evans 1963). In my present analysis sufficient lengths of continuous data have been analysed, which ought to have shown this property which was noticed by Evans, apparently from simple analysis of r.m.s. fluctuations. As, however, the effect is not clearly seen, there should be some other disturbing factors which have crept in our observational material. The observations are over the sharpest part of the line profiles, and as such the contributions over a large depth is incorporated in the measurements.

The velocity fields over a large depth may have variations which will ultimately affect the integrated results obtained. Also, the contribution functions for the formation of different lines have their characteristic variations with depth, and a direct comparison between results obtained by studying different lines may not yield accurate results.

It may, however, be pointed out that another set of measurements of shorter duration at different wing positions of certain chromospheric lines indicated monotonic increase of velocity amplitude with height. These measurements are discussed in the next chapter.

3.7. Power Spectra of individual bursts.

The analysis carried out so far yields the mean variance of the series at discrete frequency intervals for the complete record, which we have noticed to be composed of periods of bursts and quietness. In order to find out whether the power spectra analysis for different bursts gives comparable results, the analysis were repeated for periods of clear bursts in some of the lines. The burst periods have been picked up from the extended records, and only those of a reasonable length

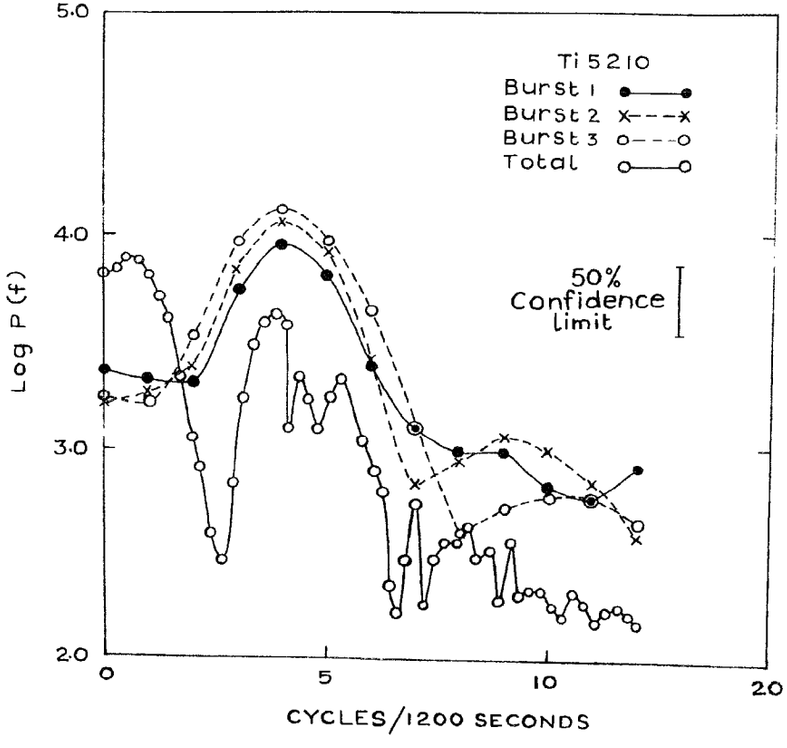
5.0
4.0
3.0
2.0
Log P (f)
0
5
10
20
CYCLES/1200 SECONDS
Ti 5210
Burst 1
Burst 2
Burst 3
Total
50%
Confidence
limit

Fig. III – 15

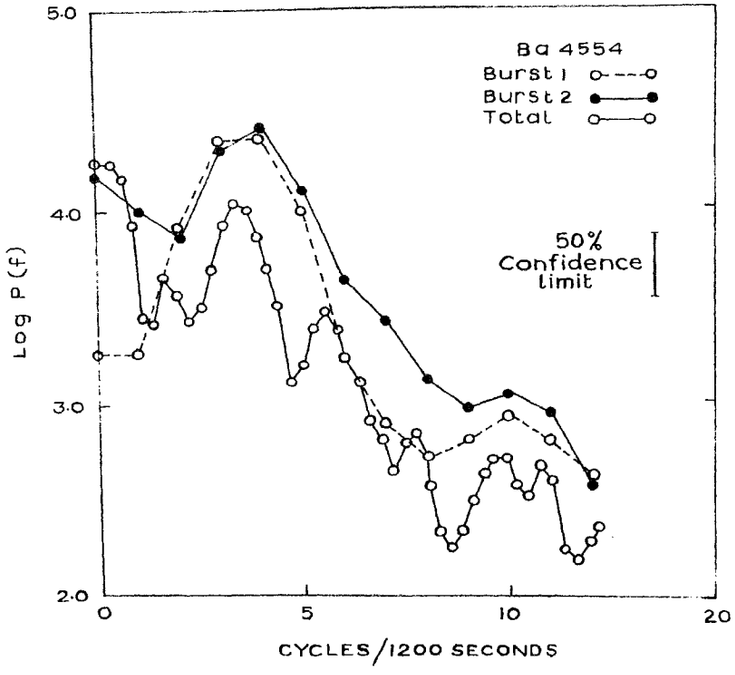
5·0
4·0
3·0
2·0
Log P(f)
0
5
10
20
CYCLES/1200 SECONDS
Bα 4554
Burst 1
Burst 2
Total
50%
Confidence
limit

Fig. III - 16

subjected to the autocorrelation and power spectra analysis. To keep the confidence level for these results and that of the extended record uniform, the maximum timeing is again limited to 20% of the data length. Since the length of data for the bursts are necessarily much shorter than the extended records, the frequency resolution in the former case is poorer. The power spectra obtained are plotted on the same scale along with the spectral curve obtained for the full record. Figures III-15 and III-16 shows the comparison between the power spectra of an extended record and those of the individual bursts for two lines. It may be seen that although discrepancies of minor nature are present between the power spectra for different individual bursts, the general nature of the curves are the same for all the bursts observed on the same line. Absolute values of spectral densities are seen to vary from burst to burst, which is not unexpected considering the random nature of the variations so far noticed in these oscillations. Comparison of these individual power spectra curves with those of the extended record for the corresponding lines, reveals two features. First, as a result of higher frequency resolution, the power spectra for extended records reveal much finer details of the spectral distribution that what can

be seen in the power spectra for individual bursts. Secondly, the mean power, and hence the mean r.m.s. amplitudes at the major peaks indicated by the extended record is less than that observed during the bursts. This is again due to the fact that, the presence of intervals in the record when no oscillations are noticed tend to lower the average value of the oscillation amplitude.

A comparison of the spectral density curves for individual bursts and the extended records summing up the bursts as well as periods of quietness gives a rough assessment of the mean percentage of time over which oscillations are observed at a fixed location. At the resonant frequency, the ratio of spectral density obtained from the extended record to that of the individual bursts should directly indicate the percentage. The figures calculated for different lines are given in Table 3.5 below:

Table 3.5

Line	Ratio $P(f)_e/P(f)_i$
H 4861	0.19
Mg 5172	0.28
Na 5890	0.27
Ba 4554	0.31
Ti 5210	0.36

It is noticed that in the lower chromosphere, about one third of the time oscillations may be expected at any particular location. My results show a tendency of this fraction to decrease with height. Other investigators have not considered this aspect of height variations but have simply noted that about one-third of the time the oscillations are noticed in any localized region (Meyer 1965).

3.8. Sizes of Oscillating cells.

By comparing the mean amplitudes of oscillation obtained by our method with those obtained by others using high dispersion photographic spectra, it is possible to estimate the average area occupied by the cells. The mean amplitude of oscillation during a burst observed in MgI 5172 line, by our method comes to 0.34 km/sec. This should be the average of all the cells and the non-oscillating spaces covered by our aperture of 1".4 x 5".6. Since the instrument integrates the line shift over the aperture, the resultant out-put is reduced in proportion to the area over which the Doppler shift is zero, this results in showing a lower velocity than in the spectral photography method. The mean r.m.s. velocity for the MgI 5172 line found by Evans and Michard is 0.81 Km/sec. Assuming that my observations with Mg 5172

as well as those of Evans and Michard have been done on representative samples of data, the total area occupied by the oscillating cells should be 3.3 square seconds of arc, i.e. about 42% of the aperture. Assuming further that our aperture covers a typical area on the average, we can estimate that on the average about 40% of the surface of the central portion of the solar disc is covered by oscillating cells.

CHAPTER IV

QUASI-PERIODIC OSCILLATIONS AT CHROMOSPHERIC HEIGHTS

4.1. The Chromospheric Oscillations.

For a more detailed study of the oscillations in the chromospheric layers, I have obtained a few extra sets of observations. The points which I wanted to study are the (i) height variation of the oscillation characteristics, (ii) the nature of oscillation wave-forms, (iii) direction of mass motions and (iv) the effect of magnetic fields on the oscillations. In what follows, I give a detailed account of the observations and analysis.

The lines chosen for these particular studies are H 4861 and MgI 5172 lines. The oscillatory characteristics were studied at various displacements from the line core of these two lines. The characteristics should then represent the properties of the layer from which the mean radiation at that point of the line profile originates. For this purpose, the magnetograph double slit was kept fixed at a measured opening and separation, and the oscillations were studied at different orders of the

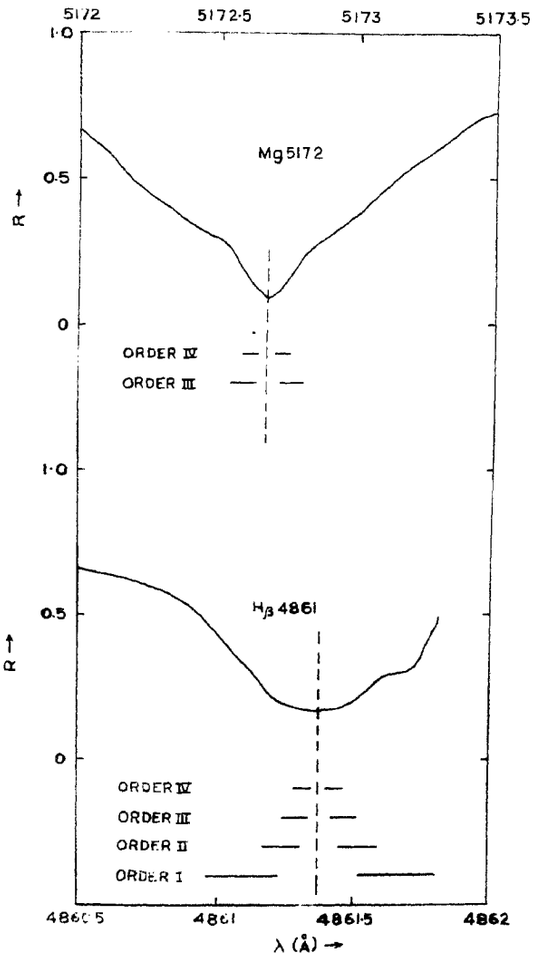
5172
5172·5
5173
5173·5
1·0
0·5
0
1·0
0·5
0
R
R
Mg 5172
ORDER IV
ORDER III
Hβ 4861
ORDER IV
ORDER III
ORDER II
ORDER I
4860·5
4861
4861·5
4862
λ (Å) →

Fig. IV-1

grating spectra, thereby changing the dispersion, and hence the measuring position on the wings of the line. The table below gives the details of the measurement.

Table 4.1

Line	Grating Order	Dispersion mm/Å	from line core Å
H 4861	1	1.1	0.29
H 4861	2	2.3	0.14
H 4861	3	3.7	0.09
H 4861	4	5.4	0.06
MgI 5172	3	3.7	0.09
MgI 5172	4	5.6	0.06

The accompanying diagram (Figure IV-1) illustrates the positions of the slit on the wings of Hβ and MgI 5172 for the different orders.

Records totalling an hour in each of the arrangements were obtained. The data were converted into velocity values following the same method as described in the previous chapter. The velocity series thus obtained were subjected to power spectra analysis, and the various oscillatory components compared.

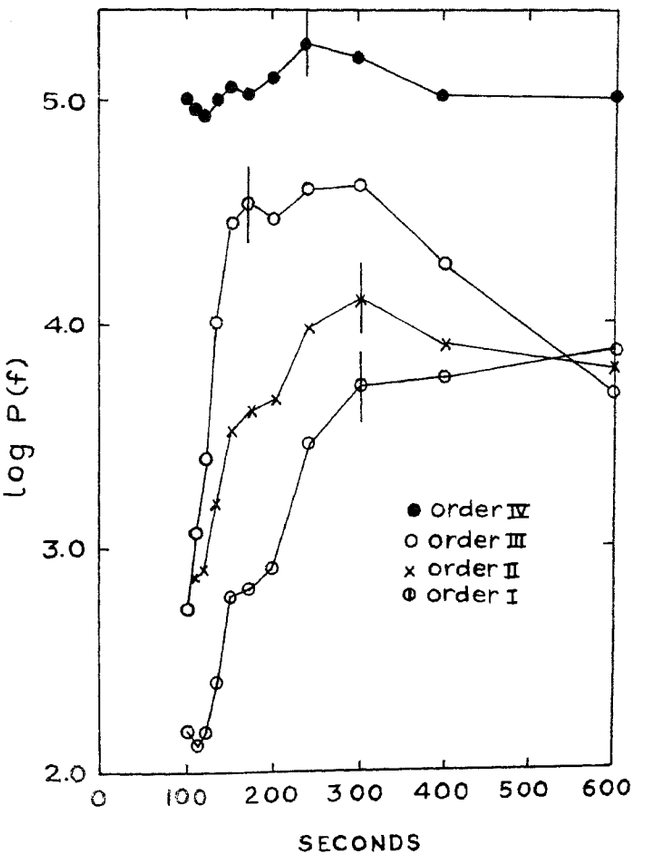
5.0
4.0
3.0
2.0
Log P(f)
0
100
200
300
400
500
600
SECONDS
● order Ⅳ
o order Ⅲ
x order Ⅱ
Φ order I

Fig. Ⅳ-2

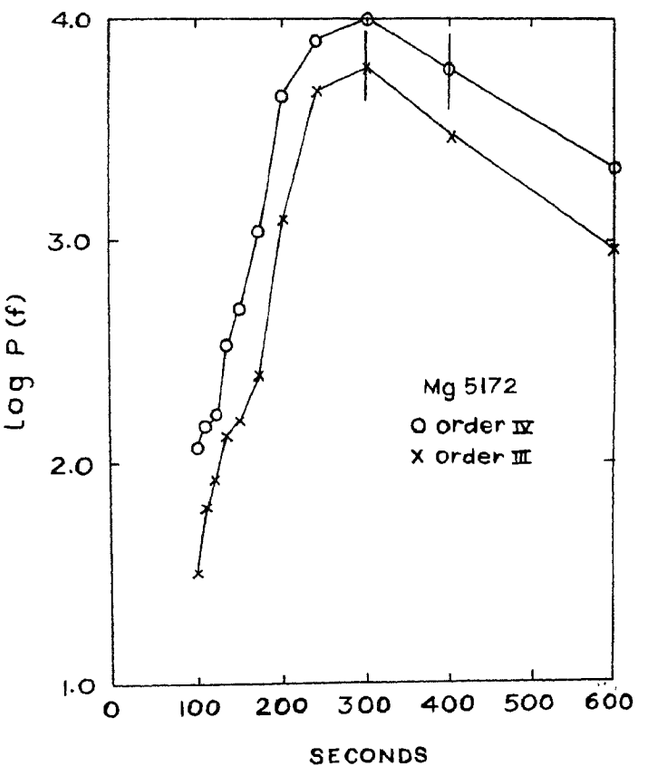
4.0
3.0
2.0
1.0
Log P (f)
0
100
200
300
400
500
600
SECONDS
Mg 5172
O order IV
X order III

Fig. IV - 3

Data on the mean heights of the formation of the different parts of the wing of these two lines is sparce in the literature. For H_β some values estimated by de Jager (1959) are utilized. For MgI 5172, Athay (1963) has calculated similar values for different displacements from the line centre, which have been used while discussing my results.

For H_β de Jagers values of h for $\Delta\lambda$= 0, 0.2, 0.4A are 3000, 2500 and 1000 kms respectively. Similar values for MgI 5172 picket up from curves calculated by Athay for $\Delta\lambda$ = 0, 0.1 and 0.2 Å are 800, 800 and 700 km approximately.

4.2. Variation of the oscillatory characteristics with height.

Figures IV-2 and IV-3 show the spectral density curves for four orders of $H\beta$ and two of MgI 5172. The curves indicate log of P(f) around several spot values of the period $T = \frac{1}{f}$. The following points are noticed from my results:

i) The amplitudes of the oscillatory components in the 100-400 second range generally increase with height in the high chromosphere.

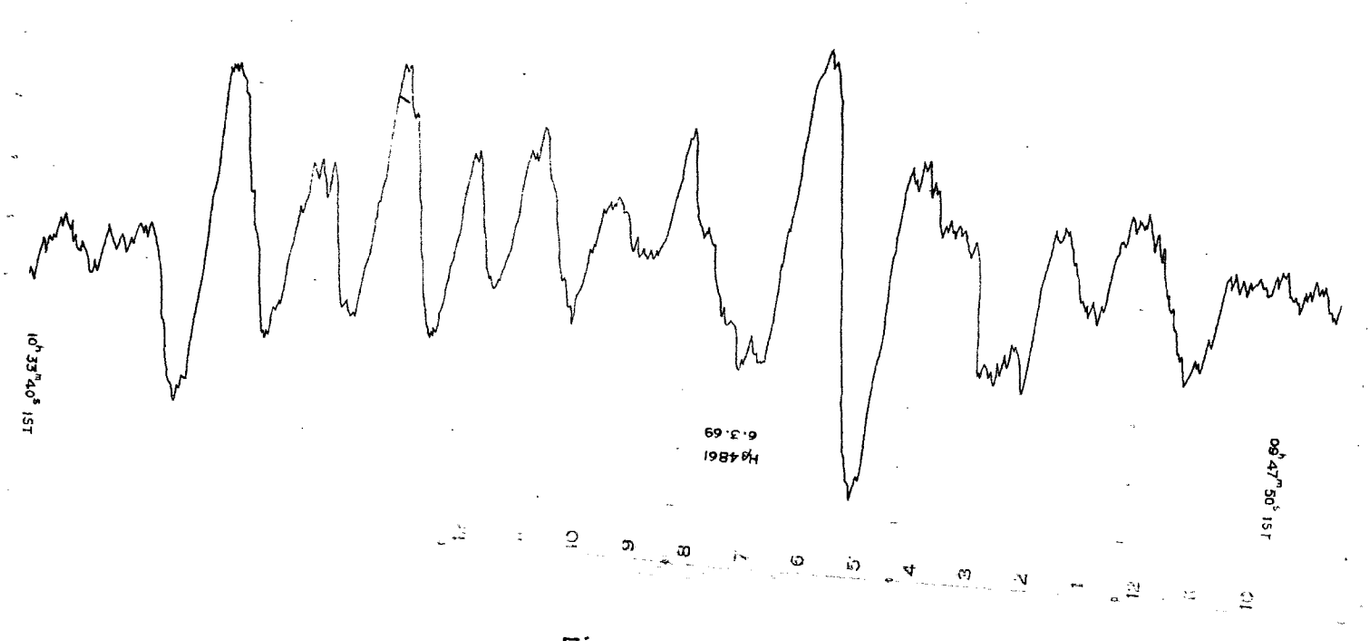

Fig. IV - 4

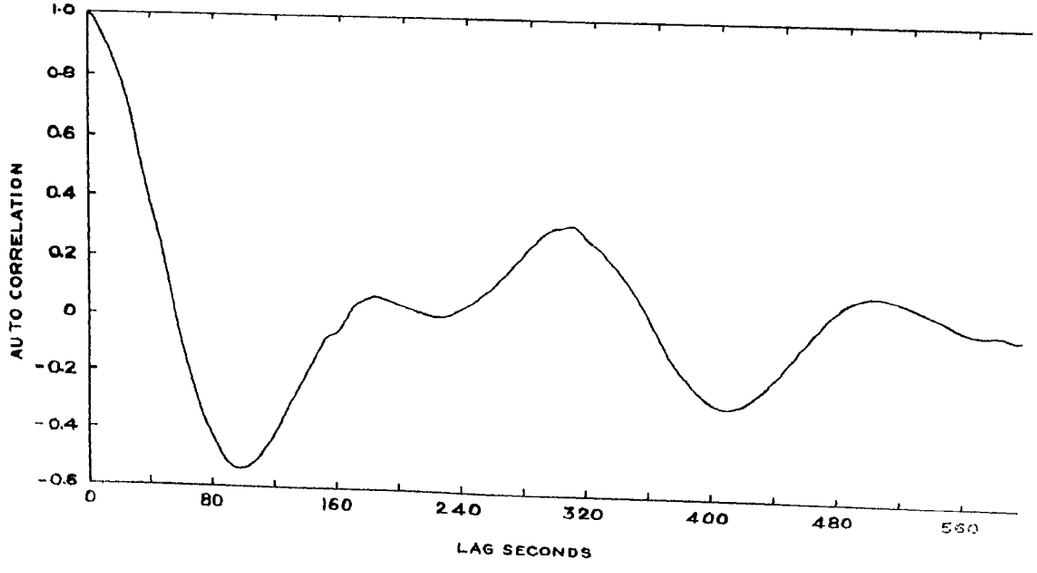
1·0
0·8
0·6
0·4
0·2
0
-0·2
-0·4
-0·6
AUTO CORRELATION
0
80
160
240
320
400
480
560
LAG SECONDS

Fig. IX - 5

ii) There is a tendency for the dominant period to decrease with increasing heights in this region.

iii) At very high heights, near the height of formation of $H\beta$ core, as noticed from the oscillations is III and IV orders in $H\beta$, a new dominant peak around 180 seconds period appears and becomes progressively more prominent.

The appearance of the prominent 180 seconds period at high chromospheric levels appears to be a feature not noticed by earlier observers. To check the consistency of this oscillation, observations were repeated on three different occasions, with identical slit settings near the core of the $H\beta$ line, and clear oscillations of a three-minute period were noticed. Figure IV-4 shows the record of one such occasion. This clearly shows the shorter period oscillation together with the normal 300 second period. The autocorrelation plot for this record is shown in Figure IV-5. While discussing these results, it may, however, be kept in mind that the oscillation amplitudes have been observed to vary from burst to burst. The variations noted in these cases, however, seem to be more than what can be expected due to variations among bursts. The root-mean square variation of the estimate

is seen to be less than the variations actually noticed. The probability that these differences are real is quite high statistically.

In the method adopted by me, viz. that of using spectral lines in different orders with fixed double slit setting, one has the disadvantage that in the lower orders, together with the shift of the observed portion of the wing, the range of the wing admitted into the slit increases proportionally. However, the order of the increasing height with higher orders of spectra remains, and the results are to be viewed with that limitation.

4.3. Waveform of the oscillations.

To determine the mean waveform of the oscillations, two long records of MgI 5172 were selected, as being most free from random noise, because of excellent observing conditions. A harmonic table was constructed as described below. The mean period was first calculated from clear peaks and troughs of the oscillations. A transparent grid overlay with this period was then prepared for picking up amplitudes at every 15° phase intervals. The amplitudes of the individual oscillations

at identical phase points are then entered in the respective columns of the phase-amplitude table. After entering all the available amplitudes, the mean amplitudes at all the twentyfour phase points were worked out. These mean values constitute the mean waveform of the oscillations as can be deduced from the available records. The mean waveforms from both the records were thus calculated and subjected to Fourier analysis. The analysis was carried out numerically, following the standard method of twelve point analysis (Karman and Biot 1940). The results of this analysis of the two records are tabulated below:

Table 4.2

Line	Slit setting from core	Fundamental m/s	Harmonics m/s			
			2nd	3rd	4th	5th
MgI 5172	0.09A	295	23	18	8	9
MgI 5172	0.06A	311	13	12	12	4

It may be noticed that the amplitudes of the Higher harmonics are small compared to the fundamental frequency; the second harmonic to fundamental ratios in the two cases being 7.8% and 4% only. The oscillations

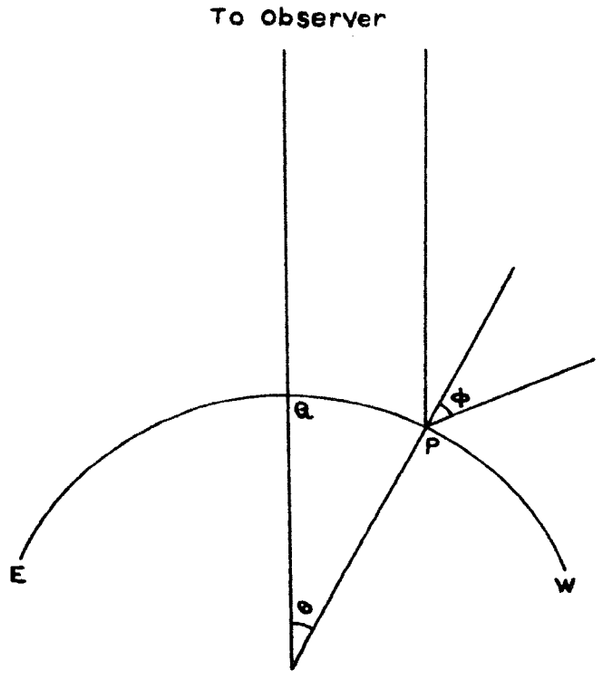

Fig. IV - 6

as such may be assumed to be almost purely sinusoidal with slight higher harmonics. From our records it is also seen that harmonic content is lower in the higher level.

4.4. Measurements at different positions from the disc centre.

Determination of the mean direction of these oscillatory motions is possible by comparing the characteristics of these oscillations at different positions of the solar disc. This is illustrated in a simplified diagram shown in Figure IV-6. If we consider a point P on the solar equator, whose heliocentric longitude is say θ ° west, and if we assume that the oscillatory motions are contained in the plane of the paper through the solar equator and directed at an angle ϕ as shown. If v be the amplitude of the oscillation, it is obvious that an observer on the earth's surface will see an apparent velocity of magnitude

$$v_a = v \cos(\theta + \phi) \qquad (4.1)$$

Denoting $\mu = \cos\theta$, this becomes

$$v_a = v\left[\mu \cos\phi - \sqrt{1-\mu^2}\sin\phi\right] \qquad (4.2)$$

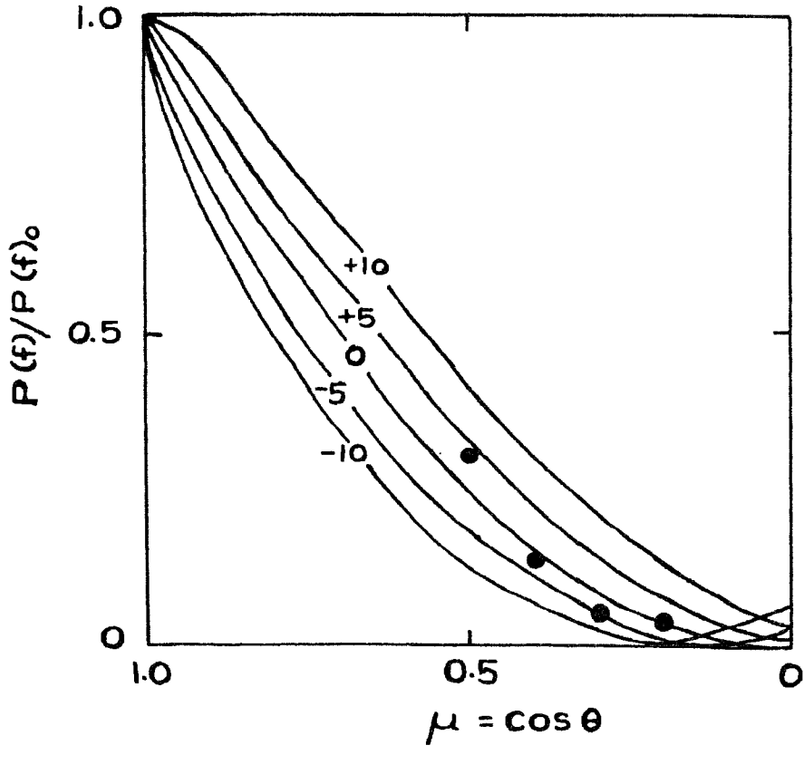

Fig. IV-7

At the position Q, $\mu = 1.0$, $v_o = v \cos\phi$

so that $$\frac{v_a}{v_o} = \mu = \sqrt{1-\mu^2}\tan\phi \qquad (4.3)$$

The corresponding spectral density functions will be related as:

$$\frac{[P(f)]_a}{[P(f)]_o} = \left[\mu - \sqrt{1-\mu^2}\tan\phi\right]^2 \qquad (4.4)$$

assuming that the depth variation of the oscillations is negligible over the range involved. A plot of the function defined above against different values of $\frac{\mu}{\lambda}$ is shown in Figure IV-7, for various values of ϕ ~~and~~ . By comparing the relative variations of the spectral densities at different μ's it is possible to have a rough estimation of the direction of the oscillatory mass motions.

Observations have been taken on the line of MgI 5172 at five positions on the solar disc with different μ's. The duration of the records was limited to about half an hour each, which is considered sufficient to give a representative sample of the velocity oscillations. The observed velocity curves were subjected to standard power spectra analysis, and the spectral

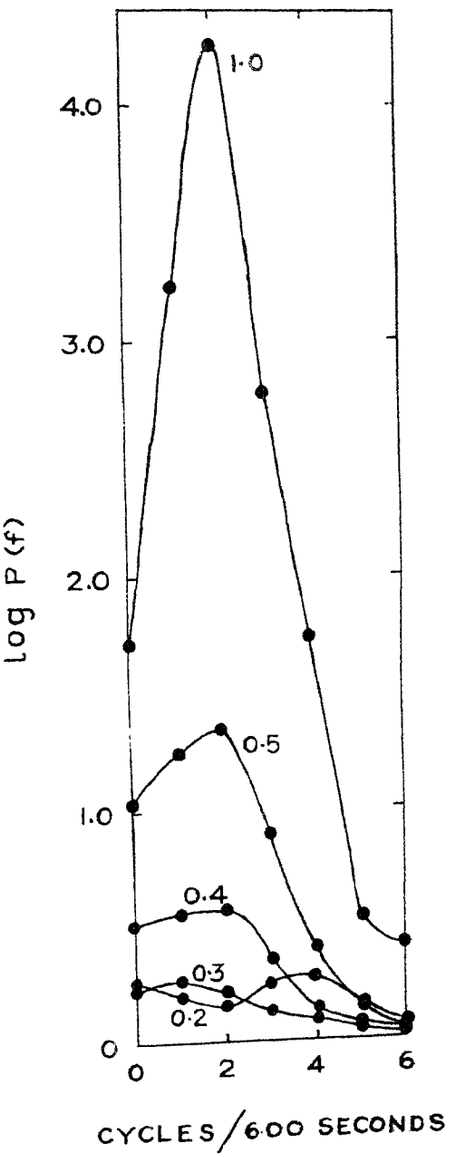

Fig. IV - 8

density curves are shown in Figure IV-8. It is evident that the oscillation amplitudes rapidly fall off with the distance from the centre of the disc. This is in general agreement with the observations of Evans and Richard, who observed that the velocities almost become undetectable below $\mu = 0.5$. With increased sensitivity of my method, it has been possible to detect weak amplitudes beyond this limit. The appearance of the high frequency peak at 150^{s} period at $\mu = 0.2$ require further observations to verify and explain.

Table 4.3

	Total power $(\text{metre/sec})^2 \times 10^{-12}$	300^{s} power $(\text{metre/sec})^2 \times 10^{-2}$	Ratios P(300)/ P(Total)
1.0	1540	426	0.277
0.5	549	137	0.255
0.4	253	57	0.225
0.3	164	23	0.140
0.2	136	17	0.125

Table 4.3 summarises the values of power density at the peak oscillation frequency at different μ values. The sum of the spectral series, i.e. the total power in

all frequencies for different μ 's are also tabulated alongside. The last column gives the fraction of the total power observed in the resonant frequency range. It is seen that the ratio decrease monotonically towards the limb, which is expected when our observations are recorded along with other types noise, e.g. seeing etc., which do not vary with μ values.

To assess the mean direction of these mass motions, normalised values of these peak spectral densities with respect to that of the centre of the disc are calculated for the different μ values. The calculated points are plotted in the graph given in Figure IV-7.

It is seen that these points indicate the direction of mass motion to be within $\pm$ 5° of the vertical. All the observed points lie within the two extreme theoretical curves corresponding to these limits.

4.5. Effect of Magnetic fields on the oscillations.

It has been observed by previous investigators that strong magnetic fields inhibit the oscillatory motions. I have taken two sets of observations to check whether the presence of strong photospheric fields affect

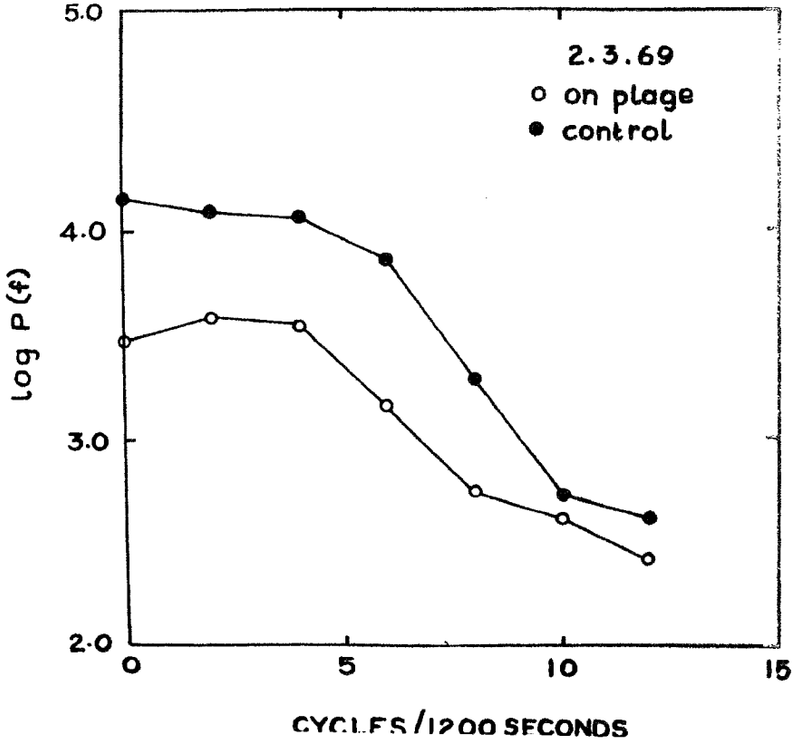
5.0
4.0
3.0
2.0
Log P (f)
2.3.69
o on plage
● control
0
5
10
15
CYCLES / 1200 SECONDS

Fig. IV - 9 (a)

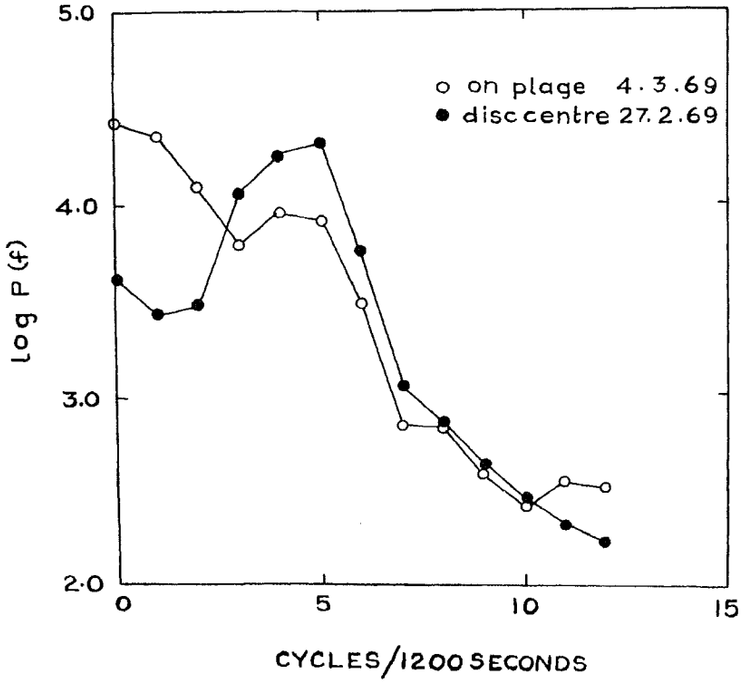
5.0
4.0
3.0
2·0
Log P (f)
o on plage 4.3.69
● disc centre 27.2.69
0
5
10
15
CYCLES/1200 SECONDS

Fig. IV - 9(b)

the oscillations in the lower chromosphere. The line chosen is again MgI 5172.7 and mass motions were recorded on two active regions, one near the centre of the disc (outside spot group 06°E,2°N, 13493 on 4-3-1969) and the other near the limb (Outside spot group 51°E, 15°N, 13495 on 2-3-1969). Line of sight component of magnetic field in either case was about 50 gauss. For the plage on the limb, control observations were taken immediately outside the plage regions. For the plage near the disc centre the velocity record taken earlier has been referred to for comparison. The two sets of velocity observations were then subjected to autocorrelation and power spectra analysis. The spectral density curves for the two cases are shown in Figures IV-9. It is seen that in both the cases, the spectral density oscillations near the dominant peak is lower in the presence of magnetic fields. No clear characteristic dominant period is noticed for the plage located near the limb, but in this case power density is lower at all periods down to 100 seconds. It is difficult to judge the effect at lower periods because of insignificant amount of power seen to be associated with lower periods.

There was low resolution of periods due to insufficiency of the available data, but within the limits, no change in value of the dominant period was noticed due to absence or presence of magnetic fields. Similar conclusions were, however, also arrived at by Howard (1967) for the photospheric levels.

CHAPTER V

A SIMULTANEOUS STUDY OF SOLAR MAGNETIC AND VELOCITY FIELDS

5.1. The Doppler recorder.

In the optical arrangement of the "Detector head" in the solar magnetograph, the two wing photomultipliers produce a balanced output when a symmetrical line is properly centred. This is irrespective of whether optical modulation is introduced, or not. This property has been utilised in operating the automatic line shifter, described in Chapter II. A very minor modification of the arrangement has enabled me to make some simultaneous recording of velocity and magnetic fields.

The arrangement is described below. The shaft of a good quality potentiometer is rigidly fixed to the shaft carrying the line shifter plate. A precisely controlled current flows through the potentiometer, so that any minute movements of the slider results in small changes of the potential of the slider contact. These changes, which are proportional to the line shifter movement are recorded on a second potentiometric recorder. The electrical arrangement is illustrated in Figure V-1.

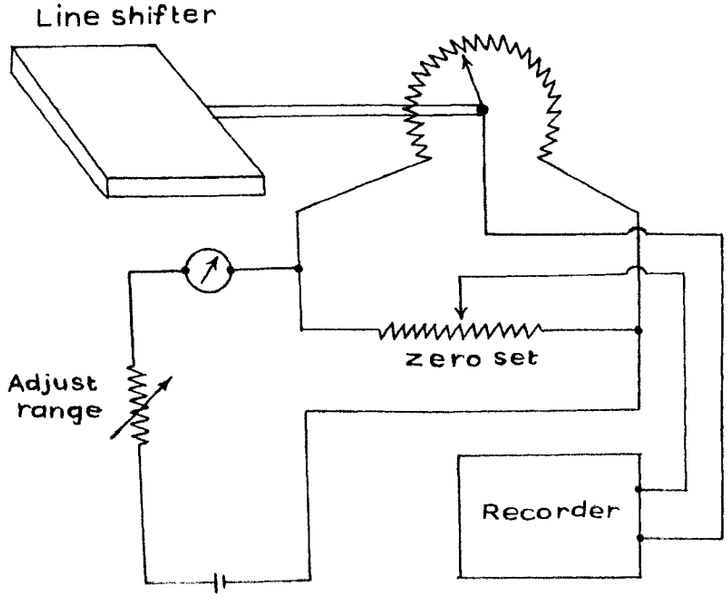

Fig. V-1

Calibration of the arrangement is done in the following manner. A line is properly centred on the detector head, as checked by zero signal of the magnetograph recorder in Doppler mode. The solar image is moved to one side so that light from either the east or west limb on the solar equator falls on the spectrograph. During the movement, as the line shifts due to solar rotational Doppler effect, the line shifter automatically moves to re-centre the line, and its movement recorded on the second recorder. The main magnetograph recorder should continue to show zero output all throughout. The deflections on the chart are then noted and with the solar image moved to the other limb, the new deflection on the chart is again noted. The difference in these two readings correspond to the difference of the rotational velocity of the sun between the two limbs on the equator, which has been taken as 4 km/sec. in our calculations. The operation thus provides a reliable calibration of the arrangement.

It is obvious from the electrical arrangement, that the scale of deflection is directly proportional to the current flowing through the potentiometer. This is of great advantage, as extra amplification of the deflections can be easily achieved when recording velocity oscillations of low amplitudes.

For operation in the magnetic mode, the second recorder thus continuously records the Doppler corrections needed to recentre the line, and the main magnetograph recorder, records the longitudinal magnetic field at the same region.

5.2. Simultaneous measurements of the magnetic and velocity fields.

The oscillatory mass motions so clearly seen, naturally raises the question whether they introduce a periodic fluctuation in the longitudinal magnetic field. If the magnetic elements are small in size, it is possible that they may be bodily carried by the mass motions, and show oscillatory fluctuations in constant phase relationship with the velocity changes. Some periodic changes in the values of the longitudinal magnetic fields have been reported recently by Severny (1967), who observed a long period of the order of 7-9 minutes in the fluctuation of the magnetic field on a plage. His observations were taken simultaneouslyon two lines FeI 5250 and FeI 6103. Observations with the Kodaikanal magnetograph were obtained on two guided locations on two plage regions, one near the centre of the disc (10°N, 6°E) and the other away from the centre

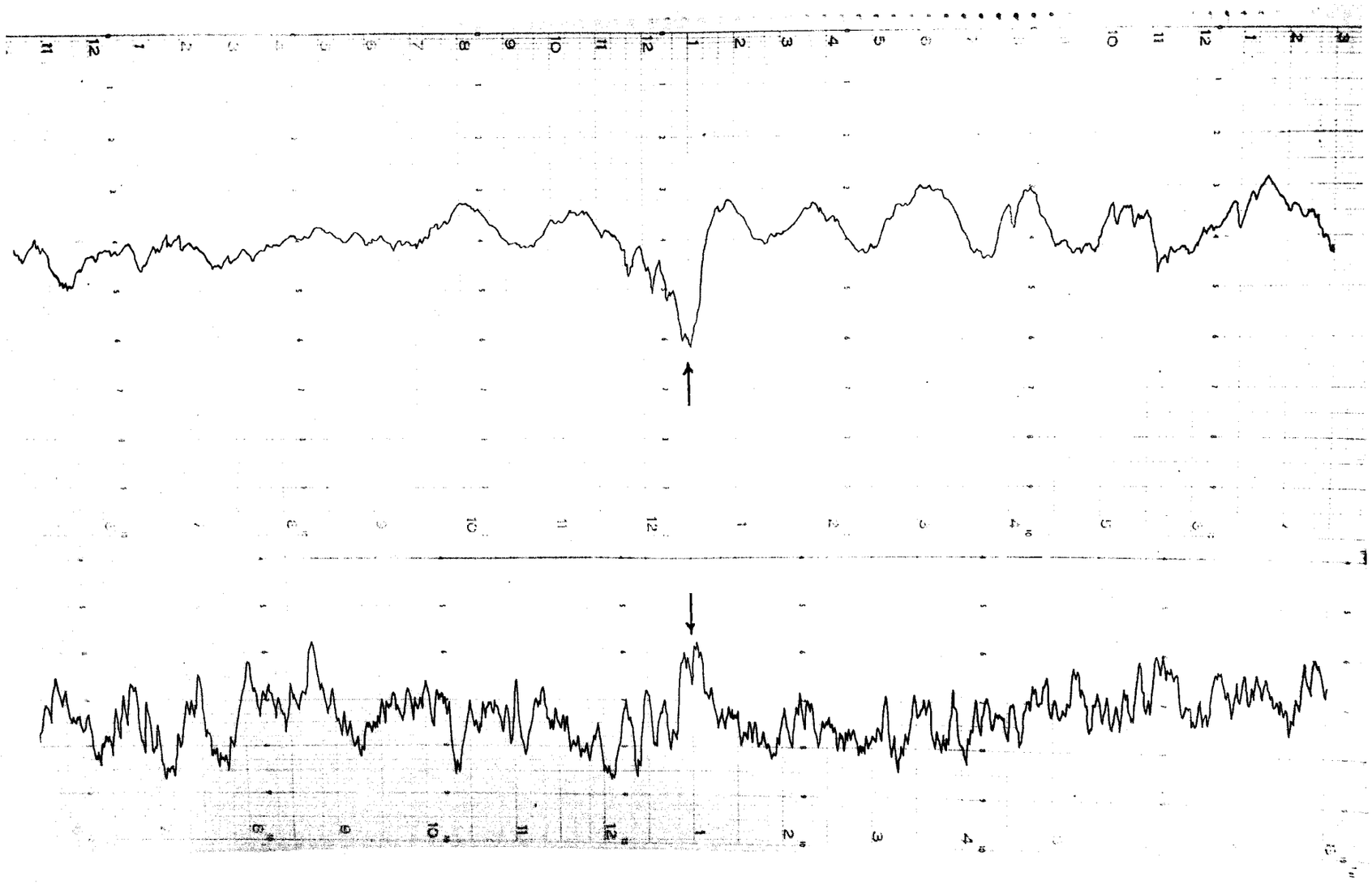

Fig. V - 2(a)

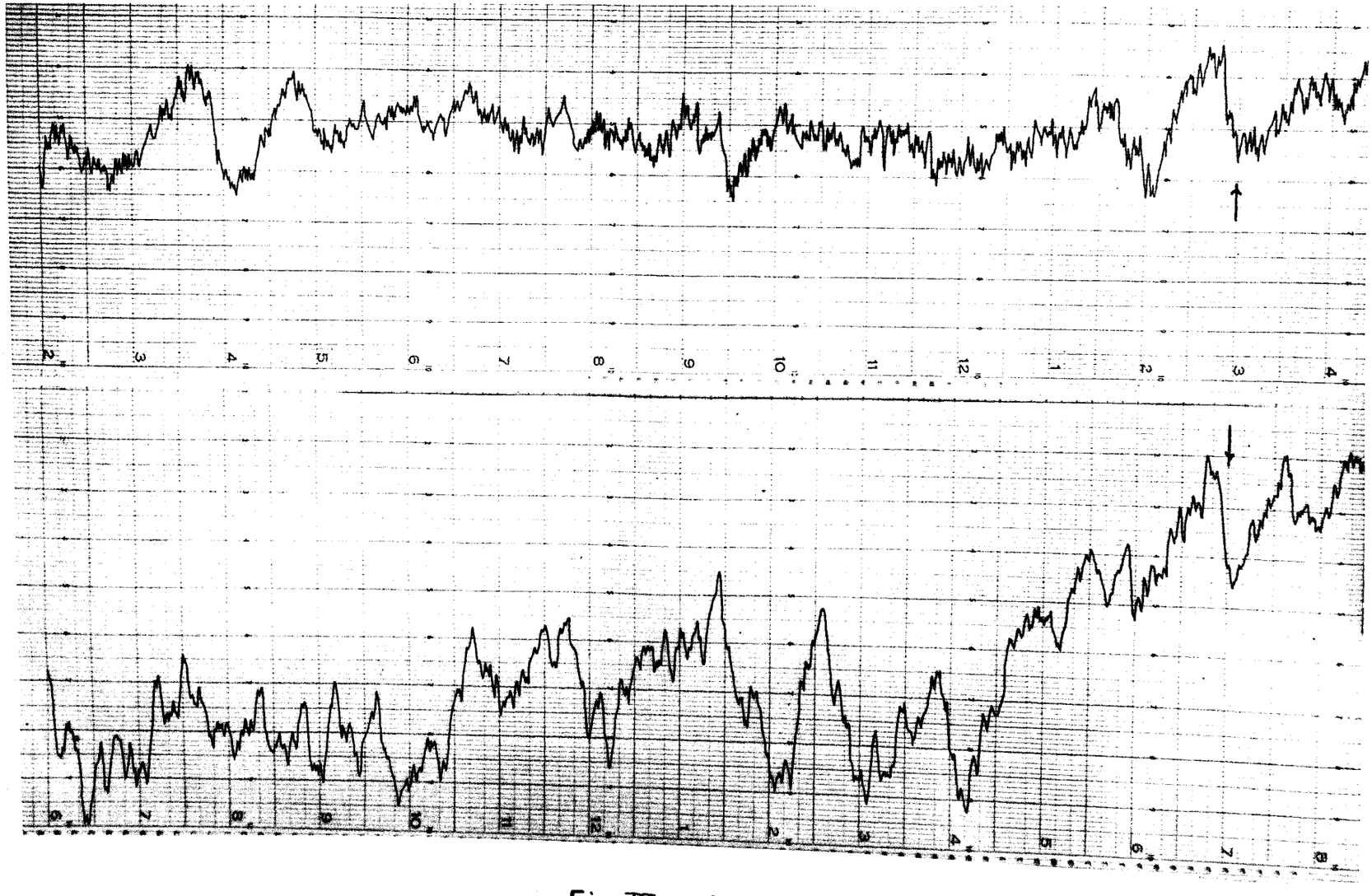

Fig. V-2(b)

(32°N, 55°W). The slit used in these two observations covered 1".4 x 11".2, on the solar surface; this is double the area used for velocity observations reported in previous chapters. This was necessary to have increased sensitivity for detecting small changes in the magnetic field. To find out whether the magnetic field changes have any correlation with the velocity changes, the magnetic field and the Doppler velocity of the area were recorded simultaneously. Each record is slightly over an hour's duration, and the solar image was manually guided, with magnified visual observation of the limbs. No solar rotation compensation was made so that, over the duration of the observation, the slow drift of the image by a few seconds of arc, thus providing a slow scan of the solar surface. The records, therefore, do not represent the changes of the values of the elements at a fixed location, but nevertheless the simultaneity of the two values is beyond doubt. Both the simultaneous records are shown in Figure V-2(a) and (b).

A superficial examination of the two records reveal certain basic information. The FeI 5250 is a photospheric line and clear bursts of oscillatory nature are seen in both the velocity records. There are variations in the magnetic field values, but apparently

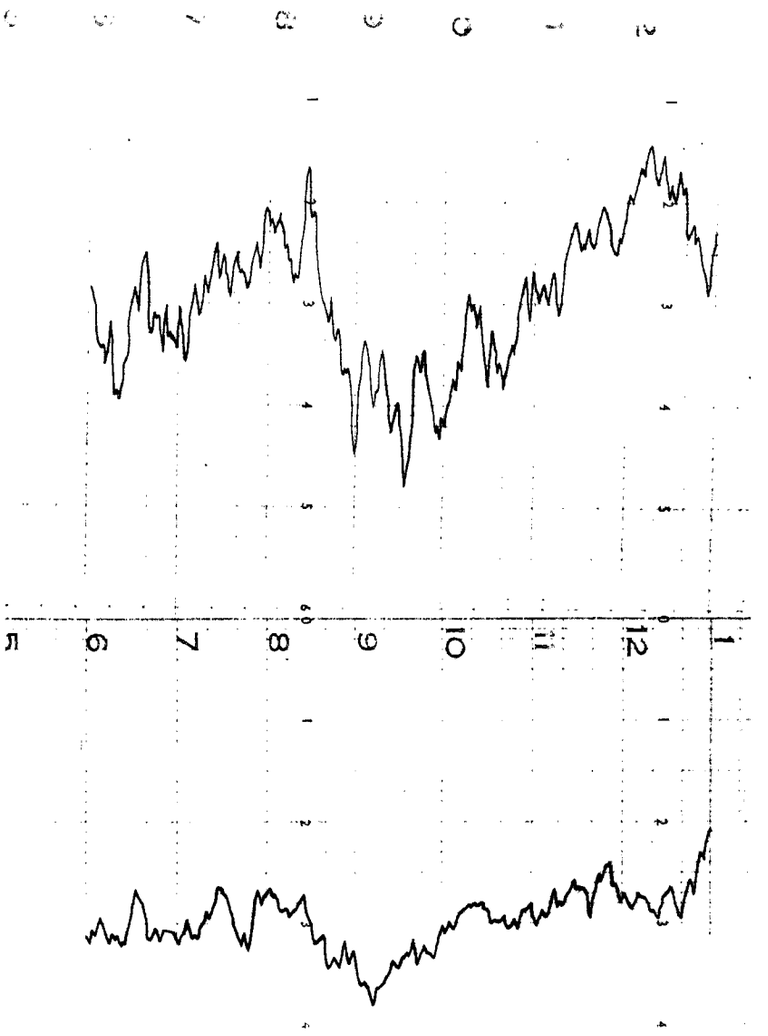

Fig. V-3

without much coherence with the velocity variations. Certain short period variations are noticed in the magnetic field records whose amplitudes are comparable to those of noise fluctuations. Only in a few isolated regions (shown by arrow marks), the velocity and magnetic field variations have almost a one-to-one correspondence. The long period variations shown in both the records particularly in the second one are most probably due to a region of non-uniform magnetic field drifting over the slit. The fact that such non-uniformities exist has been shown by the magnetic field measurements over the same area employing a very slow rate of scan. Figure V-3 shows two such scans with different amplifications used. Detailed analysis for these scans may reveal the magnetic field concentrations at the supergranular boundary levels, but such an analysis has been left out for the present.

5.3. Coherence Analysis.

The coherence between the velocity and magnetic field fluctuations has been tested following the methods of statistical coherence analysis, applied by Edmonds (1962) in his treatment of equivalent width, brightness and velocity fluctuations on the solar disc. The method is briefly described below:

We have simultaneous measurements on two fluctuating quantities viz. v(t) and H(t), let $P_v(f)$ and $P_H(f)$ denote their power spectrum as defined in chapter III, which represents the spectral densities of the two elements at any given frequency band. The relation between these two elements similarly can be represented by the Cross spectrum.

$$P_{VH}(f) = \int_{-\infty}^{+\infty} C_{VH}(\tau)\, \epsilon^{2\pi i f \tau}\, d\tau \qquad (5.1)$$

being the Fourier transform of the cross correlation function $C_{VH}(\tau)$. Generally the function $P_{VH}(f)$ is a complex quantity and can be represented by

$$P_{VH}(f) = R_{VH}(f) + i\, S_{VH}(f) \qquad (5.2)$$

the quantity $R_{VH}(f)$ being the real part of the transform, is called the co-spectrum, and $S_{VH}(f)$, the imaginary part, is called the quadrature spectrum.

The cross-correlation function, $C_{VH}(\tau)$ is composed of two parts, viz., The even part

$$C_{VH}^{+}(\tau) = \lim_{T\to\infty} \frac{1}{2T} \int_{-T/2}^{+T/2} \left[V(t).H(t+\tau) + v(t+\tau)H(t) \right] dt \qquad (5.3)$$

and the odd part

$$C_{VH}^{-}(\tau) = \lim_{T\to\infty} \frac{1}{2T} \int_{-T/2}^{+T/2} \left[v(t) \cdot H(t+\tau) - v(t+\tau) \cdot H(t) \right] dt \qquad (5.4)$$

It can be shown that (Goodman 1957)

$$R_{VH}(f) = \int_{-\infty}^{+\infty} C_{VH}^{+}(\tau) \cos 2\pi f \tau \, d\tau \qquad (5.5)$$

and $$S_{VH}(f) = \int_{-\infty}^{+\infty} C_{VH}^{-}(\tau) \sin 2\pi f \tau \, d\tau \qquad (5.6)$$

The quantity defined by

$$\gamma(f) = \left[\frac{R_{VH}^2(f) + S_{VH}^2(f)}{P_V(f) \, P_H(f)} \right]^{1/2} \qquad (5.7)$$

is known as the coherence and is a measure of the cross-correlation between the Fourier components of the two variables, and the quantity.

$$\theta(f) = \arctan \left[\frac{S_{VH}(f)}{R_{VH}(f)} \right] \qquad (5.8)$$

gives the phase difference between them for the frequency band centred around f.

Efrors in determination of these two quantities owing to finite length of data can be calculated in terms of equivalent degrees of freedom (Goodman 1957). For the phase angle $\theta(f)$, the error is given by,

$$\Delta\theta(f) = \text{arc sin}\left[\frac{1-\gamma^2(f)}{\gamma^2(f)}\left\{0.5^{-\frac{2}{k}}-1\right\}\right]^{1/2} \qquad (5.9)$$

where k is the degrees of freedom as defined by Blackman and Tukey (1959). An approximate expression for $\Delta\gamma(f)$ as given by the analysis of Van Isacker (1961),

$$\Delta\gamma(f) = \frac{\Delta P(f)}{P(f)}\left[\gamma^2(f)+1\right]^{1/2} \qquad (5.10)$$

where $\Delta P(f)$ is the probable error of one of the associated spectra. The expression is valid provided the value of r(f) is not too small.

5.4. Results of analysis.

The output values of magnetograph and Doppler recorder were picked up at 10 second intervals from the two records, and converted into values of velocity (metres/sec) and magnetic field (gauss) by use of appropriate calibration factors as described in Chapter II. The values were picked up at synchronous instants, so

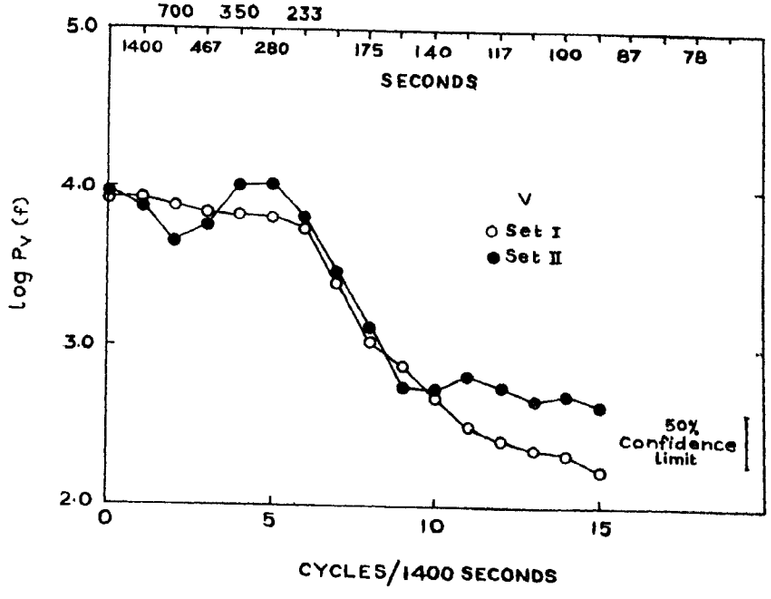
700 350 233
1400 467 280 175 140 117 100 87 78
SECONDS
5.0
4.0
3.0
2·0
Log P_V (f)
V
○ Set I
● Set II
50% Confidence limit
0 5 10 15
CYCLES/1400 SECONDS

Fig. V-4

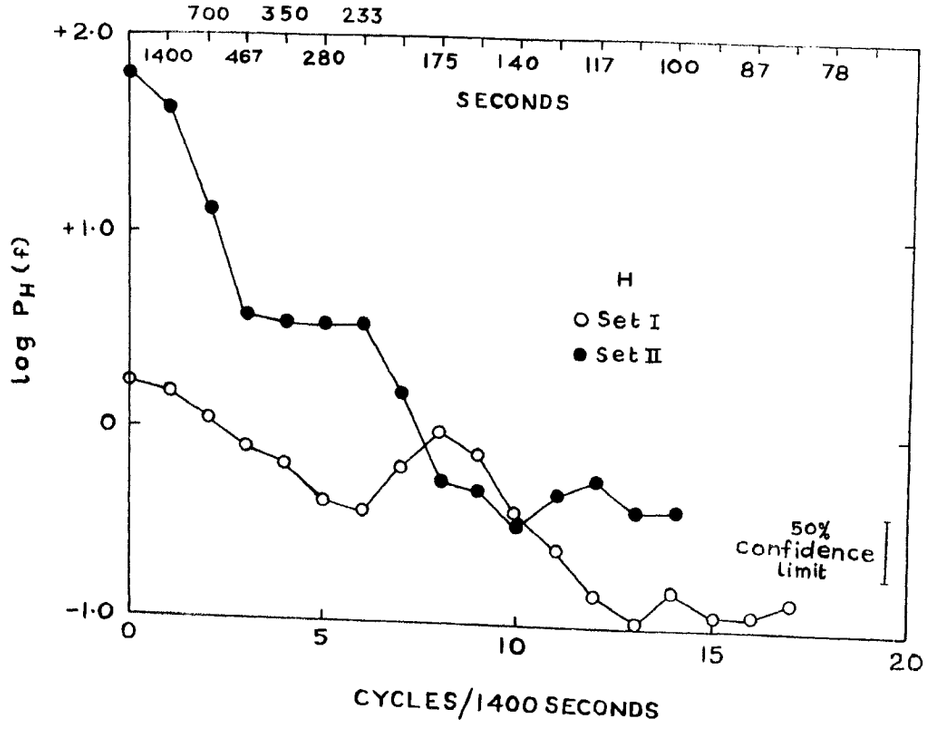
700 350 233
1400 467 280 175 140 117 100 87 78
SECONDS
+2·0
+1·0
0
-1·0
log $P_H(f)$
H
O Set I
● Set II
50% confidence limit
0 5 10 15 20
CYCLES/1400 SECONDS

Fig. X-5

that the two series thus formed, represents synchronous variation of the values of the two elements at a location. A programme written for the cross-spectrum analysis by the Colaba Magnetic Observatory was used on the CDC 3600 computor at the Tata Institute of Fundamental Research, Bombay. The results of the analysis are discussed in the succeeding sections.

Figure V-4 and V-5 show the power spectra for the two elements for the two records analysed. The absence of resonant peak around 300 seconds for the velocity record taken at the disc centre may perhaps be explained due to the continuous shift of the observed region over the spectrograph slit. For the location away from centre ($\mu = 0.6$), the linear rate of shift due to solar rotation being smaller, the resonant peak is seen better. No striking resonant peak around 300 seconds period is seen in either of the two H power spectra. A small power maximum is seen around 175 seconds period for the record taken at the centre and around 117 seconds at $\mu = 0.6$ position, the power density in both cases being small. No consistency is noticed between themselves, or with the corresponding velocity spectra.

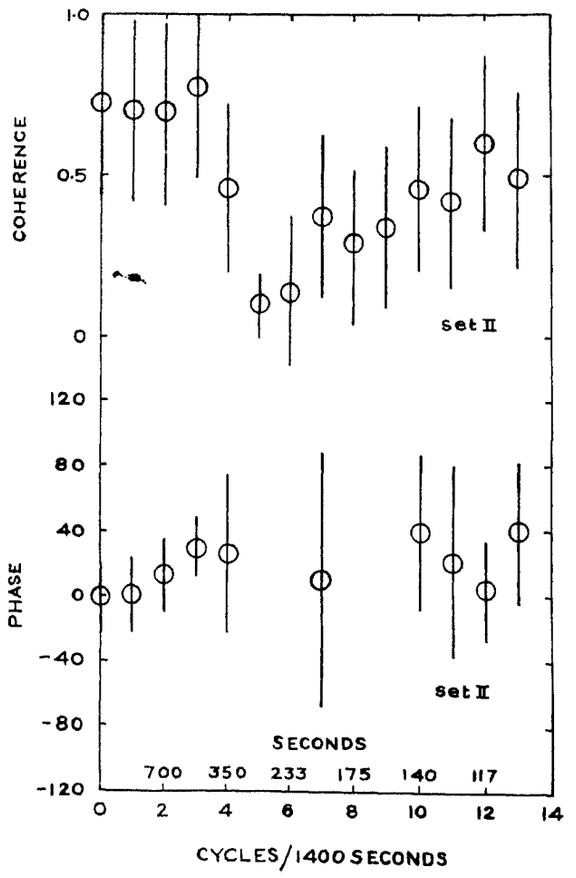
1·0
0·5
0
COHERENCE
set II
120
80
40
0
-40
-80
-120
PHASE
set II
SECONDS
700 350 233 175 140 117
0 2 4 6 8 10 12 14
CYCLES/1400 SECONDS

Fig. V-6

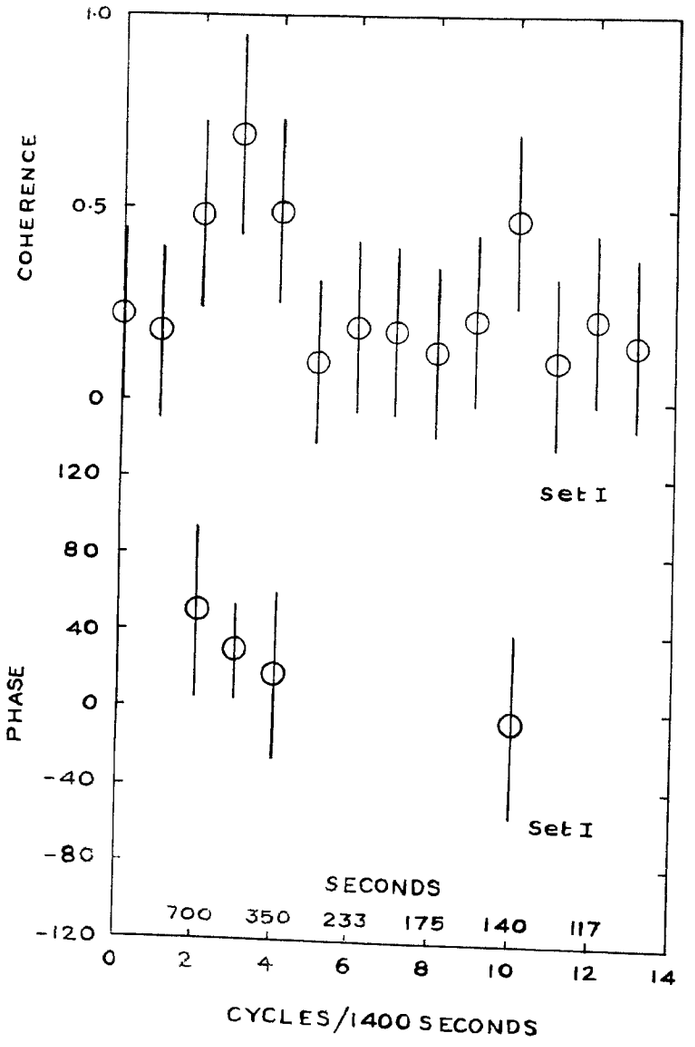
1·0
0·5
0
COHERENCE
120
80
40
0
-40
-80
-120
PHASE
Set I
Set I
SECONDS
700
350
233
175
140
117
0
2
4
6
8
10
12
14
CYCLES/1400 SECONDS

Fig. V - 7

The results of the coherence analysis is shown in Figures V-6 and V-7. Probable errors in estimation of both coherence and phase lag have been shown by vertical bars, as calculated by equations (5.9) and (5,10) wherever the value of coherence is high enough to justify the assumptions made in the equations.

The most striking point is the apparent lack of coherence around the normal velocity resonance period of 300 seconds noticed in both the records.

Coherence is better at longer periods around 500 seconds and also, at periods shorter than 300 seconds. The phase plot indicates that V and H are almost in phase for all periods.

It is interesting to note that in both the records the coherence reaches a maximum around the period of 467 seconds. Severny claims to have noticed a period around this value in the fluctuation of the magnetic field value. From the spectral curves it is seen that although no resonant peak is noticed at this period, considerable power density is available. If so, this mode of velocity fluctuation and magnetic variation should be somehow linked either at the source or during transmission through the outer solar atmosphere, interplanetary space, the

earth's atmosphere or in the instrument itself. At the present stage it is rather difficult to isolate the agency causing this apparent simultaneous changes of the two elements. From equation 2.3 and 2.4 it may be seen that changes in the apparent equivalent width or the residual intensity of the line can also produce changes in the values of these two elements measured. These apparent changes can be introduced due to scattering during the transmission path or in the instrument itself, as well as at the source in the solar photosphere.

The following reasons suggest that this coupling is introduced some where in the transmission path. If the link was at the source, it is difficult to interpret why the coherence should be maximum at any particular frequency other than the resonant peaks. If the magnetic elements are bodily shifted by mass motions, we should have expected a peak in $P_H(f)$ records also around 300 seconds, and the r(f) curve should have been more or less flat. Neither or these effects are noticed. The possibility of the simultaneity being introduced in the instrument can also be ruled out, as there are no apparent reasons for our observational equipment to couple the channels, at this particular frequency only, leaving other bands. But the possibility of the coupling

being introduced in the transmission path is open. It is true that the existence of this periodicity in the solar spectral measurements have not been specifically investigated, but a recent discussion during the Nice Symposium (1965) on cosmical gas dynamics suggests the possibilities of such periodicities. Evans reported to have found a periodicity of about five minutes period in the integrated sunlight from their observations at Sacramento Peak Observatory. This, however, is subject to verification.

Another possibility is that of chance coherence stimulated by the random "seeing" fluctuations. This can be verified only by carryingout measurements as reported herein on occasions of differing seeing quality from the best available at a site to a typically average performance.

We can summarise our observations on this question of simultaneous variation of magnetic and velocity fields on the sun as follows:

i) Resonant oscillations of about 300 second period do not have noticeable effects on the values of line-of-sight component of magnetic field.

ii) Sudden large changes in the apparent Doppler velocity have almost a one to one correspondence with

sudden changes in magnetic field as measured from its effect on the line.

iii) The variation of the two elements have a good coherence around 500 seconds period. Interpretation of this characteristic can best be done only after one can ascertain the role of "seeing" in producing such a possible coherence.

EPILOGUE

In the present dissertation, I have given a brief account of my attempts to make some extremely delicate measurements and the results obtained thereof. I did not hope to find a complete answer to the yet unsolved problems about the physical nature of the dynamics of the solar plasma, but I hope, I have been able to add something to the present store of our information about the oscillatory velocity and magnetic fields. Certain new features have been brought out by the present series of observations, some of which, I again hope, may prove vital to some future theory explaining the complete magneto-hydrodynamic behaviour of the solar plasma.

About the instrument I may like to add a few comments. In the longitudinal magnetic field measurements, we have apparently reached a point on which only marginal refinement can be made by the existing technique. On the other hand, the transverse field measurements offer a field where the varied ingenuities of any skilled experimentalist may reap major gains. A few attempts in this direction have been made, but the results so far are not very encouraging. Even, to-day, an accuracy of

only 100 gauss in the measurement of transverse fields is to be expected. For transverse field measurements some alternative means must be found. Some attempts in this direction are currently being made at Kodaikanal.

The accuracy attained by the present technique for the longitudinal field measurement is adequate for the image quality that one can possibly obtain at any ground based station. Only when better image qualities will be obtained from space platforms, one will be able to use higher sensitivities to advantage for studying fine feature of solar magnetic and velocity fields.

About the oscillatory velocity fields, the point which seem to come out my attempts is that the degree of randomness in these motions are more than what was thought to be earlier. A proper understanding of these oscillatory mechanisms, therefore, require much longer records of controlled observations. A continuous record of the "seeing" quality will be extremely useful for interpretation of the observations.

For study of the fine nature of the photospheric magnetic fields we will have to mainly depend on the best of seeing conditions, and a small aperture. I believe much useful information will come out of such studies.

Finally, it will be possible to observe a few more elements, e.g. adjacent continuum brightness, the equivalent width etc. with some modifications of the optical and electronics set up. Continuous simultaneous observations of these elements over a carefully guided location will provide valuable information about the complicated dynamical processes of the solar atmosphere.

—

REFERENCES

Alfven, H.,	1947	M.N., 107, 211 (Sec.11)
Alfven, H.,	1950	Cosmical Electrodynamics Oxford : Clarendon Press (Secs. 1, 11, 20)
Athay,	1963	Ap.J., 138, 680
Babcock, H.W.	1953	Ap.J., 118, 387
Babcock, H.W.,	1961	Ap.J., 133, 572
Babcock, H.W., and Babcock, H.D.,	1952	P.A.S.P., 64, 282
Bierman, L.,	1947	Nach. Acad. Wiss. Gott. Math. Phys. Classe 3.12
Bierman, L.,	1948	Zs. f. Ap., 25, 161
Blackman, R.B. and Tukey, J.W.,	1958	Measurement of Power Spectra Dover Publications, INC, New York.
de Jager, C.,	1959	Handbuch der Astrophysik ed. S. Flugge, 52, 80
Deubner F.L., Kiepenhuer, K.O. and Leidler, R.	1961	Zs. f. Ap., 52, 118
Dunn, R.B., Evans, J.W. Jeffries, J.T., Orral F.Q. White O.R., Zirker, J.B.,	1962	Ap.J. Supplement 15, 139
Edmonds, F.N. Jr.	1962	Ap.J. 136, 507
Evans, J.W.	1963	A.J., 68, 72.
Evans, J.W., and Michard, R.,	1962	Ap.J., 136, 493
Evans, J.W., and Michard, R.,	1962	Ap.J., 135, 812

Edmonds, F.N., Michard R, and Servajean, R.	1965	Ann. Astrophys. 28, 534
Evershed, J.	1909	M.N. 69, 454
Evershed, J.	1922	M.N.R.A.S., 82, 392
Frazier, E.N.,	1968	Ap.J., 152, 557
Goodman, N.R.,	1957	Scientific Papers No.10. Engineering Statistics Lab. New York University
Howard, R.,	1962	Ap.J., 136, 211
Howard, R.,	1966	Proceedings of Anacapri Colloquium
Howard, R.,	1967	Solar Physics, 2, 3
Karman, T.V., and Biot, M.A.	1940	Mathematical Methods of Engineering, McGraw Hill
Kiepenheuer, K.O.,	1953	Ap.J., 117, 447
Leighton, R.B.,	1960	Aerodynamic Phenomena in Stellar Atmospheres, IAU Symposium No.12, 321
Leighton, R.B., Noyes R.W., and Simon, G.W.	1962	Ap.J., 135, 474
Mc Math R.R., Mohler O.C., Pierce, A.K., and Goldberg, L.,	1956	Ap.J., 124, 1
Meyer, F.,	1965	Aerodynamic phenomena in Stellar Atmospheres, IAU Symposium No.28, 324
Moore, D.W., and Spiegel, E.A.	1964	Ap.J., 139, 48
Nikulin, N., Severny, A, and Stepanov, V.,	1958	IZV. Krym. astrofiz. Obs. 19, 3

Noyes, R.W.,	1965	Aerodynamic Phenomena in Stellar Atmospheres, IAU Symposium, No.28, 293
Orral, F.Q.,	1965	Ap.J., 141, 1131
Richardson, R.S., and Schwarzschild, M.,	1950	Ap.J., 111, 351
Schatzman, E.,	1948	C.R. Acad. Sci. Paris, 228, 738
Schatzman, E.,	1949	Ann. Astrophysics, 12, 203 (Sec.11)
Schatzman, E.,	1964	Proceedings of the 12th General Assembly, Hamburg, p. 543
Schmidt, H.U. and Zirker, J.B.	1963	Ap.J., 138, 1310
Schwarzschild, M.,	1948	Ap.J., 107, 1 (Sec 11)
Severny, A.B.,	1966	Proceedings of Anacapri Colloquium
Severny, A.B.,	1967	Astronomical Journal (USSR), 44, 481
Subrahmaniam, N.,	1965	Ph.D. Thesis, University of Madras
Thiessen, G.,	1946	Annales de Astrophysique 9, 101
Van Isacker, J.,	1961	Advances in Geophysics 7, 189
Whitney, C.,	1958	Smithsonian Contribution to Astrophysics, 2, 365

—